"ESTIMATING ANNUAL BUILDINGS GROUND FLOORS HEAT LOSSES USING A ONE-DIMENSIONAL (1-D) NUMERICAL MODEL"

By

ANDREAS GIAKOUMAKIS

The Bartlett School of Graduate Studies
University College London

A Dissertation submitted in partial fulfilment of the degree of Master of Science Built Environment: Environmental Design and Engineering

University of London

September, 2006

ProQuest LLC
789 East Eisenhower Parkway
P.O. Box 1346
Ann Arbor, MI 48106-1346

Abstract

In this work, an estimation of the annual buildings ground floors heat losses by means of numerical simulations of two different geometrical models (constructional details of buildings ground floors), using a 1-D numerical model, is attempted. Given the three-dimensional (3-D) nature of the heat transfer through the ground, the annual ground floor heat losses are first estimated using a 3-D model, constructed and simulated with the thermal analysis computer programs: "TRISCO" & "VOLTRA". Then, the 3-D model is converted to the 'respective' one-dimensional (1-D) one and the 'equalization' of the two models - for the both cases (geometrical models) - as far as the annual ground floor heat losses per unit surface area are concerned, is done by changing the values of the various simulation parameters of the used computer programs. Furthermore, since the various simulation tools, such as "TAS" thermal analysis software, generally simulate all heat transfer processes in one dimension - those through the ground floors included - and model the soil depth, in particular, to be: 1m, an estimation of the possibly introduced, in this 'methodology', errors is made, by comparing the respective results derived from the 3-D & 1-D numerical models. As far as the 'equalization' of the 1-D & 3-D numerical models is concerned, the results in question 'revealed' that, the (1-D numerical model's) soil depth, primarily and the soil thermal conductivity (λ), secondly, are the most significant simulation parameters for the achievement of this aim. Regarding the errors possibly introduced in the process of estimating the annual buildings ground floor heat losses using a 1-D numerical model (with a soil depth value of: 1m), it is shown that, the size of these errors - for the specific models examined in this work - is approximately: -38% for the first and: +59% for the second one and, furthermore, that, the definition of the 'proper' soil depth value depends on the specific numerical model (its geometry, configuration and simulation parameters), as well as, the soil type and its thermal properties, the thermal conductivity being the most significant one. However, given the limited capabilities of "VOLTRA" thermal analysis computer program and of the PCs used for the numerical simulations, as well as, the great differences between the various numerical models (regarding their: geometry, configuration, simulation parameters and soil type/ thermal properties), a generalization of the conclusions presented hereby cannot be defended.

Keywords: Annual buildings heat losses via the ground; Numerical simulations;
Thermal analysis computer programs "TRISCO" & "VOLTRA";
'Equalization' of the 1-D & 3-D numerical models;
Estimating the annual buildings ground floor heat losses
using a 1-D numerical model; "TAS" thermal analysis software;
Soil depth (of the 1-D numerical model); Soil thermal conductivity

Table of contents

List of symbols

This list of symbols is not completely exhaustive. Symbols that appear only 'locally' in the text and are not important for other parts of this work, are not included here.
To sustain conformity with the general notation in literature, sometimes different variables may be represented with the same symbol. In such cases, the exact meaning of the given symbol should be clear from the context.

Roman symbols

b: breadth	(m)
c_a: specific heat capacity of air	(J/kgK)
c_l: specific heat capacity of water	(J/kgK)
c_{salt}: concentration of salt in Eq. (4.7)	
c_v: specific heat capacity of water vapor at constant pressure	(J/kgK)
g: acceleration of gravity	(m/s^2)
h: height	(m)
h_c: convective heat transfer coefficient	(W/m^2K)
h_r: radiative heat transfer coefficient	(W/m^2K)
k_l: hydraulic conductivity of unsaturated soil	(m/sec)
k_Π: thermal gradient ratio in component Π	(-)
l_f: floor length	(m)
n_{salt}: number of molecules per mole of salt in Eq. (4.7)	
q_{cond}: heat flux per unit area generated by conduction	(W/m^2)
q_h: heat flow	(W/m^2)
$q_{h,es}$: heat flow into soil at external surface	(W/m^2)
q_l: liquid moisture flux	(kg/m^2s)
q_{lconv}: heat flux per unit area generated by liquid convection	(W/m^2)
q_m: total moisture flux	(kg/m^2s)
$q_{m,es}$: water flow into the soil at external surface	(kg/m^2s)
q_v: vapor moisture flux	(kg/m^2s)

q_{lconv}: heat flux per unit area generated by vapour convection	(W/m²)
t: time	(s)
t_0: starting time	(s)
u_a: pore air pressure	(Pa)
u_w: pore water pressure	(Pa)
$\vec{v}_l$: velocity of liquid	(m/sec)
$\vec{v}_v$: velocity of vapour	(m/sec)
w: wall thickness	(m)
x, y, z: spatial coordinates	
A: floor/ wall area	(m^2)
B: rectangular floor width	(m)
B': characteristic width	(m)
C: volumetric thermal capacity of solids, liquid, vapour and air	(J/m³kg)
C_d: volumetric thermal capacity of the solids	(J/m³kg)
CDD: cooling degree-days	
D_v: vapour diffusivity	(m²/s)
E: amount of evaporation	(kg/m²s)
E: emissivity factor in Eq. (5.1) & (5.2)	
F_d: decrement factor	
F_2: heat loss coefficient	
H: heat exchange by convection	(W/m²)
H: enthalpy	(J)
HDD: heating degree-days	
HP: heat supply by precipitation	(W/m²)
K_s: coupling coefficient in Eq. (3.12)	(W/m°C)
L: length	(m)
L_0: latent heat of vaporization of water L at temperature T_0	(J/kg)
LE: heat exchange by evaporation	(W/m²)
P: floor perimeter	(m)
P_w: pore water pressure	(Pa)
Q: heat flux	(W/m^2)
Q_A, Q_a: annual amplitude of the heat loss	(W/m^2)
Q_m: is the mean annual heat loss	(W/m^2)

R_{dif}: diffuse short wave radiation	(W/m²)
R_{dir}: direct short wave radiation	(W/m²)
R_g: long wave surface emission	(W/m²)
R_g: universal gas constant in Eq. (4.7)	(J/kgK)
R_{glob}: short wave radiation	(W/m²)
R_{ins}: thermal resistance of the insulation	(m^2K/W)
R_{se}: external surface resistance	(m^2K/W)
R_{si}: internal surface resistance	(m^2K/W)
R_{sky}: long wave sky irradiance	(W/m²)
R_t: net radiation	(W/m²)
R_w: thermal resistance of the wall	(m^2K/W)
S_r: degree of saturation	(m^3/m^3)
T: absolute temperature	(K)
T_b: basement indoor temperature	(K)
T_g: time-dependent effective ground temperature	(K)
T_o: outdoor air temperature	(K)
T_0: reference temperature	(K)
T_R: mean temperature of the slab	(K)
T_z: monthly average sub-floor temperature at a given depth z	(K)
T_i-T_s: temperature difference between the inside and the ground surface	(K)
T_R-T_S: temperature difference between the room and the soil	(K)
T_i: internal air temperature	(K)
Uf: U-value of floor	(W/m²K)
W: heat of wetting	(J/kg)

Greek symbols

α: soil surface albedo	(-)
γ_d: dry density	(kg/m^3)
γ_w: unit weight of water	(kg/m^3)
η: soil porosity	(m^3/m^3)
θ: volumetric moisture content	(m^3/m^3)
θ_a: volumetric air content	(m^3/m^3)
θ_Π: volumetric fraction of component Π	(m^3/m^3)
λ: thermal conductivity	(W/mK)
λ_e: "Earth" thermal conductivity	(W/mK)
λ_s: thermal conductivity of the solids	(W/mK)
λ_Π: thermal conductivity of component Π	(W/mK)
ρ_a: air density	(kg/m^3)

ρ_l: liquid density (kg/m^3)
ρ_v: vapor density (kg/m^3)

ω: annual frequency

$\Delta\Psi$: edge factor in Eq. (3.13) (W/m^{o}C)

Π: notation for product of multiplication

Φ: total potential for flow
Φ_L: phase lag in Eq. (3.9)

Chapter 1

Introduction

1.1 The significance of earth-contact heat losses

The total energy consumption in the UK is rising and much of this was linked, until recently, to a growing economy. While the ratio of energy use to Gross Domestic Product (GDP) has fallen in recent years, there is still plenty of scope for improving energy efficiency. Improvements can be made in every sector - domestic, industry, commerce, public sector and transport. The UK Government estimates that 30% of all UK energy consumption is wasted and much of this waste, worth £12 billion per year, could be eliminated by measures having little or no cost [1].
Buildings consume approximately 47% of the total delivered energy in the UK (see Figure 1.1 below).

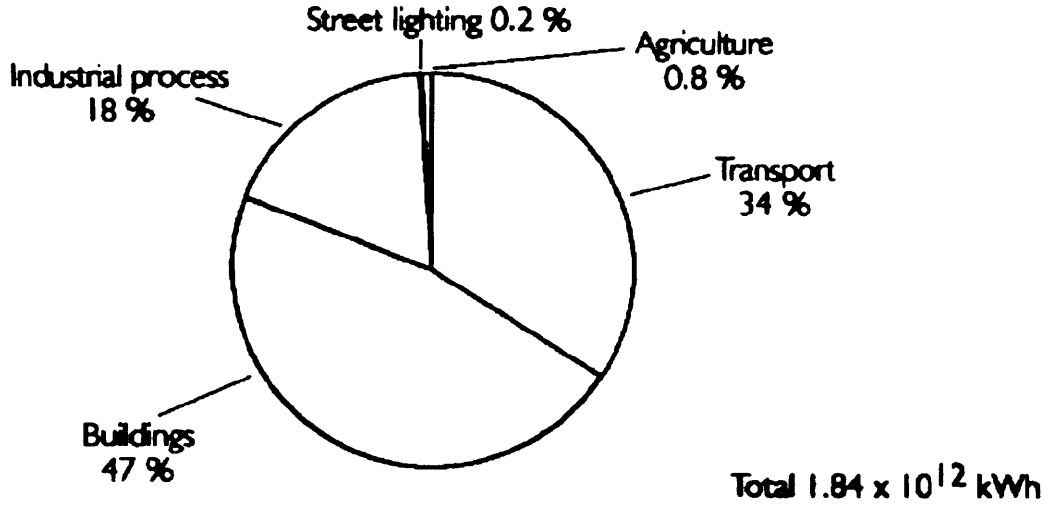

Figure 1.1: Total UK delivered energy use by sector in 2000 [1]

Of this total building energy use, 63% is used in domestic buildings (see Figure 1.2 below).

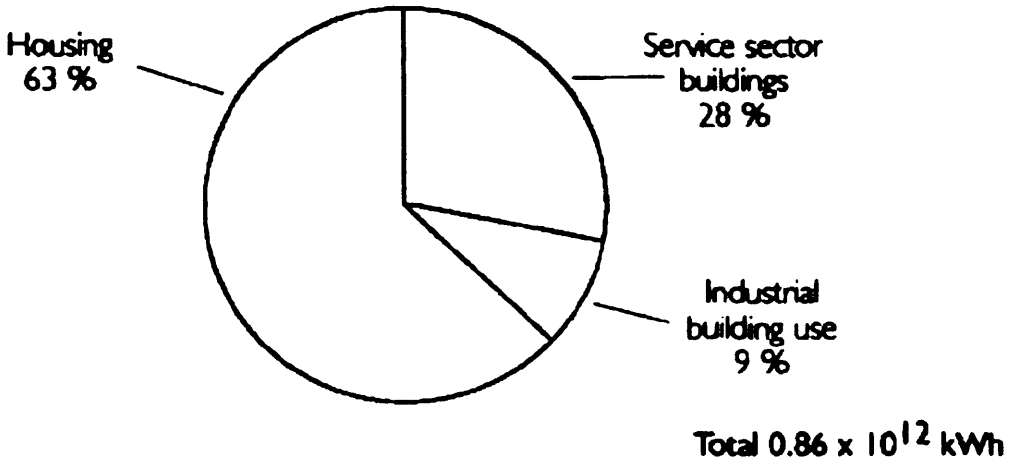

Figure 1.2: Total UK delivered energy use by building type in 2000 [1]

Energy consumption by building type in the service sector is shown in Figure 1.3 below:

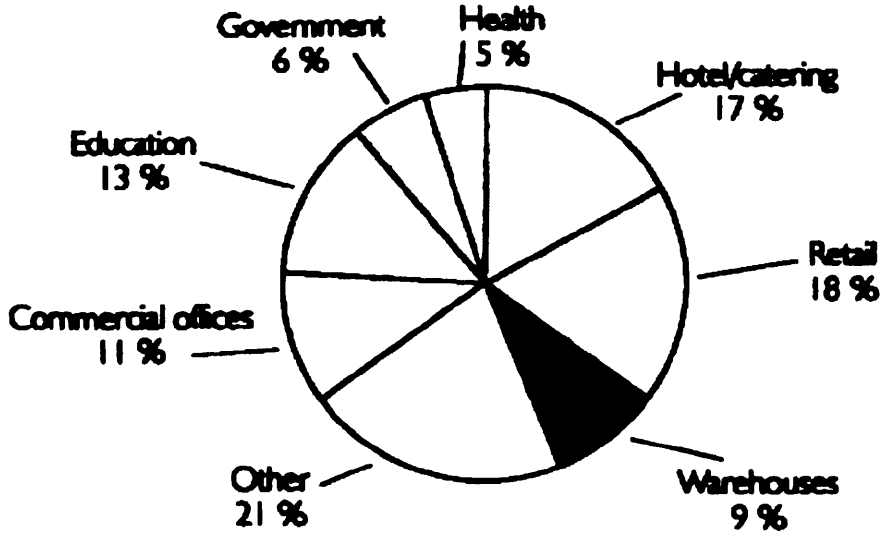

Figure 1.3: Service sector energy use by building type in 2000 [1]

The environmental impacts of energy use are numerous and they include detrimental effects from: extraction, production, transportation, storage, conversion and distribution. The final use of energy and disposal of waste products also have major environmental impacts. Particular areas of environmental concern in the energy sector include air quality, acid rain, coal mining subsidence, water pollution, maritime pollution, land use, contaminated land, visual impact, radiation, waste disposal and climate change [1].

Particularly as far as the term "climate change" is concerned, whenever fossil fuels are burned, carbon dioxide (CO_2) is emitted. This and other - so called - greenhouse gases, such as methane (CH_4), ozone (O_3) and nitrous oxide (N_2O), have been attributed to human-induced "climate change" that is likely to bring changes in global temperatures and rainfall levels and cause significant impacts to global weather systems, yielding extreme conditions, rising sea levels and crop failures. Furthermore, while fossil fuels are responsible for much of our carbon dioxide emissions, they are also responsible for several other airborne pollutants, such as carbon monoxide (CO), nitrogen dioxide (NO_2) and sulphur dioxide (SO_2) [1].
Figure 1.4 below shows the sources of carbon dioxide emissions in the UK, totalling 140 million tonnes of carbon per annum:

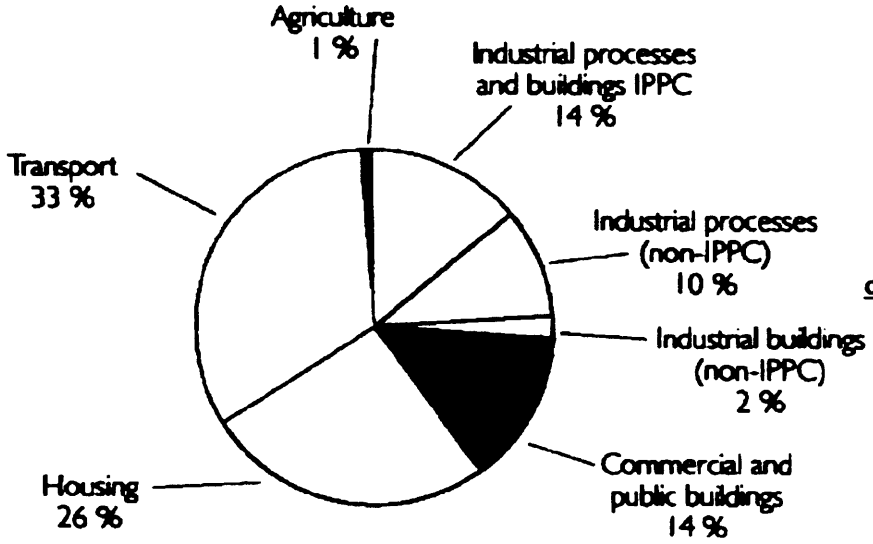

Figure 1.4: UK sources of carbon dioxide emissions [1]

As can be easily observed by the previous figure, industry, commerce and public buildings are responsible for 40% of all UK carbon dioxide emissions. Commercial and industrial buildings use substantial amounts of energy and electricity consumption has been increasing in recent years for some types of buildings. This has been explained by the increased use of information technology and associated air conditioning to remove internal heat gains. Improved building regulations, more efficient engineering systems, the application of in-passive cooling solutions and the move to thin screen technology for visual display units could help to restrain this rising trend [1].
Since the construction and operation of buildings in the UK consume almost half (1/2) of the delivered energy (see figure 1.1) and since it is acknowledged, as explained above, that, this high and continuously increasing energy demand has disastrous consequences for the environment, then energy conscious design and construction of structures, as well as, energy conservation measures, which will also provide the practical requirements for adequate indoor comfort levels, should be issues of major concern. The best time to introduce energy (and carbon) saving measures is when specifying, designing and constructing a new building. This, among others, provides the well briefed designer with the opportunity to make use of the building fabric to moderate energy needs and to reduce the heat demand by using insulation and air tight construction [1].

The UK Department of Energy suggests that, better design of new buildings could result in a 50% reduction in energy consumption and that appropriate design interventions could yield a reduction of 25% {[2], as found in [3]}. The major changes to the UK Building Regulations - firstly introduced in 2002 [4] and recently 'updated' (April 2006) [5] - which cover the conservation of fuel and power in (new) domestic buildings, aim at this direction. For example, the ongoing improvement of the insulating quality of the building envelope constitutes one of the most important developments in this particular field: this way, conductive heat losses are reduced. However, one part of the overall design process requires an evaluation of likely heat losses to the ground.

Till recently (1999), the focus of attention had been naturally directed at the thermal behaviour of the superstructure of buildings, like walls and roofs, since it was expected that, significant heat losses might, if no insulation was provided, take place [3]. However, the oil crisis in the early 1970s, did not only increase considerably the energy bills, but also had an influence on the perceived importance of heat transfer to the ground. Above-ground insulation of structures was improved and thus, thermal losses due to earth-contact became proportionally more important and could no longer be neglected. In a well documented survey carried out in the US {[6], as found in [3]}, it was suggested that a waste of about $5-$15 billion a year could be attributed to heat transfer to the ground. Another study {[7], as found in [3]} reported that, in Ohio, US, an un-insulated basement accounted for 67% of the total envelope load when the above-ground part of the building was well insulated. Furthermore, other studies claim that, in cold climates the heat loss to the ground might be responsible for up to one third (1/3) or even a half (1/2) of total heat losses {[8, 9], as found in [3] & [10], as found in [11]}.

There are, however, some other factors contributing to the growth in interest in ground heat transfer, which relate to novel construction, e.g. passive solar buildings and earth-sheltered buildings. Unconventional structures, such as these, are receiving more and more attention. The high thermal mass of the ground can be taken advantage of for heat storage and/or for moderating internal climate variations [3].

Consequently, nowadays, building heat loss via the ground has gained importance. At present, this form of heat loss can no longer be considered an insignificant part of the overall building heat loss, but it is recognised that significant heat losses may occur due to flow of heat from the inside of a building through the ground floor slab and into the foundation soils, too [3,12]. 'Building heat loss via the ground' has been the subject of numerous analytical, numerical and experimental investigations. Comprehensive literature surveys can be found in the works of: Janssen [12], Deru [14], Bahnfleth [15] and Hagentoft {[16], as found in [13]}. Furthermore, the studies of Hagentoft and Anderson {[16, 17], as found in [13]}, have recently been synthesised to form the European Standard EN ISO 13370: *"Thermal performance of buildings - Heat transfer via the ground - Calculation methods"*. This standard introduces several expressions for calculating building heat loss via the ground, appropriate for most foundation geometries and insulation strategies. It is clear, consequently, from the aforementioned that, adequate design and analysis of heat transfer and more specifically, heat loss to the ground, should be seriously taken into account.

1.2 Aim

The primary aim of the present work is to estimate the annual buildings ground floors heat losses by means of numerical simulations, using a one-dimensional (1-D) model. Given the three-dimensional (3-D) nature of the heat transfer through the ground, the annual ground floor heat losses will be first estimated using a 3-D model. Then, the specific model will be consecutively converted in the respective 2-D and 1-D models without changing anything as far as the various simulation parameters (see §5.1) are concerned. The only change, in order for this conversion to be achieved, will be made in the dimensions of the initial 3-D model (the conversion from the: 3-D to the 2-D and consecutively, from the: 2-D to the 1-D model, will be achieved by reducing the initial 3-D model's dimensions in the *X* and the *Y* axis to one meter). The resulting 1-D (and 2-D) model - which will normally differ from the initial 3-D in the results it derives - will be 'equalized' with it, so that, they both produce the same results as far as the annual ground floor heat losses are concerned. This will be achieved by changing the initial simulation parameters values (the ones initially defined during the 'construction' of the 3-D model).
Furthermore, since the various simulation tools, such as "TAS" thermal analysis software, generally simulate all heat transfer processes in one dimension - those through the ground included - and model the soil depth, in particular, to be equal to one meter, an estimation of the possibly introduced, in this 'methodology', errors will be made, by comparing the respective results derived from the 3-D & 1-D numerical models.

1.3 Methodology

The construction, simulation and, finally, 'equalization' of the numerical models (3-D, 2-D & 1-D) will be achieved using the "TRISCO" (version 10.0w - 2002) and "VOLTRA" (version 4.0w - 2003) thermal analysis programs, both products of the PHYSIBEL SOFTWARE. Therefore, a brief presentation of the two programs, as the one given below, is considered proper:

- **"TRISCO": Computer program to calculate 3D & 2D steady-state heat transfer in objects described in a rectangular grid using the energy balance technique [18]**

"TRISCO" is a thermal analysis computer program for steady state[1] heat transfer in three-dimensional rectangular objects consisting of different materials and submitted to different boundary conditions. The geometry is described with a list of rectangular blocks, which vertices lie on grid points of a rectangular grid. Materials and surface boundary conditions with different thermal properties are identified using separate colors. Each geometry block is part of either a material or a surface boundary condition region and has a reference to one of these colors. Node boundary conditions with fixed temperature or power are possible and can be placed in grid point locations. Also, since version 10.0w - the one used in this work - border face boundary conditions in the interface between two color regions with fixed temperature or heat flux are possible.
After input of geometry and thermal properties, a system of linear equations is calculated based on the energy balance technique and solved using a fast iterative method ("*finite difference method*"). Possible non-linear behavior is solved by use of different cycles of adjusted linear systems.

[1]: Under steady state conditions, the linear heat flux is constant (independent of time) and the temperatures on a part do not vary over time [19].

The RADCON module allows a more realistic simulation of the separate heat transfer by radiation and convection in enclosures and between material objects and the environment. Without the RADCON module, simplified combined convection and radiation is supposed, characterized by a global heat transfer coefficient.
Clear graphic and alphanumeric output containing temperatures and heat flows allow the thermal evaluation of the calculated problem.

- **"VOLTRA": Computer program to calculate 3D & 2D transient heat transfer in objects described in a rectangular grid using the energy balance technique [20]**

"VOLTRA" is a thermal analysis computer program for transient[2] heat transfer in three-dimensional rectangular objects. "VOLTRA" is an extension for time-dependent (transient) boundary conditions of the steady-state program "TRISCO". Also, additional phenomena can be studied: temperature dependent thermal properties (thermal conductivity and specific heat capacity) and the thermal influence of ventilation flows. The object modeling is completely identical as in "TRISCO". "TRISCO" data files can be taken as starting data in "VOLTRA" (as happened in this work).
The time-dependent boundary conditions are described with functions, either built-in functions based on variable parameters or external user-defined functions based on function values given at a fixed time interval. The thermal conductivity and specific heat capacity of any material can refer to temperature dependent functions.
"VOLTRA" allows creating time-dependent graphic animations of the temperature and heat flux field in the studied object. Alphanumeric lists of time functions of temperatures in individual nodes or heat flows through given surfaces through the object can be made. Graphs using the text output data can be drawn e.g. in Microsoft Excel.
Some additional information, concerning the program's: functions, materials thermal properties and calculation parameters, as well as the minimum system requirements, are presented in the attached Appendix A.

1.4 Outline of the work

Four main parts can be distinguished in this work. Chapter 2 will concisely analyze the ground heat transfer mechanisms. Specific attention will, furthermore, be given to the soil thermal properties which play a very important role on the heat transfer via the ground 'phenomenon': thermal conductivity and (volumetric) heat capacity.
The available calculation methods of building heat loss via the ground (simplified, analytical & semi-analytical, design guides and numerical methods) will be reviewed in Chapter 3. Particular mention of the design guides calculation methods will be made, as far as the cases in which each is best to be used are concerned.
In Chapter 4, the influence of soil stratification and ground water flow, as well as, of soil moisture transfer on buildings heat losses via the ground will be advanced. The fact that, the couplings between soil heat and soil moisture transfer cannot be assumed having a negligible influence will be highlighted and analyzed.
The most influential (soil) simulation parameters, as well as, the simulation study itself will be presented in Chapter 5, along with a validation of the used methodology, as far as its precision is concerned. Finally, in Chapter 6, the conclusions derived by the simulation study will be summarized.

---

[2]: Transient heat transfer analysis predicts the outcome when temperatures on a part vary over time [21].

Chapter 2

Ground heat transfer mechanisms and soil thermal properties

A sensitivity study [22] made on the results derived from the simulation of a 3-D numerical model of a test room showed that, the soil thermal conductivity is comparatively the most important parameter among those analysed, as far as the earth-contact heat transfer part of the overall simulation process is concerned. However, an increase in the values of the soil conductivity and heat capacity had opposite effects since a higher thermal conductivity led to higher heat losses while a higher thermal capacity (or density) led to greater heat storage.
In this chapter, a concise analysis of the ground heat transfer mechanisms will be made. Specific attention will be given to the above mentioned soil thermal properties, which play a very important role on the heat transfer via the ground 'phenomenon': thermal conductivity and (volumetric) heat capacity.

2.1 Ground heat transfer mechanisms

The transport of heat in porous media may be induced by several mechanisms. The three most influential mechanisms are conduction, convection and the transfer of heat due to water phase change, also known as latent heat of vaporisation. Radiation is often assumed to be negligible and excluded from formulations [3].
Heat conduction is a process whereby heat is transferred from one region of the medium to another, without visible motion in the medium. The heat energy is passed from molecule to molecule. According to Fourier's Law, the heat flux per unit area (q_{cond}) generated by conduction, may be written as [3]:

$$q_{cond} = -\lambda \nabla T, \qquad (2.1)$$

where: λ is the thermal conductivity of the medium, T is the temperature and ∇ is the gradient operator.

For example, consider a body of thickness d, bounded by two plane parallel and isothermal faces of temperatures T_1 and T_2, each of these faces having an area A. The lateral edges bounding the main faces of this body are assumed to be adiabatic (impermeable to heat transfer) and perpendicular to them. Suppose that the material form of which the body is made is stable, homogeneous and isotropic (or anisotropic with a symmetry axis normal to the main faces). In such conditions, the following relationships, derived from Fourier's law {Eq. (2.1)} under steady state conditions, apply if the thermal conductivity λ or thermal resistivity r is independent of temperature [23]:

$$\lambda = \frac{1}{r} = \frac{\Phi d}{A(T_1 - T_2)} = \frac{d}{R} \tag{2.2}$$

$$R = \frac{A(T_1 - T_2)}{\Phi} = \frac{d}{\lambda} = rd \quad , \tag{2.3}$$

where: Φ is the heat flow rate in: W (quantity of heat transferred to or from a system divided by time) and: R is the thermal resistance in: m^2K/W (temperature difference divided by the density of heat flow rate in the steady state condition).
Heat convection refers to the transport of heat in a fluid by means of circulation flows. Particle movement, therefore, exclusively induces convection effects. In soils, it is usually assumed that the soil structure (solid phase) is static and thus, convection effects are only attributed to liquid and vapour transport. The heat flux per unit area generated by liquid convection (q_{lconv}) is, then, given as [3]:

$$q_{lconv} = c_l \rho_l \vec{v}_l (T - T_0) \quad , \tag{2.4}$$

where: c_l is the specific heat capacity of soil water, ρ_l is the density of soil water, $\vec{v}_l$ is the vector of water velocity and T_o is the reference temperature. Similarly, the heat flux per unit area generated by vapour convection (q_{vconv}) can be written as [3]:

$$q_{vconv} = c_v \rho_l \vec{v}_v (T - T_0) \quad , \tag{2.5}$$

where: c_v is the specific heat capacity of soil vapour and $\vec{v}_v$ is the vector of vapour velocity.
Latent heat of vaporisation is used when taking into account heat transfer caused by the transport of vapour in the medium and arises due to phase change. The magnitude of this contribution to the overall heat transfer will be dependent on the quantity of vapour transfer occurring and can be relatively significant when dry conditions prevail. The classical theory for heat transfer expresses the heat flux (q_{lat}) due to this contribution as [3]:

$$q_{lat} = L_0 \rho_l \vec{v}_v \quad , \tag{2.6}$$

where: L_o is the latent heat of vaporisation at T_o.

Radiation occurs across air spaces (or within a transparent medium) by heat energy propagated as electromagnetic waves. The temperature of the radiating body is the most important factor, the flow of heat being proportional to the fourth power of the absolute temperature. In soils, radiation usually makes a negligible contribution to heat transfer. Its effect in sand, for example, is less than 1% of the overall heat transfer at normal atmospheric temperatures. On the other hand, radiation can play a significant part in heat transfer in dry, coarse, crushed-stone materials. For example, using a particle size of 20mm gravel, it has been shown that the effect of radiation could amount to 10% of total heat transfer at normal temperatures {[24], as found in [3]}.
Since radiation is assumed to be negligible, it is excluded from formulas. Therefore, the total heat transfer (q_h) may be defined as [3]:

$$q_h = q_{cond} + q_{conv} + q_{vconv} + q_{lat} \quad (2.7)$$

2.2 Soil thermal conductivity

The basic process of heat conduction has been described in the previous paragraph. The constant of proportionality that relates the rate at which heat is transferred by conduction to the temperature gradient in a material is known as the *"thermal conductivity"*. Its SI units are: W/mK and it is symbolized with the Greek letter *"lambda (λ)"*. Since, then, the soil thermal conductivity plays a very important role on the heat transfer by conduction via the ground, it is given some further consideration below [3].
The 'overall' (bulk) soil thermal conductivity of soil is dependent on the thermal conductivity of its individual components (solid, water, air). The thermal conductivity of the solid grains is much greater than that of water. Furthermore, the thermal conductivity of the air phase is much lower than the other components. It is clear, therefore, that any increase in the proportion of air in the void space of a soil can be expected to have a significant effect on its bulk thermal conductivity [3]. Table 2.1 below shows some typical thermal conductivity values of soil materials.

Substance	Thermal conductivity (W mK)	Specific heat capacity (J kg K)	Density (Kg m^3)
Quartz	8.79	2010	2660
Clay minerals	2.93	2010	2650
Organic matter	0.25	2512	1300
Water	0.57	4186	1000
Ice	2.18	1884	920
Air	0.025	1.256	1.25

[a] These values have been converted to SI units from the original reference.

Table 2.1
Thermal conductivity and heat capacity of some soil materials - [24], as found in [3] [a]

The soil volume fractions can be calculated from the following expressions:

$$f_1 = 1 - n \quad \text{(solid fraction)} \quad (2.8)$$

$$f_2 = nS_l \quad \text{(water fraction)} \quad (2.9)$$

$$f_3 = n(1 - S_l) \quad \text{(air fraction)} \quad (2.10)$$

where: η is the porosity of the soil and S_r is the degree of saturation[3] [26].
However, measuring accurately the soil thermal conductivity is not an easy task. Consequently, only scarce and in many cases, inaccurate data of soil thermal conductivity are available. As a response to this lack of fine data and to the arduous and costly procedure involved in acquiring measurement data, numerous predictive models have been developed, some of which are presented in Appendix B of this work [12].
As can be clearly concluded by the Eq. (B.15) & (B.18) of Appendix B, the soil thermal conductivity is implicitly dependent on the degree of saturation (or moisture content) of the soil. This is clearly an important parameter, whose influence on the heat transfer and, subsequently, the building heat loss through the ground, will be separately analyzed and presented in Chapter 4.

2.3 Soil (volumetric) heat capacity

It is well established that, the bulk thermal properties of soils are quite strongly dependent on the combined properties of their liquid, air and solid components {[3], as found in [28]}. This fact, does not apply only for the soil thermal conductivity, as shown in §2.2, but also for the soil (volumetric) heat capacity, as described below.
The 2-D transient (time dependent) form of the heat conduction is given by the following equation [28]:

$$\lambda\left(\frac{\partial^2 T}{\partial x^2}\right)+\lambda\left(\frac{\partial^2 T}{\partial z^2}\right)=\rho c\left(\frac{\partial H}{\partial T}\right)\left(\frac{\partial T}{\partial t}\right). \qquad (2.11)$$

where: H is the enthalpy, T is the temperature, t is the time, x and z are the Cartesian co-ordinates, λ is the soil thermal conductivity, c is the soil specific heat capacity and ρ is the soil density. The term ρc represents the soil volumetric heat capacity, 'C'. In effect, the specific heat capacity (c) defines the amount of energy stored in a material per unit mass per unit change in temperature (SI units J/kg K). Similarly, the volumetric heat capacity (C) defines the amount of energy stored in a material per unit volume per unit change in temperature (SI units J/m^3 K) [3, 28].
In the above Eq. (2.11), two independent thermal properties define the quantity of heat transferred, namely the soil thermal conductivity and the soil volumetric heat capacity. Therefore, the successful application of this equation for time dependent problems clearly depends upon the use of representative values for the specific material thermal properties [28].
As far as the volumetric heat capacity is concerned, the densities of the individual soil constituents dictate the magnitude of this parameter. Hence gaseous materials are less able to store thermal energy than liquid matter. The large thermal inertia of soils may allow thermal energy to be stored for some periods of time resulting in a time lag effect of heat transfer [28].
De Vries {[29], as found in [28]} provided the following approach for the determination of soil volumetric heat capacity:

$$C=\chi_s\rho_s c_s+\chi_w\rho_w c_w+\chi_a\rho_a c_a. \qquad (2.12)$$

[3] :Soil moisture saturation means that all voids are filled with water and thus, all surfaces are wetted; the degree of saturation represents the ratio of soil water volume to its voids volume - the sum of the soil water and air phase volumes [25]

where: the subscripts *s*, *w* and *a* refer to the solid, water and air phases, respectively. Therefore, c_s, c_w and c_a are the specific heat capacities, ρ_s, ρ_w and ρ_a, the densities and χ_s, χ_w and χ_a, the volume fractions, respectively, of each phase. As mentioned in §2.2, the volume fractions of a soil can be calculated from consideration of the soil porosity η (volume of voids/ total volume) and the degree of saturation S_r (volume of water/ volume of voids) {see Eq. (2.8), (2.9) & (2.10)}.

It is apparent from the above Eq. (2.12) that the soil volumetric heat capacity continues to increase as the water content increases. For many soils, the air phase occupies a relatively small proportion of the void space and has a small density. It is, therefore, often excluded from the above calculation. However, water vapour present in the voids can increase *c* and ρ and may need to be considered. The volumetric heat capacity of a soil having more than three constituents can be calculated by simply adding more terms into Eq. (2.12) [3, 28].

Some typical thermal properties for the constituents of a number of soils are summarised in the Tables 2.2 & 2.3 below:

Thermal properties of soil constituents at 20 °C and 1 atm

Material	Density (ρ) (kg m^{-3})	Specific heat (c) (J kg K)	Vol. heat capacity (C) (J m^{-3} K) × 10^6	Thermal conductivity (λ) (W m K)	Thermal diffusivity (δ) (10^{-6} m^2 s)
Quartz	2650	733	1.94245	8.4	4.3
Many soil minerals[a]	2650	733	1.94245	2.9	1.5
Soil organic matter[a]	1300	1926	2.5037	0.25	0.10
Water	1000	4187	4.187	0.6	0.142
Air	1.2	1005	0.001206	0.026	0.021

NB. These values have been converted to SI units from the original reference.
[a] Typical values.

Table 2.2
Thermal properties of soil constituents at 20°C and 1atm - [30], as found in [28] [a]

Material	Specific heat capacity (J kg K)	Density (kg m^{-3})
Quartz	799	2650
Kaolin	937	2600
Calcium carbonate	870	2710
$CaSO_4$	816	2450
Fe_2O_3	690	5240
Al_2O_3	908	3700
$Fe(OH)_3$	946	3600
Orthoclase	812	2560
Oligaclase	858	2640
Potash mica	870	2900
Magnesia mica	862	2900
Hornblende	816	3200
Apatite	766	3200
Dolomite	929	2900
Talc	874	2700
Granite	803	2600
Syenite	833	2700
Diorite	812	2900
Andesite	833	2400
Basalt	891	3000

Table 2.3
Specific heat capacity and density of selected materials - [31], as found in [3]

While in this Chapter a concise description of the ground heat transfer mechanisms and the most influential on the heat transfer via the ground 'phenomenon' soil thermal properties was made, the next Chapter - Chapter 3 - will deal with the available methods for the calculation of the heat losses from buildings through the ground.

Chapter 3

Methods for calculating heat losses from buildings through the ground

The basic problem of building heat loss via the ground is intrinsically more complex than heat loss through above grade building parts. The most significant reasons for this are:

- Heat loss via the ground is in essence a three-dimensional phenomenon,
- The large thermal inertia of the ground necessitates non-stationary calculations and,
- The ample variation in geometries and insulating strategies leads to large numbers of parameters to consider {[17], as found in [12]}.

Given the growing importance of ground floor heat losses, as described in Chapter 1 of this work, an increasing need for accurate calculation methods of building heat loss via the ground arises. For this purpose, simplified, analytical & semi-analytical, design guides and numerical methods-solutions can be used. In this Chapter, an outline of the aforementioned available calculation methods is made. Furthermore, as far as the design guides are concerned, the cases in which each is best to be used are cited.

3.1 Analytical and semi-analytical methods

Analytical methods[4] of heat transfer equations were the first available and generally assume some simplification of the problem [3]. Because of this fact, a number of outstanding problems cannot be considered within the framework of simple, analytical and semi-analytical methods, namely {[33], as found in [26]}:

- The spatial inhomogeneity of the thermal properties of the floor slab and ground;

[4]: Analytical models are mathematical models that have a closed form solution, i.e. the solution to the equations used to describe changes in a system can be expressed as a mathematical analytic function [32].

- The variation in time and location of the thermal properties of the floor and ground, mainly due to varying moisture content and ground types;
- The effect of the flow of ground water flow beneath the floor;
- The variation in the annual cyclic temperature pattern for different years and location.

However, in certain cases (simple configurations) these methods can be very powerful since they provide fast exact solutions. Semi-analytical methods are similar in the mathematical approach they use, but generally require a computer-based solution to be developed (e.g. to efficiently perform numerical integration) [3].

A number of solutions to the steady-state heat conduction equation can be found in the literature. For example, Latta and Boileau [34], as found in [3] analyzed a measured temperature profile in the ground surrounding a basement. During a winter period, it was observed that the flow of heat to the Earth's surface followed circular paths (see fig. 3.1 below). Knowing the thermal conductivity of the soil λ (W/m °C) and calculating the length of these paths (arcs) from a point in the below-grade wall, the heat loss Q_z (W/m^2) at depth z (m) was given by:

$$Q_z = \frac{T_i - T_s}{R_w + R_{ins} + (\pi z/2\lambda)}, \qquad (3.1)$$

where: T_i-T_s is the temperature difference between the inside and the ground surface, R_w is the thermal resistance of the wall and R_{ins} is the thermal resistance of the insulation.

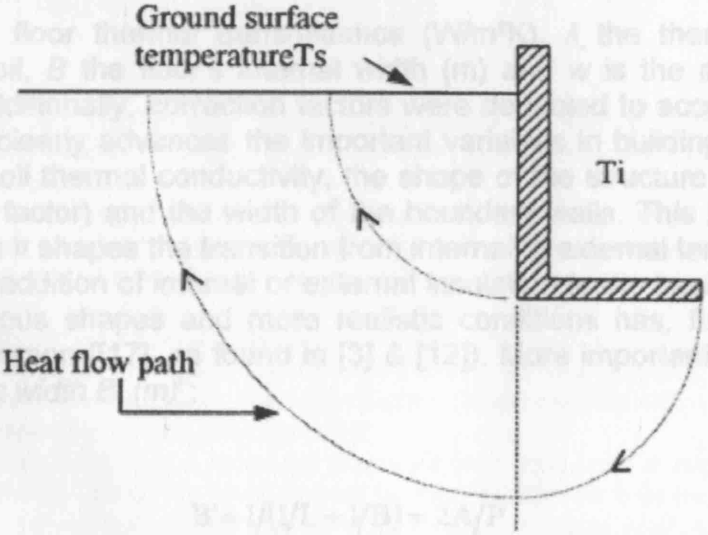

Figure 3.1 - Assumed heat flow paths {[33], as found in [3]}

The ASHRAE Guide {[35], as found in [3]} adopted this method and some modifications were included in 1985. However, some criticisms of the method have arisen:

- The method ignores heat loss to the ground at depth, which is a limitation for summer period calculations and,

- When the walls are partially insulated, the heat flow paths are no longer concentric as described, but have a shape somewhere between circular and vertical lines.

A semi-analytical method using Green's functions to solve a three-dimensional dynamic heat flow equation was presented by Kusuda and Bean {[36], as found in [3]}. The solution was provided in the following form for an insulated slab-on-grade floor:

$$Q = \frac{\lambda}{L}(T_R - T_z) \quad (3.2)$$

where: Q is the floor heat flux (W/m^2), λ the soil thermal conductivity (W/m °C), L the thickness of earth (m) and T_R is the mean temperature of the slab (°C). T_z is calculated by Green's technique and is the monthly average sub-floor temperature at a given depth z. An approximation was also included to take into account the effect of floor insulation.

Other work has focused on the determination of solid floor U-values. In general, this type of research utilises and develops work originally proposed by Macey {[37], as found in [3] & [12]}. Based on a circular arc approximation, he derived an analytical expression for the thermal transmittance of a non-insulated infinitely long floor:

$$U = \frac{2\lambda}{\pi B}\ln\left(\frac{2B}{w}+1\right) \quad (3.3)$$

where: U is the floor thermal transmittance (W/m^{2}K), λ the thermal conductivity (W/mK) of the soil, B the floor's internal width (m) and w is the above grade wall thickness (m). Additionally, correction factors were deducted to account for the finite length. Eq. (3.3) clearly advances the important variables in building heat losses via the ground: the soil thermal conductivity, the shape of the structure (B and the finite length correction factor) and the width of the boundary walls. This last parameter is also important, as it shapes the transition from internal to external temperature.

A method for the addition of internal or external insulation to the basic framework and extension to various shapes and more realistic conditions has, furthermore, been proposed by Anderson {[17], as found in [3] & [12]}. More importantly, he introduced the "*characteristic width B' (m)*":

$$B' = 1/(1/L + 1/B) = 2A/P \quad (3.4)$$

where: L, B, A and P (all in m) are the length, width, area and perimeter of a rectangular floor. The "*characteristic width B'*" tends to B, for: $L \rightarrow \infty$ and similarly to L, for $B \rightarrow \infty$. Anderson replaced B with B' in Eq. (3.3) and attained a good approximation of the exact expression for three-dimensional heat losses from rectangular floors [12]. Muncey and Spencer {[38], as found in [12]} had already confirmed that the same principle held for non-rectangular floors. Anderson {[17], as found in [12]} hence proposed to generalise any two-dimensional expression by replacing B with B'. A comparison with numerical data supported his proposal [12].

Recently, the methods and concepts of Hagentoft {[16], as found in [12]} and Anderson {[17] & [39], as found in [12]} have been combined in the European Standard EN ISO 13370: "*Thermal performance of buildings - Heat transfer via the ground - Calculation methods*".

A summary of some of the above methods along with some comments regarding their scope and limitations can be found in [3], Table 8, p.234.

3.2 Numerical methods

As opposed to analytical methods, numerical methods allow greater flexibility. Numerical simulations can represent:

- Almost any geometrical configuration,
- Transient or steady-state conditions,
- Heat flux or temperature boundaries (constant or time varying),
- User defined initial conditions,
- Multi-dimensional effects and,
- A variety of different material properties.

Of course, as a consequence of increased sophistication, potentially prohibitive computer run-times and reduced operability arises [3].
Numerical models [5] generally use either "*finite difference*" [6] or "*finite element*" [7] techniques (or some combination of both). Each method has its advantages and disadvantages. Perhaps the most significant aspects relate to the balance between the relatively fast solution times offered by the finite difference method and flexibility offered by the finite element method, in terms of its ability to easily accommodate irregular geometry, etc [3].

---

[5]: Numerical models are mathematical models that use some sort of numerical time-stepping procedure to obtain the models behaviour over time. The mathematical solution is represented by a generated table and/or graph [40].

[6]: Finite-difference time-domain (FDTD) is a popular computational electrodynamics modeling technique. It is considered easy to understand and easy to implement in software. Since it is a time-domain method, solutions can cover a wide frequency range with a single simulation run.
The FDTD method belongs in the general class of differential time-domain numerical modeling methods. Maxwell's equations (in partial differential form) are modified to central-difference equations, discretized and implemented in software. The equations are solved in a "leapfrog" manner: the electric field is solved at a given instant in time, then the magnetic field is solved at the next instant in time, and the process is repeated over and over again [41].

[7]: Finite Element Analysis (FEA) is a computer simulation technique used in engineering analysis. It uses a numerical technique called the finite element method (FEM). The finite-element method (FEM) originated from the needs for solving complex elasticity, structural analysis problems in civil engineering and aeronautical engineering Its development can be traced back to the work by A. Hrennikoff (1941) and R. Courant (1942). While the approaches used by these pioneers are dramatically different, they share one essential characteristic: mesh discretization of a continuous domain into a set of discrete sub-domains. Hrennikoff's work discretizes the domain by using lattice analogy while Richard Courant's approach divides the domain into finite triangular sub-regions for solution of second order elliptic partial differential equations (PDEs) [42].
Mathematically, the finite element method (FEM) is used for finding approximate solution of partial differential equations (PDE), as well as, of integral equations such as the heat transport equation. The solution approach is based either on eliminating the differential equation completely (steady state problems) or rendering the PDE into an equivalent ordinary differential equation, which is then solved using standard techniques, such as finite differences In mathematics, a finite difference is like a differential quotient, except that it uses finite quantities instead of infinitesimal ones [42].

3.3 Simplified methods

Simplified methods are generally derived from analytical, numerical or experimental calculations. As discussed previously, earth-contact heat transfer may be influenced by a number of factors (e.g. climatic data, thermo-physical properties, geometric configuration, insulation, etc.).
Therefore, methods which have necessary simplifications of the physical problem have limited applicability. However, within the context of their stated aims, e.g. to yield accurate calculations with a minimum of parameters, these methods have been found to provide useful information about the thermal performance of structures. Some of these methods are reviewed here [3].
Within the context of a comprehensive study of large earth-sheltered buildings at the University of Minnesota, a two-dimensional implicit finite difference model to simulate heat transfer to the ground was developed {[43], as found in [3]}. The model was used to calculate annual heating season and cooling season heat flows, Q, for various cases (insulation, slab-on-grade, basement, crawl-space configuration, etc.). The results obtained were simplified to the following regression equation {[7], as found in [3]}:

$$Q = B_0 + \frac{B_1}{R} + B_2(HDD/100) + B_3(CDD/100) + B_4\frac{(HDD/100)}{R} + B_5\frac{(CDD/100)}{R} + B_6(HDD/100)(CDD/100) + B_7R(CDD/100) \quad (3.5)$$

where: B_0-B_7 are tabulated coefficients for various configurations, R is the thermal resistance of the structure, *HDD* stands for heating degree-days and *CDD* stands for cooling degree-days. The coefficients B_0-B_7 alter if a different base temperature for degree-day calculation is used. A limitation of this method comes from the single set of soil thermal properties and the fixed indoor temperature used to develop the correlation. Further work on this approach has also been carried out {[44] & [45], as found in [3]}, where the temperature setting assumptions have been removed to allow a more general application of the technique.
A further method, known as the Decremented Average Ground Temperature method (DAGT), is also available {[46], as found in [3]}. This approach takes into account the change of ground temperature due to the heat loss from the building. A finite difference program was used to compute the heat flow to the ground and the results obtained were used to determine the following expression:

$$Q = F_d U A (T_R - T_S) \quad (3.6)$$

where: U is the U-value of the wall (W/m^2 °C), A the wall area (m^2) and T_R-T_S is the temperature difference between the room and the soil (°C). The coefficients F_d are tabulated "*decrement factor*" values and are given as functions of soil thermal conductivity and wall thermal resistance. This method applies only for entirely underground walls and is not applicable to floors.

In 1983, Mitalas presented a detailed method for predicting the heat loss from basements and slab-on-grade floors {[47] & [48], as found in [3]}. It was one of the first methods to allow the determination of heat transfer to the ground at any time of the year. Underground walls and floors were divided into five segments and the total heat flow was estimated by summing the losses of the different zones Q_n (n = 1-5) using "linking" factors. Q_n was expressed as follows:

$$Q_{n,t} = Q_{m,n} + Q_{A,n,t} \sin\frac{2\pi t}{12}, \tag{3.7}$$

where: Q_m is the annual heat loss (W/m^2), Q_A is the annual amplitude of the heat loss (W/m^2) and t is the time. Two- and three-dimensional finite element models were used to compile tables of heat loss factors for a variety of configurations (insulation, foundation type). Experimental data were used to validate the approach.
Yard et al. {[49], as found in [3]} presented a two-dimensional finite element analysis applied to simulate heat losses from a basement. Expressions were developed in terms of non-dimensional parameters. As with Mitalas' theory, the ground temperature was assumed to be a sinusoidal function of time and heat loss from the basement can be determined at any time of the year. The total heat flow to the ground was calculated from the sum of the floor (f) and the wall (w) components:

$$Q = U_f A_f (T_b - T_{g,f}) + U_w A_w (T_b - T_{g,w}), \tag{3.8}$$

where: A is the floor area (m^2), T_b is the basement indoor temperature (°C) and T_g is the time-dependent effective ground temperature (°C). Relations were given for the calculation of U-values U_f and U_w (W/m^2 °C). These were expressed as functions of the soil conductivity, insulation configuration and basement depth.
Using the Interzone Temperature Profile Estimation technique (ITPE), in which the ground, slab or basement is divided into several zones of rectangular shape, a simplified method for heat loss calculations from both slab-on-grade and basements has been presented recently {[50], as found in [3]}. Non-linear regression was used to develop an expression for heat loss from the foundation to the ground where Q (W/m^2) varies sinusoidally with time and is written as:

$$Q = Q_m + Q_a \cos(\omega t - \Phi_L), \tag{3.9}$$

where: Q_m is the mean annual heat loss (W/m^2), Q_a is the annual amplitude (W/m^2), ω is the annual frequency and Φ_L is the phase lag between heat loss and soil surface temperature. These three coefficients are taken as functions of soil properties, foundation dimensions, insulation U-values and configuration, indoor air temperature and ground surface temperature.

3.4 Design guides

The design guides presented below are generally based on research undertaken with specific end-users in mind. They are typically coordinated by organizations representing practitioners; for example, the American Society of Heating

Refrigeration and Air Conditioning Engineers (ASHRAE) or in the UK, the Chartered Institution of Building Services Engineers (CIBSE) [3].
The method presented in the ASHRAE Handbook {[35], as found in [3]} is probably one of the most widely used and is based on the work of: Boileau, Latta and Wang {[34] & [51], as found in [3]}. For basements, tables provide heat loss values for one type of soil conductivity (1.38 W/m °C) according to various depths, path lengths and insulation. For slab-on-grade floors, the heat flow to the ground is given as:

$$Q = F_2 P (T_i - T_o) \quad , \tag{3.10}$$

where: P is the perimeter of the exposed edge of floor (m), T_i and T_o are, respectively, indoor and outdoor temperatures and F_2 are tabulated heat loss coefficients, provided for different insulation/wall configurations (W/m °C).
In the UK, the CIBSE Guide [52] is one of the primary guidance documents and is essentially based on Macey's steady-state formula {[37], as found in [3]}. It is only valid for non-insulated rectangular slab-on-grade floors. The following expression gives the floor U-values (W/m^2 °C):

$$U = \frac{2\lambda_e}{1/2b\pi} \arctan h\left(\frac{1/2b}{1/2b + 1/2w}\right) \exp\left(\frac{1/2b}{l_f}\right) \quad , \tag{3.11}$$

where: λ_e (W/m °C) is the "Earth" thermal conductivity, b and l_f are, respectively, the breadth and the length of floor (m) and w is the thickness of wall (m). The CIBSE Guide describes modification of the above equation to include insulation.
The French Guide, published by the "*Association des Ingénieurs de Climatisation et de Ventilation de France*" (AICVF), gives expressions for the calculation of heat losses from floors and walls in contact with the ground. In all cases the heat flow Q (W) is written as [3]:

$$Q = K_s L (T_i - T_o) \quad , \tag{3.12}$$

where: L is the length of the exposed edge, T_i is the indoor temperature, T_o is the outdoor temperature and K_s (W/m °C) is a coupling coefficient, which depends on the configuration (floor or wall), the depth, the thickness, soil and basement thermal conductivities and convective coefficients. For each case, an expression is given for calculating K_s values.
The European Standard: *BS EN ISO 13370* {[53], as found in [3]} is the most detailed of those dealt with in this Chapter and accommodates a large number of configurations. The general formulation for the calculation of U-values (W/m^2 °C) is as follows:

$$U = U_0 + 2\Delta\Psi / B' \quad , \tag{3.13}$$

where: U_o is the basic thermal transmittance of slab-on-grade floor (W/m^2 °C), $\Delta\Psi$ is an edge factor (W/m °C) and B' is the characteristic dimension of floor (m). The procedure requires calculation of the U_o, ignoring edge insulation but, including any overall insulation. Then the edge factor, $\Delta\Psi$, is calculated for either horizontal or vertical edge insulation. $\Delta\Psi$ is described in the Standard as a correction factor

related to the detail of the floor edge. The procedure for its determination is fully described in the Standard.
Amongst the group of design guides available, the new European Standard appears to be the most detailed and flexible. However, the ASHRAE method is the most widely used, although there are potential problems associated with summer basement predictions using this method. Whilst the CIBSE method is limited to floors, the French AICVF method is more generally applicable. These guides remain critically important in practice as they define thermal requirements in construction [3].
The results derived from the analysis of three case studies [54], using some of the established design guides mentioned above, showed that, such simplified calculation procedures may significantly over or under-estimate the actual value of heat loss (by up to 31% in the studied cases).
This is perhaps understandable if one considers that the fundamental aim of the simplified calculation procedures is to provide a rapid estimate of ground heat transfer. So, because of this, all the parameters and processes involved in earth-contact heat transfer cannot be taken into account in such simplified algorithms. On the other hand, when it is not possible to use design guides (e.g. basements using CIBSE or complex configurations, like the BRE building case described in [54]), the alternative is to use analytical or numerical models. Nevertheless, design guides may well be considered for relatively simple cases. However, the choice approach to be used to calculate ground heat losses is clearly not straightforward. The following circumstances may help the decision making process:

- Soil thermal properties not known: use ASHRAE [35].
- Earth-contact through basement: CIBSE [52] does not apply.
- Heated slab-on-ground floors; ASHRAE considers four pre-determined cases only. Numerical tools are more appropriate.
- Non uniform wall insulation: use ASHRAE, Krarti's method [50] or numerical tools.
- Monthly heat loss required: use CEN [55], Krarti's method or numerical tools.
- Hourly outcome required: use numerical tools.

Chapter 4

The influence of soil stratification, ground water flow and soil moisture on buildings heat losses via the ground

4.1 The influence of soil stratification and ground water flow

In the previous Chapter, a concise outline of the available calculation methods of building heat loss via the ground was made. Summarily, it can be concluded that the knowledge on the essential issues concerning this field is fairly well developed and that appropriate calculation methods exist for most common geometries and insulating strategies. However, two substantial deficits of the research domain have already been mentioned [12]:

- Certain geometric topics have not been adequately studied yet: Combinations of ground floor and basement, effects of nearby buildings, thermal bridging and,
- The available research results remain fairly dispersed and isolated: Integration and validation of the numerous different contributions is necessary.

Other less studied - but possibly important - topics in the field of ground heat loss are [12]:

- The influence of soil stratification: The ground domain is commonly stratified, and cannot be assumed homogeneous. Stratification leads to differing thermal conductivities, which will affect the heat loss via the ground and,
- The effect of ground water flow: The heat lost to the ground domain will heat up any eventual ground water. The flow of ground water will hence result in a simultaneous drain of heat, affecting the foundation heat loss.

Krarti and Gabbard {[56], as found in [12]} studied the heat loss from a partially insulated ground floor, situated on a layered ground domain and they found that, stratification of the soil domain (two or five layers with different thermal conductivities) did affect the steady state heat losses through the floor. Hagentoft {[16], as found in [12]} analysed a similar problem, assuming a granite layer (conductivity: 3.5 W/mK, soil conductivity: 1.5 W/mK), present at a certain depth *H* under the ground floor. He demonstrated that, a weighting procedure for the steady state losses produces a quite accurate approximation of the exact results: based on the thermal properties and the dimensions of floor and soil layers, a weighted average between two extremes (H = 0m and H = ∞m) was calculated.
Delsante {[57], as found in [12]} examined the influence of water table depth on steady state heat losses through a ground floor and observed significant heat loss rises when the water table neared the floor.
To conclude, the knowledge on the particular effects of stratified soil and ground water flow is not fully complete. However, the contributions of Hagentoft {[16] & [58], as found in [12]} mainly, have introduced appropriate procedures to quantify their influence, which, nevertheless, should not be generalised for other geometries and insulating strategies.

4.2 The influence of soil moisture transfer

4.2.1 Is the hypothesis: "*The influence of soil moisture on buildings heat losses via the ground is generally negligible*", valid?

Most of the existing research work on foundation heat loss is based on one important hypothesis: "the couplings between soil heat and soil moisture transfer can be assumed having a negligible influence". For example, most of the authors referenced above, assume soil thermal conductivity and soil thermal capacity constant in space and time, ignoring their dependence on soil moisture content. Furthermore, a fixed surface temperature is generally imposed as external boundary condition or it is assumed that, surface heat transfers are governed exclusively by the air temperature in combination with a constant surface heat transfer coefficient. Additional heat transfer phenomena, as short and long wave radiation, evaporation or condensation, are usually not accounted for. Finally, usually only conduction is considered as the only soil heat transfer mechanism [12].
However, the following phenomena are not accounted for [13]:

- The soil thermal conductivity and capacity are highly dependent on soil moisture content,
- The transfer, storage and/or phase change of moisture result in a concurrent transfer and/or storage of sensible and/or latent heat and,
- Evapo-transpiration forms an integral part of the surface heat balance.

The primary reason for the above mentioned hypothesis is that, constant soil thermal properties, heat transfer by thermal conduction only and a fixed or linear surface balance reduce the coupled, non-linear problem of soil heat and moisture transfer to a common linear problem of thermal conduction. This simplification makes analytical solutions and simple numerical schemes for the simulation of the heat transfer between buildings and the ground acceptable [12]. Is it valid, however?

Janssen [12] studied the influence of couplings between soil heat and soil moisture transfer. Results derived from coupled and uncoupled simulations of building heat losses via the ground were compared and significant deviations were observed: it was shown that an uncoupled calculation of the foundation heat loss could yield underestimations of up to 15% for the heating season heat losses, 10% for the steady state thermal permeances and 20% for the periodical thermal permeances. Obviously, such differences cannot be regarded as insignificant. Thus, the influence of soil moisture transfer on building heat losses via the ground has been proved to be non-negligible and so, the above mentioned hypothesis is not completely valid.
Given the importance of the couplings between soil heat and soil moisture transfer on building heat losses via the ground, special mention of it is made in the following paragraphs of the present Chapter. First, though, a brief presentation of the ground water content changes and their influence on soil heat transfer will be made, followed by the outline of the moisture and heat migration processes in soils. Since the moisture migration processes are governed by the soils hydraulic properties, the latter will be concisely discussed, too. For similar reasons, the moisture and heat balance at the soil surface will be analyzed, since it affects the couplings between soil heat and moisture transfer.

4.2.2 The influence of ground water content changes on heat transfer

As stated in Chapter 2, the thermal properties of soils are fundamentally linked to the properties and proportions of their individual constituents (water/air/solid). From these considerations it is clear that, the moisture content of a soil is an important factor contributing to the average thermal properties of the bulk material (see fig. 4.1 below).

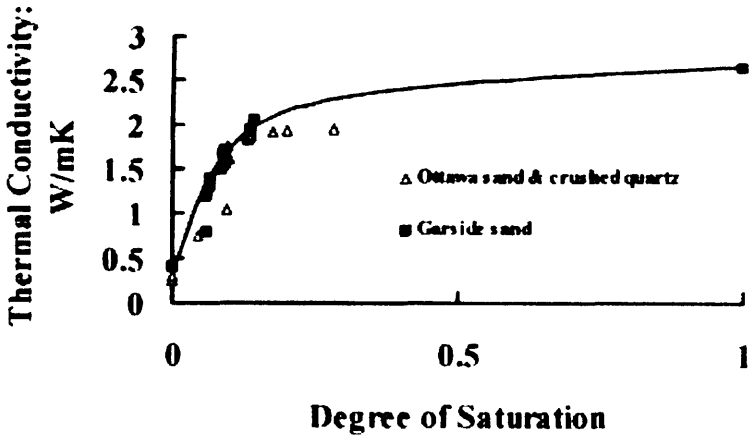

Figure 4.1 - Thermal conductivity as a function degree of saturation - [59], as found in [3]

A variety of circumstances can lead to changes in the ground water regime near buildings [3]. For example:

- Precipitation: Depending on local conditions (cover/slope, etc.) some rainfall is lost as runoff and some will percolate into the ground, changing the water content of the soil,
- Evaporation: Severe drying and possible shrinkage cracking of soils can occur depending primarily on temperature and wind speed,
- Transpiration: Soil moisture deficit can be caused by vegetation demands,

- Alteration to existing vegetation: Removal of established trees can change local ground water content profile quite significantly,
- Construction/demolition/ground works,
- Ground water abstraction for potable or industrial supply,
- Changes in ground water level: Natural or anthropogenic and,
- Buried services: The presence of water supply systems, sewerage networks, distributed heating systems, etc. will all have some affect on ground water conditions.

The occurrence of such phenomena may lead directly to a change in the thermal conductivity of the ground beneath or adjacent to a building and can therefore be expected to have some contribution to the ground heat transfer processes that occur. Under uncoupled (soil moisture and heat transfer) saturated conditions, the bulk soil thermal conductivity will be at its highest: a saturated soil will conduct heat at a faster rate than the unsaturated material (see Chapter 2 - §2.2). If the ground water is static, then attention need only be placed on obtaining a reasonable estimate of bulk soil thermal conductivity and standard design procedures may suffice. However, in some cases reasonably high flow rates may occur which have the potential to create a heat sink - with heat being transferred from the source into the water course and dissipated at some distance from the structure, this also depending on the permeability of soils, which defines the ground water flow rates and so, the ability of the water to "convect" heat [3].

Notwithstanding the importance of the saturated conditions, the ground beneath and adjacent to many earth-contact structures is likely to be unsaturated much of the time. The region of soil that lies between the water table and the soil surface is referred to as the "*unsaturated zone*". In this region the soil moisture content is dictated by capillary and gravitational forces (see §4.2.3.2 below), in addition to the usual influence of climatic boundary conditions. The soil in this region may therefore include a significant air phase and its degree of saturation will vary with depth - increasing to approximately 100% at the water table. Analysis of the moisture transfer in the near surface zone will require solution of an unsaturated flow equation, which in turn will require the determination (or estimation) of a number of hydraulic properties of the soil [3, 26]. These two specific topics - moisture transfer in soil and soils hydraulic properties - are discussed below.

4.2.3 Moisture transfer in soil

The moisture transfer equation, which will be used for the derivation of the soil heat transfer equation, is discussed below [12].

4.2.3.1 Conservation of mass

The total mass of water per unit volume of the soil medium is:

$$\rho_l \theta + \rho_v \theta_a \qquad (4.1)$$

where: ρ_l is the liquid water density, θ the volumetric moisture content (m^3/m^3), ρ_v the vapor density (kg/m^3) and θ_a the volumetric air content (m^3/m^3).

Mass conservation results in:

$$\frac{\partial}{\partial t}(\rho_l\theta + \rho_v\theta_a) = -\nabla q_m \quad , \tag{4.2}$$

where: t is the time (s) and q_m the total moisture flow (kg/m²s).

4.2.3.2 Transfer of moisture

The transfer of moisture takes place both in the liquid and the gaseous (vapor) phase. Buckingham's-Darcy's law {[60], as found in [3]} is assumed valid for the description of the liquid transfer. Fick's law can be applied for the transfer in the vapor phase, if diffusion is the only vapor transfer mechanism [12]:

$$q_m = q_l + q_v = -\rho_l K\nabla(\psi + z) - D_v\nabla\rho_v \quad , \tag{4.3}$$

where: q_l is the liquid flux (kg/m²s), q_v vapor flux (kg/m²s), K the hydraulic conductivity of the soil matrix (m/s), z the vertical coordinate (m, positive upward) and, D_v is the effective molecular diffusivity (m²/s).
The simplest and most obvious mechanism inducing liquid transport is isothermal liquid water flow, due to a potential gradient. In unsaturated media this mechanism will cause flow to occur from a zone of greater potential to a zone of lesser potential. The Buckingham-Darcy law {[60], as found in [3]} states that:

$$\bar{v}_l = -k_l\nabla\Phi \tag{4.4}$$

where: $\bar{v}_l$ is the liquid velocity, k_l is unsaturated hydraulic conductivity and Φ is the total potential for flow. The total potential is made up from contributions of several smaller potentials. The three most relevant of these were defined by Yong and Warkentin {[60], as found in [3]}, as follows:

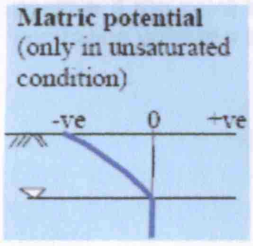

- The capillary (or matric) potential[8]: the work required per unit distance to transfer a unit quantity of soil solution from a reference pool at the same elevation and temperature as the soil, to a point in the soil:

$$\psi_c = \frac{u_w - u_a}{\gamma_w} \tag{4.5}$$

where: u_w is the pore water pressure, u_a is the air pressure and γ_w is the unit weight of water.

[8]: **Matric potential (only in unsaturated condition)** of soil water results from the capillary and adsorptive forces due to the soil matrix. These forces attract and bind water in the soil and lower its potential energy below that of bulk water. Matric potential is expressed negatively; the term matric suction has been used as the absolute value of matric potential. In saturated soil the matric potential is zero [61].

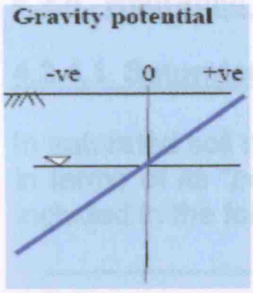

- The gravitational potential [9]: the work required per unit distance to transfer water from the reference elevation to the soil elevation. The gravitational potential may be given as:

$$\psi_g = -\rho_l g h \tag{4.6}$$

where: g is the acceleration due to gravity, h is the height from the reference elevation and ρ_l is the unit mass of water.

- The osmotic potential[10]: the work required per unit distance to transfer water from a reference pool of pure water to a pool of soil solution at the same elevation, temperature, etc:

$$\psi_o = n_{salt} R_g T c_{salt} \tag{4.7}$$

where: n_{salt} is the number of molecules per mole of salt, R_g is the universal gas constant (J kg^{-1} K^{-1}), T is the absolute temperature and c_{salt} is the concentration of salt.

In most mathematical formulations for liquid transfer, it is usually the case that, for simplicity and because of its magnitude, the osmotic potential is neglected and the total potential is assumed to be equal to the sum of the capillary and gravitational potentials.

---

[9]: **Gravitational potential** of water at each point is determined by the elevation of the point relative to some arbitrary reference level. This is negative if the point in question is below the reference point and positive if the point is above the reference point. Gravitational potential energy of mass m of water occupying volume v is [61]:

$$E_g = mgz = \rho_w vgz \qquad \frac{kg}{m^3} m^3 \frac{m}{s^2} m = N.m = J$$

Gravitational potential head (energy per unit weight) is:

$$h_g = \frac{E_g}{mg} = z$$

[10]: **Osmotic Potential** [61]:

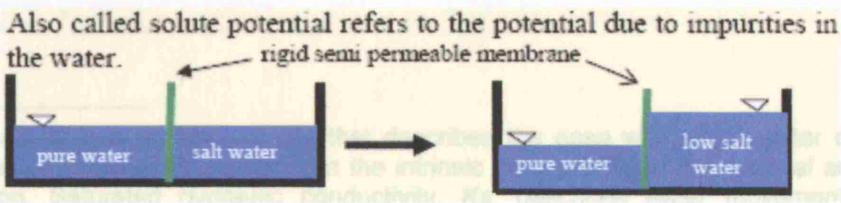

4.2.4 Hydraulic properties of soils

4.2.4.1 Saturated and unsaturated hydraulic conductivity

In saturated soil mechanics, it is usual to refer to the hydraulic conductivity k_l of a soil in terms of its "*permeability*" (SI units: m/s). Typical values of soils permeability are included in the following Table 4.1 [3]:

Soil type	Permeability, k_l (m/s)
Gravel	$k_l > 10^{-2}$
Clean sand	$10^{-2} > k_l > 10^{-5}$
Silt	$10^{-5} > k_l > 10^{-8}$
Fissured clay	$10^{-4} > k_l > 10^{-8}$
Intact clay	$k_l < 10^{-9}$

Table 4.1 - Saturated permeability - [62], as found in [3]

In general, a single value is often used to represent the saturated state of the soil. However, heterogeneity and other factors can cause significant variations in permeability even within a fully saturated soil.
On the other hand, the hydraulic conductivity[11] of an unsaturated soil is more difficult to define. Moreover, a single value of hydraulic conductivity is not adequate to describe unsaturated flow, mainly due to the fact that, the ability of a soil to transmit water is strongly dependent on its water content. In addition, when the soil is in an unsaturated state, there is a capacity for the amount of water stored within the pore space to change. This aspect of the hydraulic response of an unsaturated soil is described via the use of the "*specific moisture capacity*" and is strongly dependent on the soil moisture content [3]. The most well known mathematic relationships for the estimation of the "*unsaturated hydraulic conductivity*" are summarized in [3] - §7.3, pp.246-248.

4.2.4.2 Water retention curves

Let's consider an unsaturated soil in which water is flowing under suction (or matric potential). At any given suction, there is some water remaining in the soil pores, i.e., the soil has a certain water content. This water content is a function of soil type, structure, organic mater content, etc. Therefore, the water content will vary by soil type. In fact, it can actually vary within a soil type of different structure caused by the type of mechanical operations taking place on the soil. The relationship between water content versus suction (or matric potential) is called the "*soil water characteristic curve*" or "*soil water retention curve*". Examples of "*water characteristic curves*" for various soil types are given in the figures 4.2-4.4 below [61]:

[11]: Hydraulic conductivity is a property of soil that describes the ease with which water can move through pore spaces or fractures. It depends on the intrinsic permeability of the material and on the degree of saturation. Saturated hydraulic conductivity, *Ks*, describes water movement through saturated media [63].

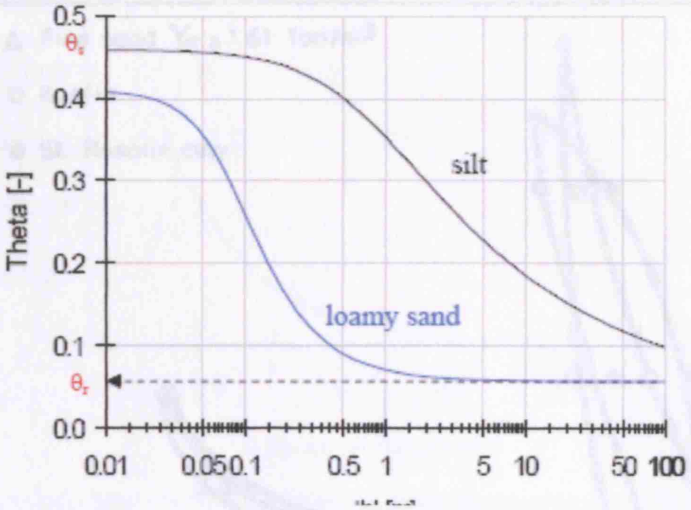

Figure 4.2 - Water retention curve [61]

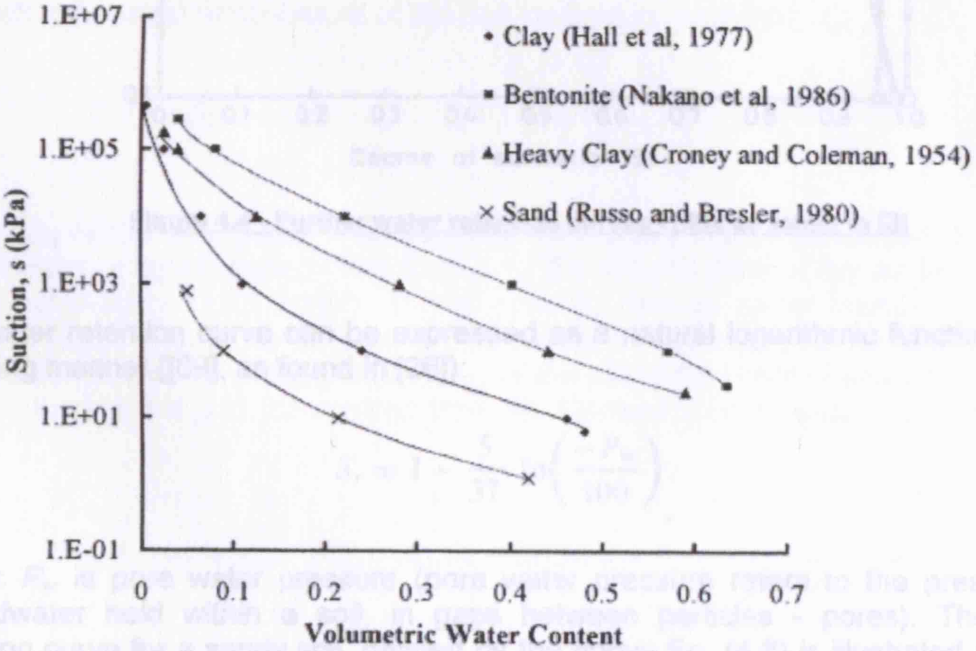

Figure 4.3 - Typical water retention curves {[64]-[67], as found in [3]}

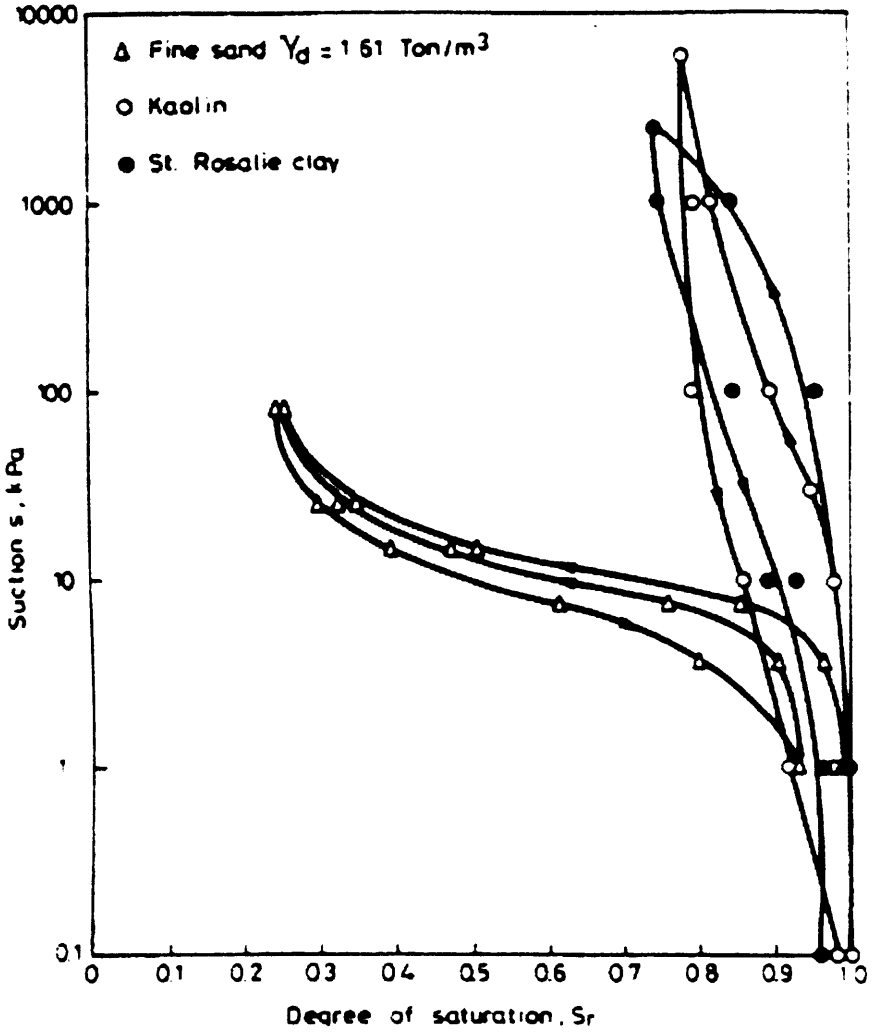

Figure 4.4 - Further water retention curves - [68], as found in [3]

The water retention curve can be expressed as a natural logarithmic function in the following manner {[69], as found in [26]}:

$$S_r = 1 - \frac{S}{37} \ln\left(\frac{P_w}{100}\right), \tag{4.8}$$

where: P_w is pore water pressure (pore water pressure refers to the pressure of groundwater held within a soil, in gaps between particles - pores). The water retention curve for a sandy soil, defined by the above Eq. (4.8) is illustrated in figure 4.5 in the following page:

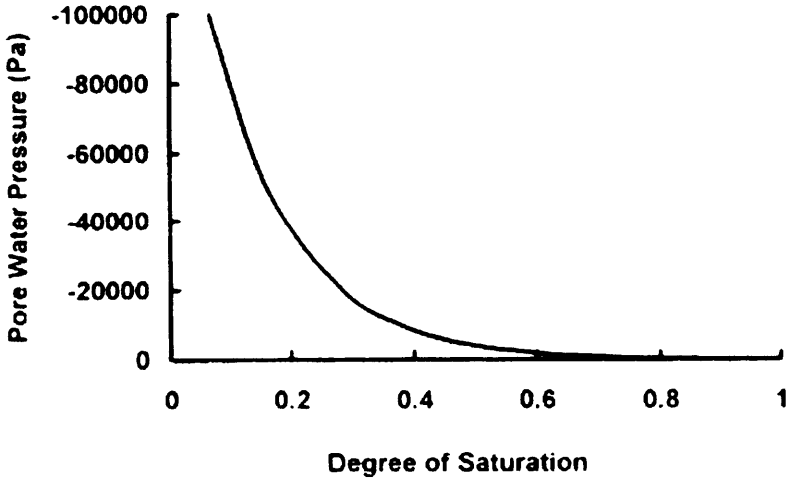

Figure 4.5 - Degree of saturation vs pore water pressure [26]

4.2.5 Heat transfer in soil

While in §4.2.3 the outline of the moisture transfer in soil was made, the respective 'phenomenon' for heat will be dealt with in this one.

4.2.5.1 Conservation of energy

The bulk volumetric heat content of the soil medium is given by [12]:

$$(C_d + c_l\rho_l\theta + (c_a\rho_a + c_v\rho_v)\theta_a)(T - T_0) + L_0\rho_v\theta_a - \rho_l\int_{t_0}^{t} W\frac{d\theta}{d\kappa}d\kappa \quad (4.9)$$

where: C_d is the volumetric heat capacity of the dry soil material (J/m³K), c_l the specific heat of liquid water (4180 J/kgK), c_a the specific heat of dry air (990 J/kgK), ρ_a the air density (1.23 kg/m³), c_v the specific heat of water vapor at constant pressure (2050 J/kgK), T_0 an arbitrary reference temperature, L_0 the latent heat of vaporization of water L at temperature T_0, W the differential heat of wetting (J/kg) and t and t_0 the current and the starting time (s). Conservation of energy then leads to [12]:

$$\frac{\partial}{\partial t}\left[(C_d + c_l\rho_l\theta + (c_a\rho_a + c_v\rho_v)\theta_a)(T - T_0) + L_0\rho_v\theta_a - \rho_l\int_{t_0}^{t} W\frac{d\theta}{d\kappa}d\kappa\right] = -\nabla q_h \quad (4.10)$$

where q_h is the total heat flow (W/m²).

4.2.5.2 Transfer of heat

Heat can be transferred through the porous medium both by conduction and as sensible and latent heat linked to moisture transfer in the liquid and vapor phase. Macroscopic heat transfer by advection[12] with the soil air is assumed negligible. The total heat flow through the soil medium is hence represented by [12]:

$$q_h = -\lambda^* \nabla T + c_l (T - T_0) q_l + (c_v (T - T_0) + L_0) q_v \quad (4.11)$$

in which λ^* is the bulk medium's thermal conductivity (W/mK). Note that, λ^* stands for the thermal conductivity of the soil medium in the hypothetical case that no moisture movement occurs.

4.2.6 "*Atmospheric excitation*" at the soil surface

As already mentioned (see §4.2.1), in most research on building heat loss via the ground the heat transfer at the surface is usually believed driven by the air temperature, habitually combined with a constant surface heat transfer coefficient. However, an even more complete description of the surface heat balance should include convection, short and long wave incoming radiation and transfer of latent and sensible heat by evaporation and precipitation. Furthermore, as a completely coupled analysis of ground heat loss involves the moisture transfer as well, "*atmospheric excitation*" should, moreover, include the surface moisture balance, which is made up by evaporation and precipitation. The effects of vegetation and seasonally surface cover (e.g. snow) should also be taken into account [12]. The specific 'phenomena' are discussed below.

4.2.6.1 Heat balance at the soil surface

The conservation of energy at the soil surface requires that {[71], as found in [12]}:

$$q_{h,es} = H + R_t + LE + HP \quad (4.12)$$

where: $q_{h,es}$ is the heat flow into the soil, H the heat transfer by convection, R_t the net incoming radiation, LE the latent heat transfer by evaporation and HP the sensible heat transfer by precipitation (all in: W/m²). Heat flows are considered positive when they add heat to the soil domain.

[12]: The term advection refers to the transport of something from one region to another. There are essentially two (2) types of advection: positive and negative. In positive advection higher values of a variable (for example, temperature) are advected towards lower values. The end result of positive advection in this case, is to increase the temperature values in the direction the wind is blowing. On the other hand, in negative advection lower values of a variable (in our case temperature) are advected towards higher values of the same variable. The end result of such a negative advection is to decrease the temperature values in the direction the wind is blowing [70].

4.2.6.1.1 Convection H

The heat transfer by convection is commonly described by {[72], as found in [12]}:

$$H = \frac{\rho_a c_a (T_e - T_{es})}{r_e} \quad (4.13)$$

in which: ρ_a is the density of air (1.23 kg/m³), c_a the specific heat of dry air (990 J/kgK), T_e the air temperature (°K), T_{es} the outer surface temperature (°K) and r_e the aerodynamic resistance (s/m).

4.2.6.1.2 Net incoming radiation R_t

The net incoming radiation R_t is given by [12]:

$$R_t = (1 - \alpha).R_{glob} + R_{sky} - R_g \quad (4.14)$$

where: α is the soil surface albedo[13] (-), R_{glob} the incoming short wave radiation (W/m²) - sum of direct (R_{dir}) and diffuse (R_{dif}) radiation - R_{sky} the long wave sky irradiance (W/m²) and R_g is the long wave surface emission (W/m²).

4.2.6.1.3 Latent heat transfer by evaporation

The evaporation or condensation of moisture at the soil surface induces a simultaneous transfer of heat, as the phase transfer of the moisture involves the heat of vaporisation. During evaporation, heat is transferred from the surface to the atmosphere, while during condensation the reverse is true. The associated heat flow LE is described by [12]:

$$LE = (L + c_l(T_{es} - T_0))\frac{\rho_{v,e} - \rho_{v,es}}{r_e} \quad (4.15)$$

where: E is the evaporation rate (kg/m²s).

4.2.6.1.4 Sensible heat transfer by precipitation

Precipitation falling down on the surface produces an input of sensible heat contained in the arriving volume of moisture. The transfer of sensible heat related to precipitation is to be calculated as [12]:

$$HP = c_l(T_e - T_0)P \quad (4.16)$$

in which P is the precipitation flow (kg/m²s).

[13]: Albedo is a ratio of scattered to incident electromagnetic radiation power, most commonly light [73].

4.2.6.2 Moisture balance at the soil surface

4.2.6.2.1 Evaporation and precipitation

As long as the soil surface remains unsaturated, the transfer of moisture to and from the surface is made up by evaporation and precipitation [12]:

$$q_{m,es} = E + P \qquad (4.17)$$

where: $q_{m,es}$ is the moisture flow (kg/m²s) into the soil.

4.2.6.2.2 Vegetation

The effects of vegetation and root water uptake on the surface heat and moisture surface should also be accounted for [12].

4.2.6.2.3 Snow and soil freezing

Gilpin and Wong {[74], as found in [12]} analysed the effects of seasonally varying surface cover (snow, for example) on soil temperatures. It was indicated that, the insulating properties of the snow seriously affect soil temperatures: the average soil temperature was significantly higher when the presence of snow on the surface was accounted for. Hagentoft {[16], as found in [12]} similarly studied the effect of surface snow cover on the heat loss from buildings via the ground. It was likewise demonstrated that, snow adds a large surface thermal resistance, thus reducing the foundation heat losses. Furthermore, a sensitivity study, made on the results derived from the simulation of a 3-D numerical model of a test room [22], demonstrated that, when the snow and the rain are non-negligible components of the weather (i.e. duration, depth) over the simulated period, a discrepancy can arise between calculated and measured data when their effects are not modelled.

4.2.7 The couplings between soil heat and soil moisture transfer

As aforementioned in §4.2.1, the comparison between results derived from a fully coupled simulation of building heat loss via the ground with respective ones from a linear (uncoupled) thermal simulation demonstrated that, the influence of soil moisture transfer on building heat loss via the ground is non-negligible. An in depth analysis of the specific results showed that, this influence can be brought back to three main coupling effects [12, 13]:

- The increased amplitude of the soil surface temperature, due to the inclusion of evaporation and radiation in the surface heat balance,
- The variation of the thermal properties with soil moisture content and,
- The advection of sensible heat with liquid moisture transfer.

A fourth coupling effect, the latent heat transfer by thermal vapor diffusion, is commonly included in all - even linear - simulations, by application of the "effective soil thermal conductivity" (λ)[14].

[14]: The effective thermal conductivity (λ), represents the combination of conduction heat flow and the flow of latent heat by temperature induced vapour diffusion [12].

A parameter study - for different soil types, climates and foundation structures - made on the resulting differences between the coupled and the linear heating season heat loss [13] is presented in figure 4.6 below. It is apparent from this graph that, 'soil type' and 'basement width' do not affect the influence of coupling significantly: the relative differences between coupled and linear heat loss do not change appreciably for different soil types or basement widths. Since the effect of climate and precipitation amount on the coupling influence is significant enough, it ultimately appears that, the climate governs the hygro-thermal behavior of the soil. All in all, it was concluded that the coupled simulation of building heat loss via the ground increases:

- The heating season heat loss with up to 15%,
- The surface temperature amplitude 25%,
- The steady-state floor thermal permeance 10%,
- The periodical floor thermal permeance 20%,
- The steady-state wall thermal permeance 10% and,
- The periodical wall thermal permeance 10%,

when compared to their respective linear values. Such differences cannot, obviously, be regarded as insignificant.

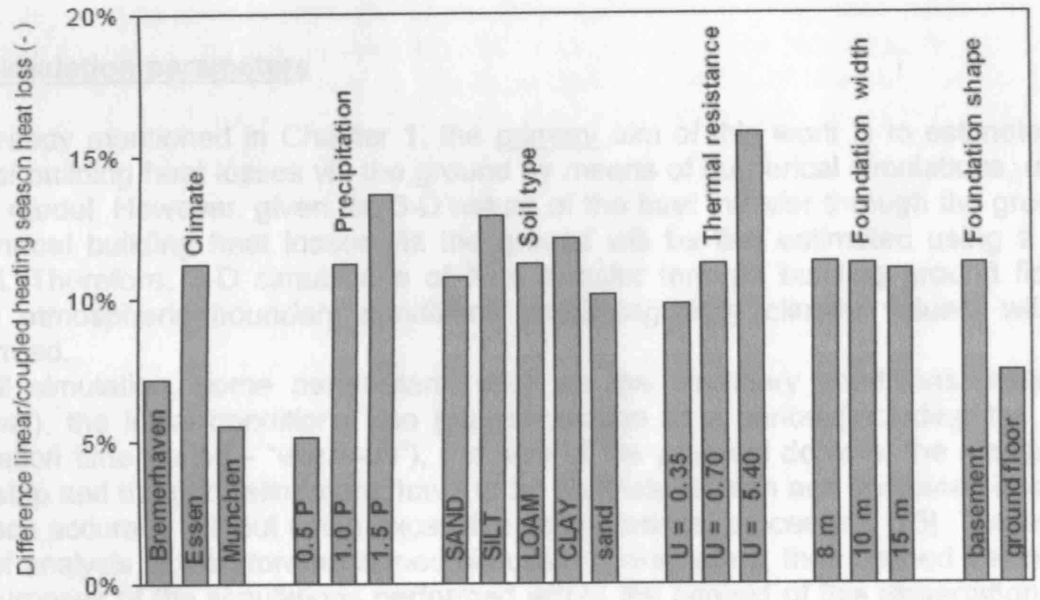

Figure 4.6 - Differences between the coupled and the linear (uncoupled) heating season heat loss for all cases considered in the parameter study [13]

At this point, it must be noted that, the currently available standard building heat loss via the ground calculation methods {EN ISO 13370 - [53]} do not account for the coupling effects between soil moisture and soil moisture transfer. However, due to the limitations which Janssen's work [12] is subject to and due to the insufficient accuracy of the EN ISO Standard, the implementation of the coupling influences in such standard calculation methods can not be defended at present. For these reasons, the inaccuracies resulting from the EN and from the soil thermal properties are still large enough [12, 13].

Chapter 5

Computational considerations and simulation study

5.1 Simulation parameters

As already mentioned in Chapter 1, the primary aim of this work is to estimate the annual building heat losses via the ground by means of numerical simulations, using a 1-D model. However, given the 3-D nature of the heat transfer through the ground, the annual building heat losses via the ground will be first estimated using a 3-D model. Therefore, 3-D simulations of heat transfer through building ground floors, under atmospheric boundary conditions employing daily climate values, will be performed.
In soil simulation, some parameters, such as the boundary conditions (internal-external), the initial conditions, the total simulation time period (including the pre-simulation time period - "*warm-up*"), the size of the physical domain, the simulation time step and the grid refinement, have to be carefully chosen and combined in order to reach accuracy without using excessive computational processing [75]. Therefore, a brief analysis of the aforementioned simulation parameters, their defined values for the purposes of the simulations performed within the context of this dissertation and how these values were defined, is considered to be most necessary in order for any reader to completely understand the magnitude of the work presented hereby.

5.1.1 Boundary conditions

5.1.1.1 Internal

The internal boundary condition air temperature for all the numerical simulations is represented by a constant function with a value of: 20°C, which lies within the thermal comfort zone's limits recommended by CIBSE (for low air speeds) [76].

The internal (global) surface heat transfer coefficient was set to: 7.69W/m^{2}K. According to: [77] - Table 3 - p. 22, the internal surface resistance for heat flow rate calculations is: 0.13m^{2}K/W. However, the internal surface resistance is given by [78]:

$$R_{si} = \frac{1}{\sigma_S E h_r + h_c} \tag{5.1}$$

where: R_{si} is the internal surface resistance (m^{2}KW^{-1}), E is the emissivity factor, h_r is the radiative heat transfer coefficient (Wm^{-2}K^{-1}) and h_c is the convective heat transfer coefficient (Wm^{-2}K^{-1}). Since it is assumed that, there is no heat transfer by radiation, then the reciprocal of the internal surface resistance (1/0.13 W/m^{2}K = 7.69 W/m^{2}K) is equal to the internal (global) surface heat transfer coefficient.
The boundary condition heat flux (W/m^2) was set to: zero, since the boundaries of the internal 'domain' are assumed to be "*adiabatic*" (i.e. zero heat flow) [77].

5.1.1.2 External

In most investigations of non-steady state heat loss via the ground the variations of the air or surface temperature are implicitly simplified to a sinusoidal pattern with a one-year period, since the penetration depth for shorter term temperature variations is considered to be limited, due to the large thermal inertia of the soil domain [12]. Delsante et al. {[79], as found in [12]} were the first to study this issue and employed an analytical expression to demonstrate that the periodic heat loss only becomes significant for periods much larger than a day. Hagentoft {[16], as found in [12]} and Bahnfleth {[15], as found in [12]} similarly showed that, hourly variations of the soil surface temperature only resulted in slight 'ripples' on the yearly heat losses curve. The results from Geving {[80], as found in [12]} are, however, far from exhaustive and cannot definitively establish the use of daily averaged climate data in simulations of coupled soil heat and moisture transfer. The use of such averaged data imports a substantial benefit though: less extreme fluctuations of the boundary condition are obtained and, more importantly, larger time steps can be allowed, resulting in serious reductions of the calculation times. Conclusively, use of daily averaged climate data - even in fully coupled simulations of building heat loss via the ground, which, of course, is not the case in this work - is allowed for the quantification of both the thermal permeance of the foundation structure and of the soil surface temperatures [12].
In this work, the external boundary condition air temperature - for all the numerical simulations performed - is represented by a sinusoidal function (see figure 5.1 in the following page) with:

- A mean value of: 10°C,
- An amplitude value of: 20°C (so, it fluctuates between: -10°C and: +30°C),
- A period of: 525,600 min (1 year - 365 days) and,
- An offset (distance from *Y*-axis/ Temperatures axis) of: 0min.

The specific internal time-dependent function is one of the five built-in program functions (see Appendix A - §A.2), defined by one or more parameters, as mentioned previously. The values of the specific parameters were set as above, because they are thought to best represent the annual air temperature fluctuation in the region of London, UK.

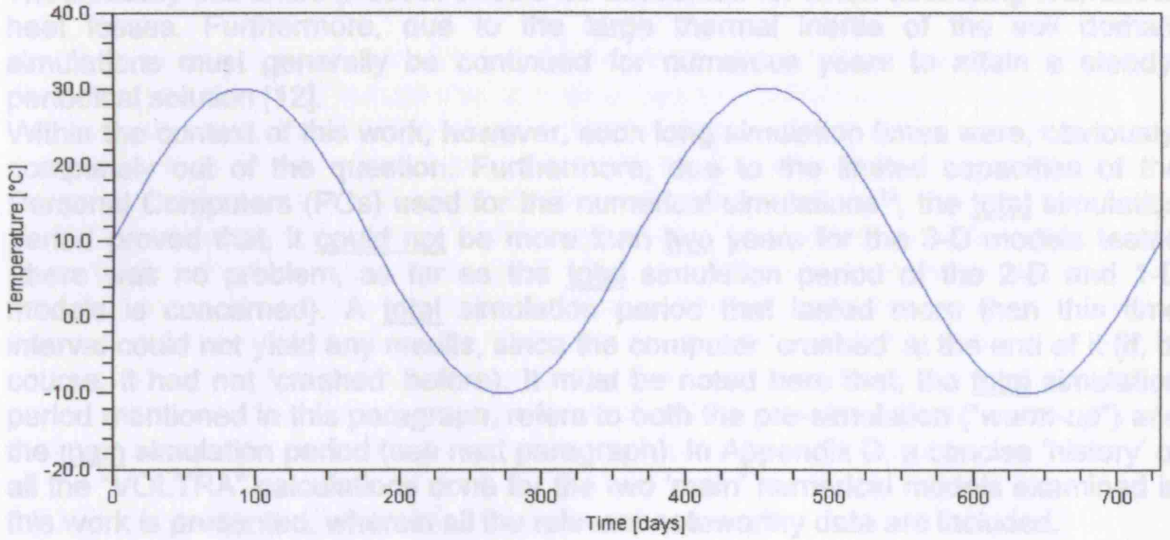

Figure 5.1 - External boundary condition air temperature vs Time [20]

As mentioned in Appendix A, the program FUNCEDIT, which is a utility program to edit and visualise function files for use in non-steady state PHYSIBEL programs, like "VOLTRA", is not included in the program's version used for this work [20]. Therefore, any representation of real climatic data (from previous years' records for the specific region), with a function that could be imported and used in "VOLTRA", was not possible for this work. For the same reason, a 'comparison' of "VOLTRA" with "TAS" thermal analysis software [81], as far as the calculation of the internal ground floor surface temperatures are concerned, cannot be defended.
The external (global) surface heat transfer coefficient was set to: 25W/m^{2}K. According to: [77] - Table 3 - p. 22, the external surface resistance for heat flow rate calculations is: 0.04m^{2}K/W. On the other hand, the external surface resistance is given by [78]:

$$R_{se} = \frac{1}{E h_r + h_c} \qquad (5.2)$$

where: R_{se} is the external surface resistance (m^{2}KW^{-1}). Since it is assumed that, there is no heat transfer by radiation, then the reciprocal of the external surface resistance (1/0.04 W/m^{2}K = 25 W/m^{2}K) is equal to the external (global) surface heat transfer coefficient.
The boundary condition heat flux (W/m^2) was set to: zero, since the boundaries ("*cut-off planes*" - see next page) of the external 'domain' (both on the soil surface and in the soil domain) are assumed to be "*adiabatic*".

5.1.2 Total simulation period

Building heat loss via the ground is essentially a transient process. At a certain moment in time, the newly created building starts to disturb the common hygro-thermal behaviour in the ground domain. The climate data are neither invariant from year to year, giving rise to a continuously varying hygro-thermal regime in the ground domain.

Theoretically this entire process should be accounted for when assessing foundation heat losses. Furthermore, due to the large thermal inertia of the soil domain simulations must generally be continued for numerous years to attain a steady-periodical solution [12].
Within the context of this work, however, such long simulation times were, obviously, completely out of the question. Furthermore, due to the limited capacities of the Personal Computers (PCs) used for the numerical simulations[15], the total simulation period proved that, it could not be more than two years for the 3-D models tested {there was no problem, as far as the total simulation period of the 2-D and 1-D models is concerned}. A total simulation period that lasted more than this time interval could not yield any results, since the computer 'crashed' at the end of it (if, of course, it had not 'crashed' before). It must be noted here that, the total simulation period mentioned in this paragraph, refers to both the pre-simulation ("*warm-up*") and the main simulation period (see next paragraph). In Appendix D, a concise 'history' of all the "VOLTRA" calculations done for the two 'main' numerical models examined in this work is presented, wherein all the relevant noteworthy data are included.

5.1.3 Initial conditions and pre-simulation period ("*warm-up*")

Determination of representative initial conditions for foundation heat losses is always a difficulty [28]. In this work, however, taking into consideration the limitations imposed by the capacities of the PCs used for the simulations and the total period that was defined for them (two years, as explained previously), the initial conditions were set at the end of one year (pre-simulation period), after which the main simulation period started. So, each of the pre-simulation and the main simulation period lasts one year, while the total simulation period lasts two years (the sum of the two periods). It must be noted at this point that, the results derived from the simulations performed for the two 'main' numerical models demonstrated that, the differences in the foundation heat losses between: one year of pre-simulation period, combined with one year of main simulation period and: two years of main simulation period, with no pre-simulation period, are negligible in most cases (see Appendix D).

5.1.4 Size of the physical domain

The size of the soil domain (location of the cut-ff planes[16]) was defined according to: [77] - Table 1, p.13 & figure 7b, p.14. Furthermore, due to symmetry, only one quarter (1/4) of the whole domain was modelled in each case. So, since in both geometrical models the dimensions of the ground floor were: 20x20 m^2, then the size of the soil domain was set to: 50m (2.5 x 20m), in all the three directions (*X, Y, Z axis*), while the size of the internal domain (ground floor's dimensions) was set to: 10m (0.5 x 20m) in the two directions (*X & Y axis*) and to: 1m (above the slab) in the third one (*Z axis*) [77] - §5.1.1.

---

[15]: Due to compatibility problems with the program's hardware key, all the simulations were performed in the UCL's EDE Cluster Room at Torrington Place 1-19 building, second (2^{nd}) floor. The Operational System of the specific computers is: WINDOWS XP, while their memory size is: 512 Mb RAM.
[16]: Cut-ff planes are those construction planes that are boundaries to the 3-D model or 2-D model by separating the model from the remainder of the construction [77].

5.1.5 Simulation time-step

As mentioned in Appendix A - §A.4 of this work, the (simulation) time step is the time distance between two successive dynamic system calculations. In this work, the definition of the 'optimum' time step - the time step, which would produce the most accurate results in the soonest calculation time - was a serious decision. Given the limited capacities of the PCs used for the numerical simulations - at least as far as the 3-D models are concerned - and the experience gained from the simulation of the three 'trial' numerical models (see §5.2 below), several calculations were performed (see Appendix D) with the intention of defining the 'optimum' time-step. For the 2-D and 1-D models there were no problems having to do with the duration of the calculation times. Detailed information about the 'setting' of the time-step interval and the duration of the calculation time, for each of the two 'main' numerical models examined within the context of this work, are presented in §5.3 below.

5.1.6 Grid refinement (optimization)

As aforementioned, simulation time reduction has been a primary issue during the development of the numerical models of this work and therefore, the use of the 'optimum' grid is a significant measure. The 'optimum' grid is the one with as few nodes as possible without introducing notable errors in the resulting numerical solutions.
Optimisation of the 3-D nodal grid was the most important thing to be done, as far more nodes and hence, far greater calculation time reductions, are involved. The use of symmetry (see §5.1.4) can be assumed a first optimisation: only one quarter (1/4) of the foundation structure and the soil-surface domain needed to be modelled.
Furthermore, with the intention of achieving as accurate results as possible, fine "*discretisation*"[17], particularly near the soil surface (boundary between the foundation structure and the soil domain), is needed. Another important parameter to be taken into account, is that, the used PCs' memory capacity (512Gb RAM) allows to solve a system of about 1,000,000 nodes (see Appendix A - §A.1).
Taking all the above into consideration, the 'optimum' grid for the first 3-D numerical model (a slab-on-ground, with insulation below the slab and an un-insulated compact external wall) consisted of: 979,120 nodes, while the respective one for the second 3-D numerical model (a ground bearing floor, with insulation above the slab and an insulated cavity external wall) was made up of: 791,504 nodes. As far as the respective 2-D & 1-D numerical models - the ones that 'came up' from the 3-D models following the procedure described in Chapter 1 - §1.2 - are concerned, the following apply:

- Slab-on-ground model:
  - 2-D model: 11,258 nodes,
  - 1-D model: 224 nodes,

and:

- Ground bearing floor model:
  - 2-D model: 15,244 nodes,
  - 1-D model: 208 nodes.

[17]: In mathematics, "*discretization*" concerns the process of transferring continuous models and equations into discrete counterparts. This process is usually carried out as a first step toward making them suitable for numerical evaluation and implementation on digital computers [82].

5.2 Validation of the used methodology

In order for the methodology described in Chapter 1 - §1.3 to be validated for its precision, three different geometrical ('trial') models, as presented below {[77] - Annex A, pp.28-30}, were modelled and simulated with the use of the: "TRISCO" [18] & "VOLTRA" [20] thermal analysis programs - first modelled and simulated in "TRISCO" and then, imported and simulated in "VOLTRA", too. The results derived from the numerical simulation of the three models, using the methodology chosen for this work and the respective ones, as they are given by the analytical solution of the models, according to the calculation method described in [77], are presented in Appendix C of this work. It must be noted that, for the 'check' points shown in each geometrical model, the difference between the temperatures calculated by the method being validated and the temperatures listed, shall not exceed 0.1K for all the three cases (models). Furthermore, for the second model, the difference between the heat flow calculated by the method being validated and the heat flow listed, shall not exceed 0,1 W/m, while for the third model, the difference between the heat flows calculated by the method being validated and the heat flows listed, shall not exceed 2% of the listed values. As can be concluded from the comparison of the respective results, the used methodology is highly precise.

- First model: 1-D heat transfer (half a square column)

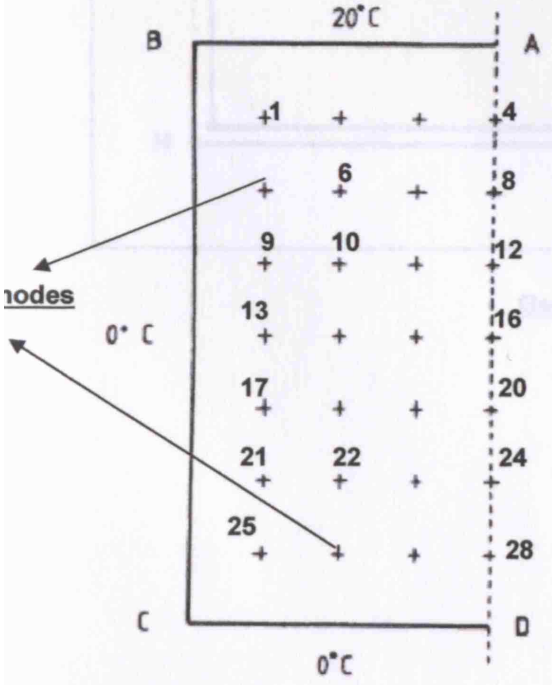

Geometrical model [77]

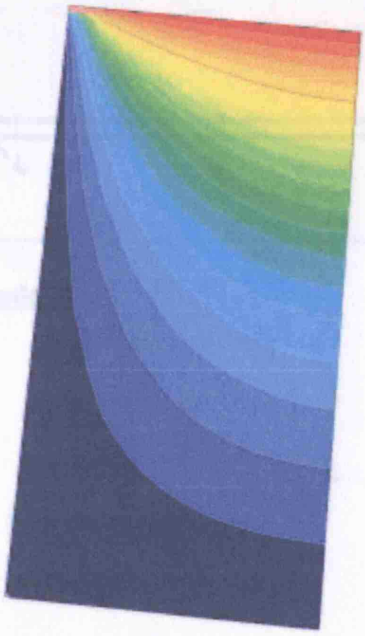

'Numerical' model

Temperature range (°C)

- Second model: 2-D heat transfer

Description of the model

Geometry (mm)	Thermal conductivities W/m·k	Boundary conditions
AB = 500	1: 1.15	AB: 0 °C with R_{se} = 0.06 m² K/W
AC = 6	2: 0.12	HI: 20 °C with R_{si} = 0.11 m² K/W
CD = 15	3: 0.029	
CF = 3	4: 230	
EM = 40		
GJ = 1.5		
IM = 1.5		
FG-KJ = 1.5		

Numerical solution temperatures, in °C: **Total heat flow rate: 9.5 W/m**

A: 7.1		B: 0.8
C: 7.9	D: 6.3	E: 0.8
F: 16.4	G: 16.3	
H: 16.8		I: 15.3

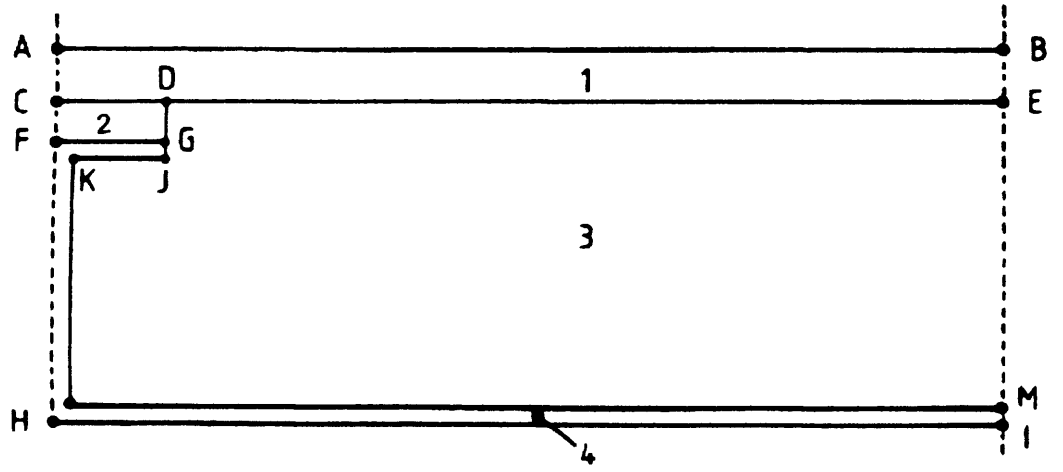

Geometrical model [77]

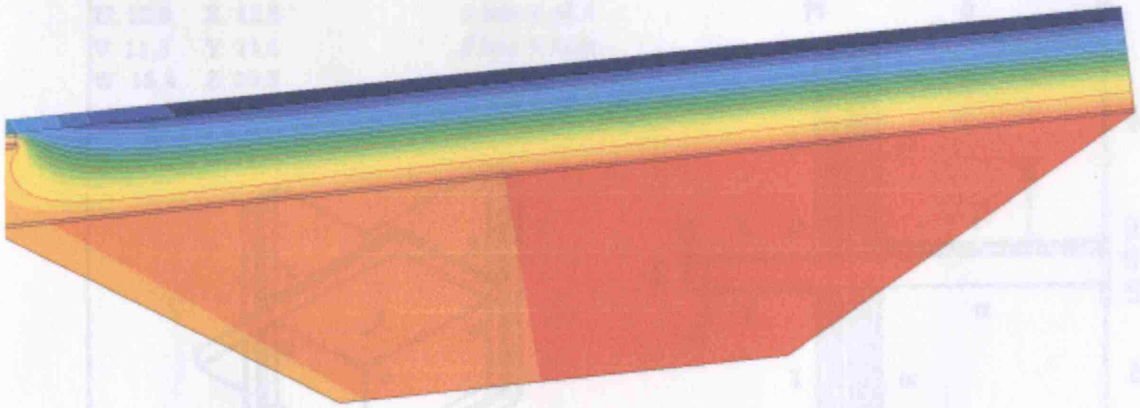

'Numerical' model

Temperature range (°C)

- Third model: 3-D heat transfer

Description of the model

Geometry mm		Thermal conductivities W/(m·K)
AB =	1 300	1: 0,7
BD = HI =	100	2: 0,04
DE = LJ =	50	3: 1,0
EF = JK =	150	4: 2,5
FL = KL =	1 000	5: 1,0
CG =	1 150	**boundary conditions:**
GH =	600	α: 20 °C 0,20 m²·K/W
MP = ST =	1 000	β: 15 °C 0,20 m²·K/W
QR =	50	γ: 0 °C 0,05 m²·K/W
RS =	150	δ: adiabatic
NQ =	950	
OP =	600	

Horizontal section

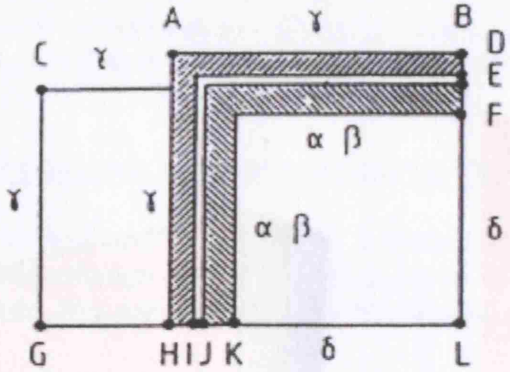

Numerical solution

Temperature, in °C:

U: 12,9	X: 12,6	α loss = 46,3
V: 11,3	Y: 11,1	β loss = 14,0
W: 16,4	Z: 15,3	γ gain = 60,3

Perspective

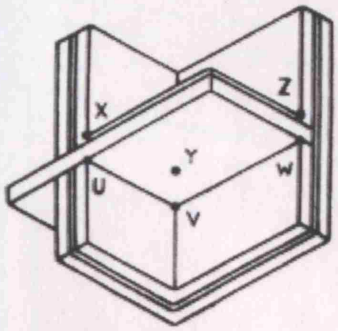

Vertical section

Heat flows, in W:

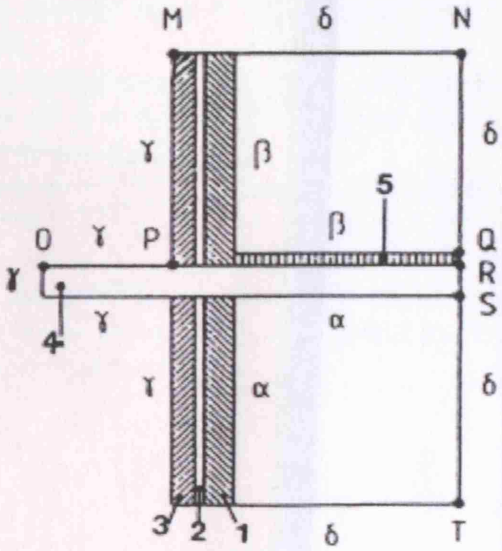

Y and V are three-dimensional corners

Geometrical model [77]

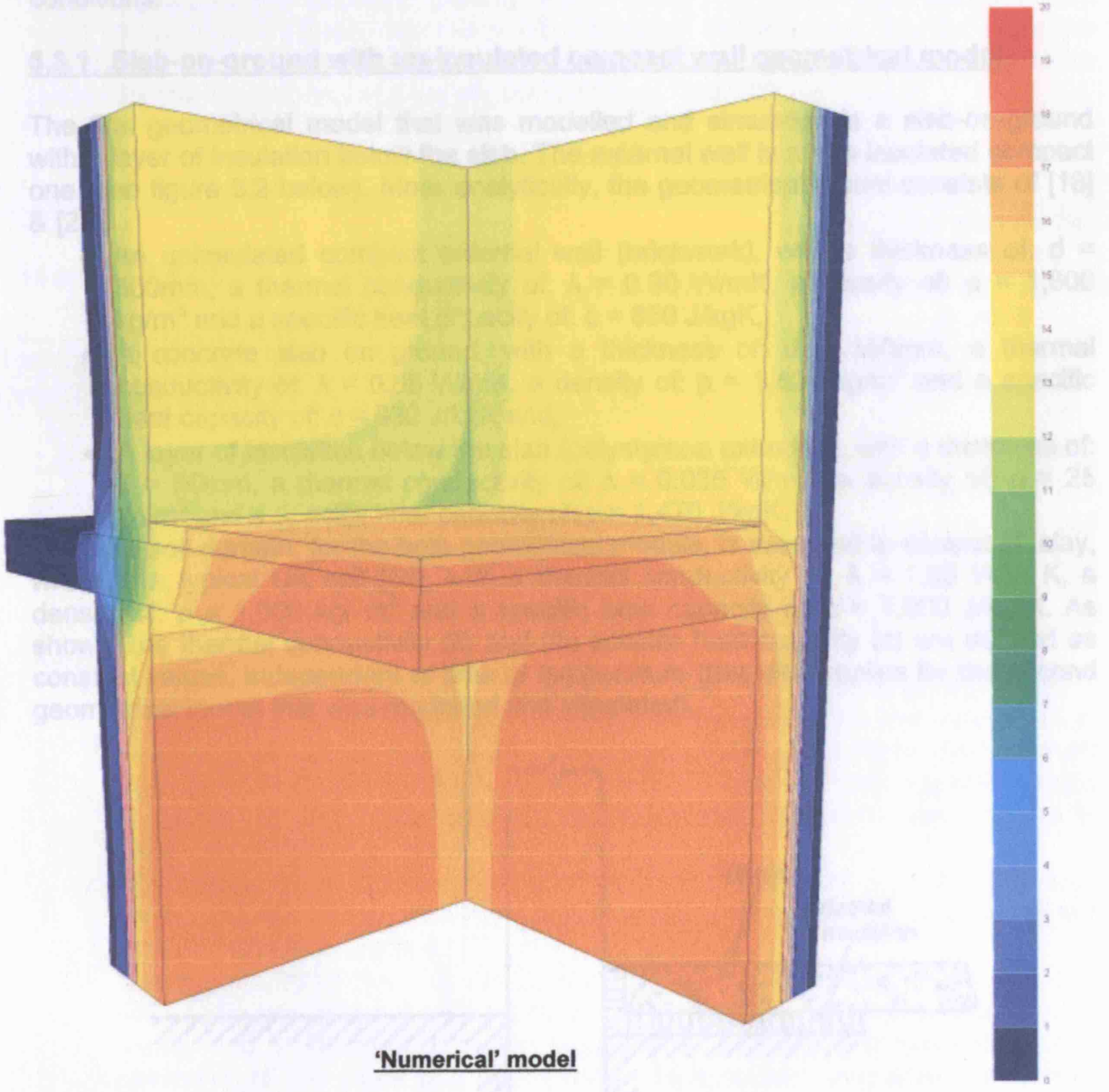

'Numerical' model

Temperature range (°C)

5.3 Modelling and simulation of the geometrical models

In the next two sub-paragraphs the presentation of the two geometrical models (ground floor constructional details) that were modelled and simulated, using the thermal analysis computer program "VOLTRA", with the intention of calculating the annual ground floor heat losses, is made. As already mentioned in §5.2, the two geometrical models were first modelled and simulated in "TRISCO" under steady state conditions and then, imported and simulated in "VOLTRA", under transient conditions.

5.3.1 Slab-on-ground with un-insulated compact wall geometrical model

The first geometrical model that was modelled and simulated is a slab-on-ground with a layer of insulation below the slab. The external wall is an un-insulated compact one (see figure 5.2 below). More analytically, the geometrical model consists of [18] & [20]:

- An uninsulated compact external wall (brickwork), with a thickness of: d = 300mm, a thermal conductivity of: λ = 0.90 W/mK, a density of: ρ = 1,800 kg/m^3 and a specific heat capacity of: c = 850 J/kgK,
- A concrete slab on ground, with a thickness of: d = 150mm, a thermal conductivity of: λ = 0.85 W/mK, a density of: ρ = 1,600 kg/m^3 and a specific heat capacity of: c = 930 J/kgK and,
- A layer of insulation below the slab (polystyrene extruded), with a thickness of: d = 50mm, a thermal conductivity of: λ = 0.035 W/mK, a density of: ρ = 25 kg/m^3 and a specific heat capacity of: c = 1,470 J/kgK.

Last, the soil domain, for the both geometrical models, is assumed to consist of: clay, which is a typical UK soil [54], with a thermal conductivity of: λ = 1.50 W/m K, a density of: ρ = 1,000 kg/ m^3 and a specific heat capacity of: c = 1,000 J/kg K. As shown, the thermal conductivity (λ) and the specific heat capacity (c) are defined as constant values, independent of time or temperature (this also applies for the second geometrical model that was modelled and simulated).

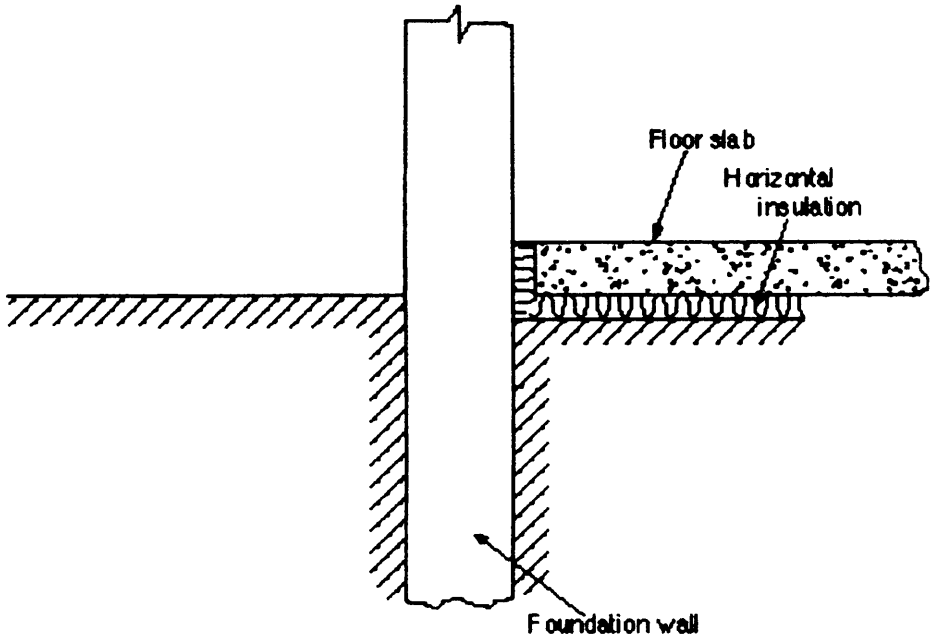

Figure 5.2 - Slab-on-ground with uninsulated compact wall geometrical model [53]

The following calculation parameters were set in the Calculation Parameters dialog box of the "VOLTRA" software (for the calculation of the 3-D numerical model):

- Time step interval: 10 days.
- Start-up calculation duration (pre-simulation period) to get 'dynamic' start values: 1 year.
- Calculation duration (simulation period): 1 year.

After the calculation of the 3-D numerical model, which lasted 110 minutes, the annual ground floor heat losses were found to be: ~20,305,494.72 kJ or, if the surface area of the model's ground floor ($100m^2$) is taken into consideration: ~203,054.95 kJ/ m^2. Then, the 2-D & 1-D numerical models were 'derived' from the 3-D model, following the procedure described in Chapter 1 - §1.2. The respective results for the specific models are presented in the Table 5.1 below:

Table 5.1

Numerical model	Annual ground floor heat losses (kJ)	Ground floor surface area (m^2)	Annual ground floor heat losses per unit surface area (kJ/m^2)
Two-dimensional (2-D)	~ 1,139,814.72	10	~ 113,981.47
One-dimensional (1-D)	~ 8,830.08	1	~ 8,830.08

Last, the 'equalization' of the 1-D with the 2-D & 3-D models, as far as the annual ground floor heat losses per unit surface area are concerned, was done. For the 1-D & 2-D models, it was found that, setting the value (in the 1-D model) of the soil thermal conductivity (λ) equal to: ~ 59.89 W/mk (from: 1.5 W/mk), a 'match' of the two models was achieved. On the other hand, the 'equalization' process of the 1-D & 3-D models, which, besides, constitutes the primary aim of this work, derived the following results:

- Setting the value (in the 1-D model) of the soil thermal conductivity (λ) to: ~ $2.5x10^6$ W/mk (from: 1.5 W/mk), a 'match' of the two models was achieved by: ~84.7% {the annual ground floor heat losses per unit surface area derived from the 1-D model were 84.7% (171,983.52 kJ/m^2) of the respective ones (~203,054.95 kJ/m2) derived from the 3-D model}. Further increase of the 'λ' value, did not result in 'match' of the two models,
- The change of the soil density (ρ) or the soil specific heat capacity (c) values (in the 1-D model) had almost no effect on the 'equalization' process of the two specific numerical models,
- The soil depth of the 1-D model was turned out to be the most significant simulation parameter, as far as its influence on the annual ground floor heat losses and, consequently, on the 'equalization' process is concerned. A **90%** decrease of the initial soil depth (from: 50m to 5m) increased the annual ground floor heat losses by: **~691%** (from: **~8,830.08kJ/m^2** to: **~61,020.00kJ/m^2**), while a **98%** decrease of the soil depth (from: 50m to 1m) increased the annual ground floor heat losses by: **~1,428%** (from: **~8,830.08kJ/m^2** to: **~126,118.08kJ/m^2**)! In this specific case (soil depth: 1m), the annual ground floor heat losses per unit surface area derived from the 1-D model were: **~62.11%** of the 3-D model's respective ones **(~203,054.95 kJ/m^2)**.

In other words, the annual ground floor heat losses (per unit surface area) derived from a numerical model which simulates the heat transfer through the ground in one-dimension and 'incorporates' a soil depth of: 1m - as, namely, is the common practice in "TAS" simulations - were: **~62.11%** of the respective ones 'representing' best the real conditions, given the three-dimensional nature of heat transfer through the ground and,

- Setting the soil thermal conductivity to: 17.31 W/mK (from: 1.5 W/mk) and the soil depth to: 1m (from: 50m), a 'match' of the two models was achieved. The same 'match' could have also been achieved with combinations of different values for the specific simulation parameters.

The initial 3-D & 2-D models, as well as, the 1-D numerical models that, 'matched' them, as far as the annual ground floor heat losses per unit surface area are concerned, along with a graphical representation of these models heat loss rate (W) change in relation with time (sec), are presented in the figures 5.3-5.11 below. A detailed presentation of the whole 'equalization' process is made in the attached Appendix D.

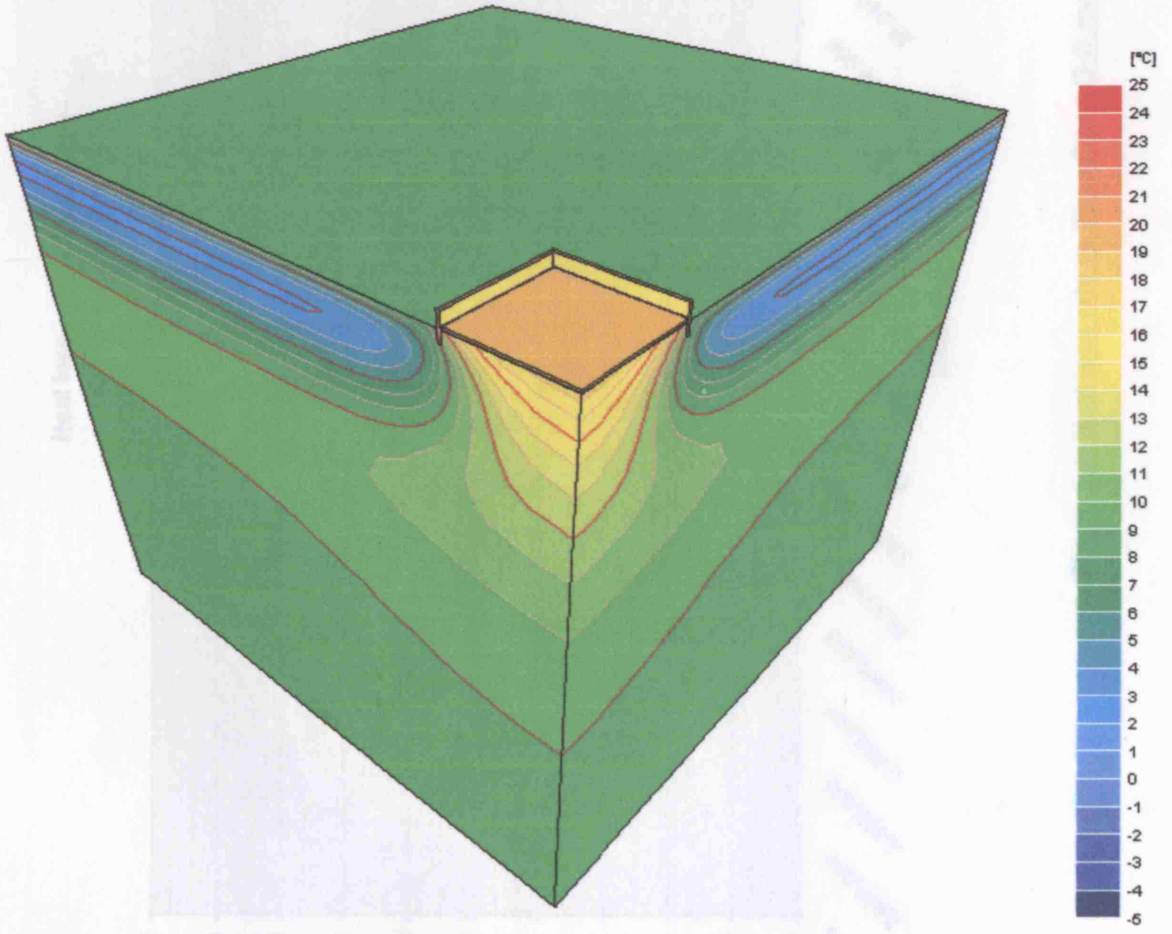

Initial 3-D Numerical model (calculated) Temperature range

Figure 5.3: Temperature results of the 3-D numerical model's calculation

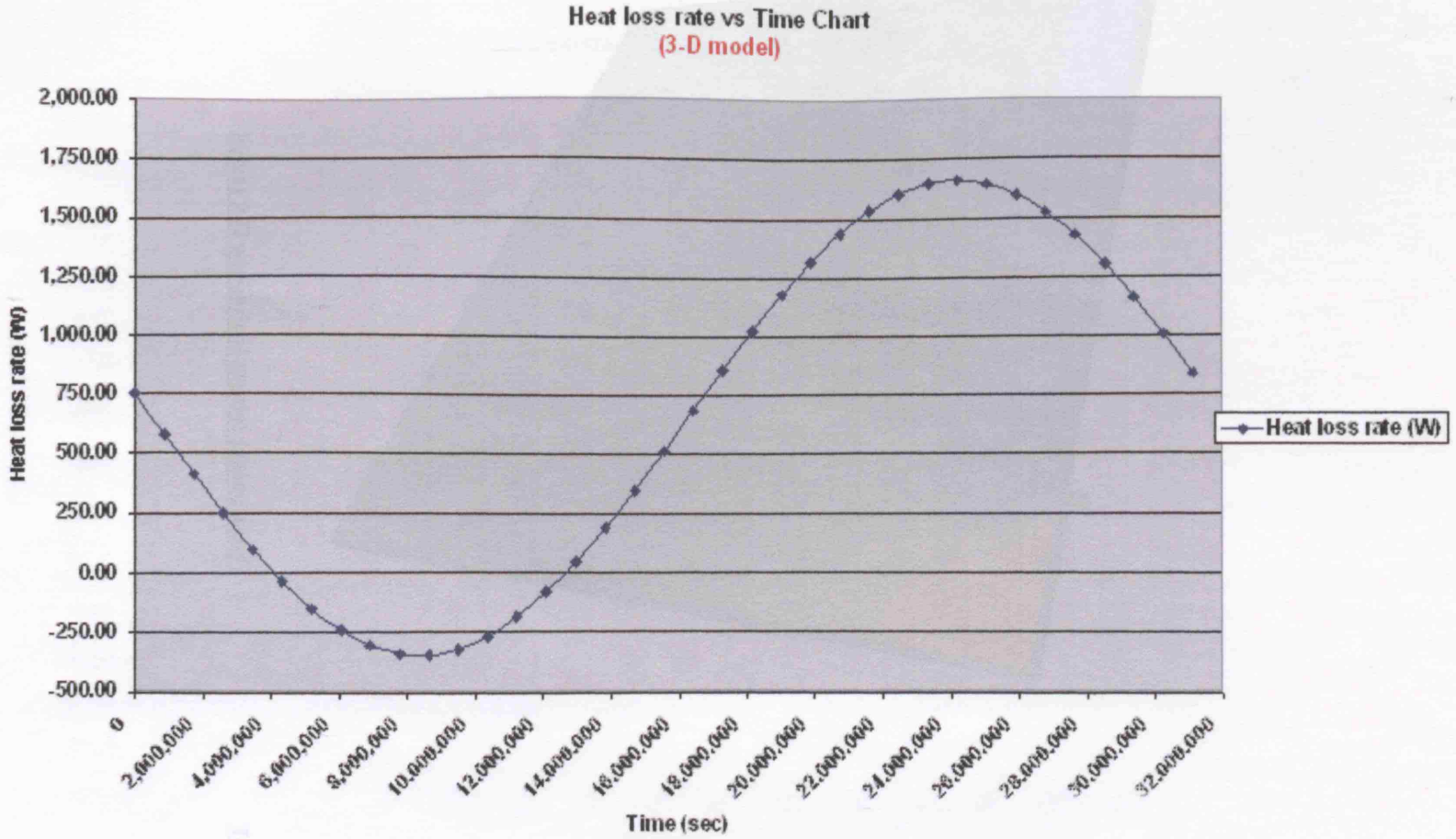

Figure 5.4: Heat loss rate vs Time Chart (3-D model)

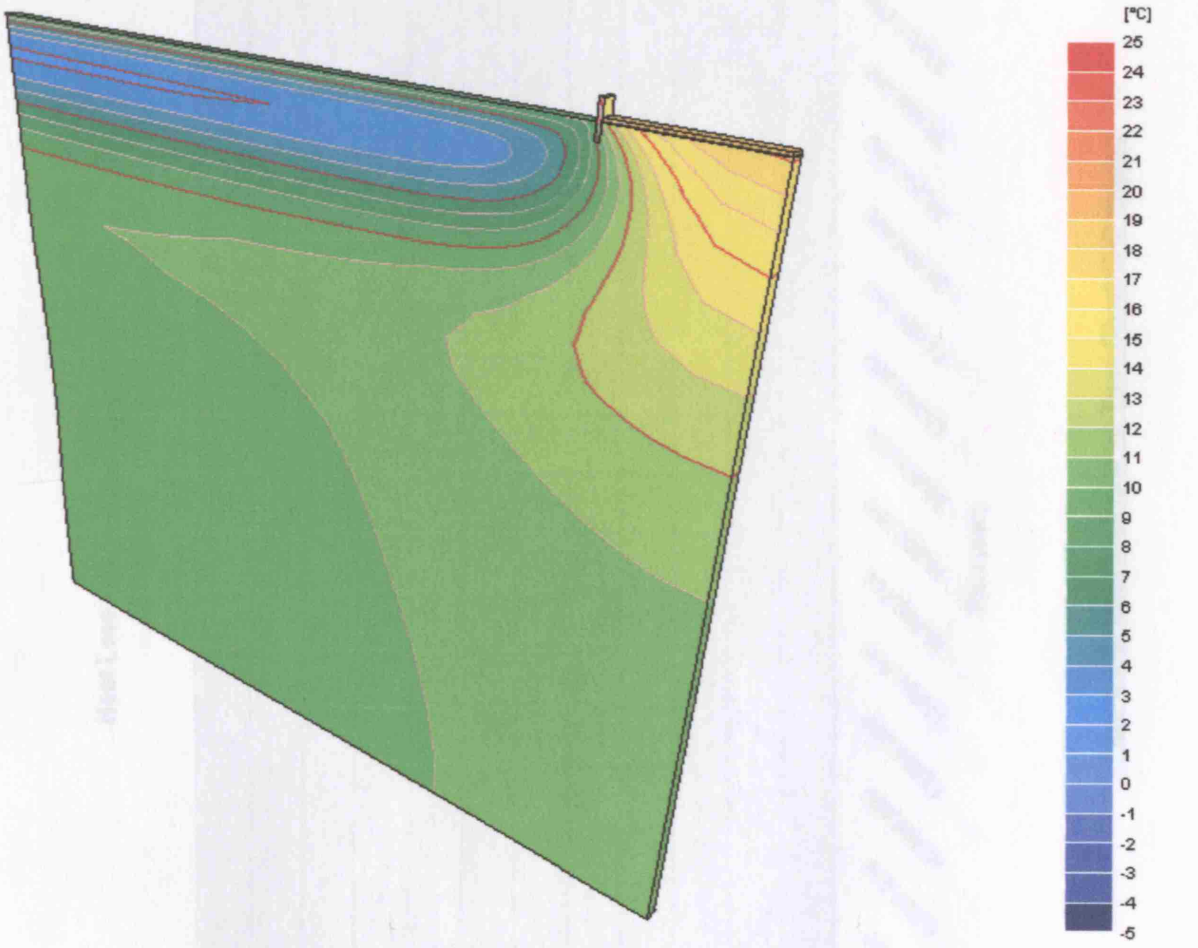

Initial 2-D numerical model (calculated)

Temperature range

Figure 5.5: Temperature results of the 2-D numerical model's calculation

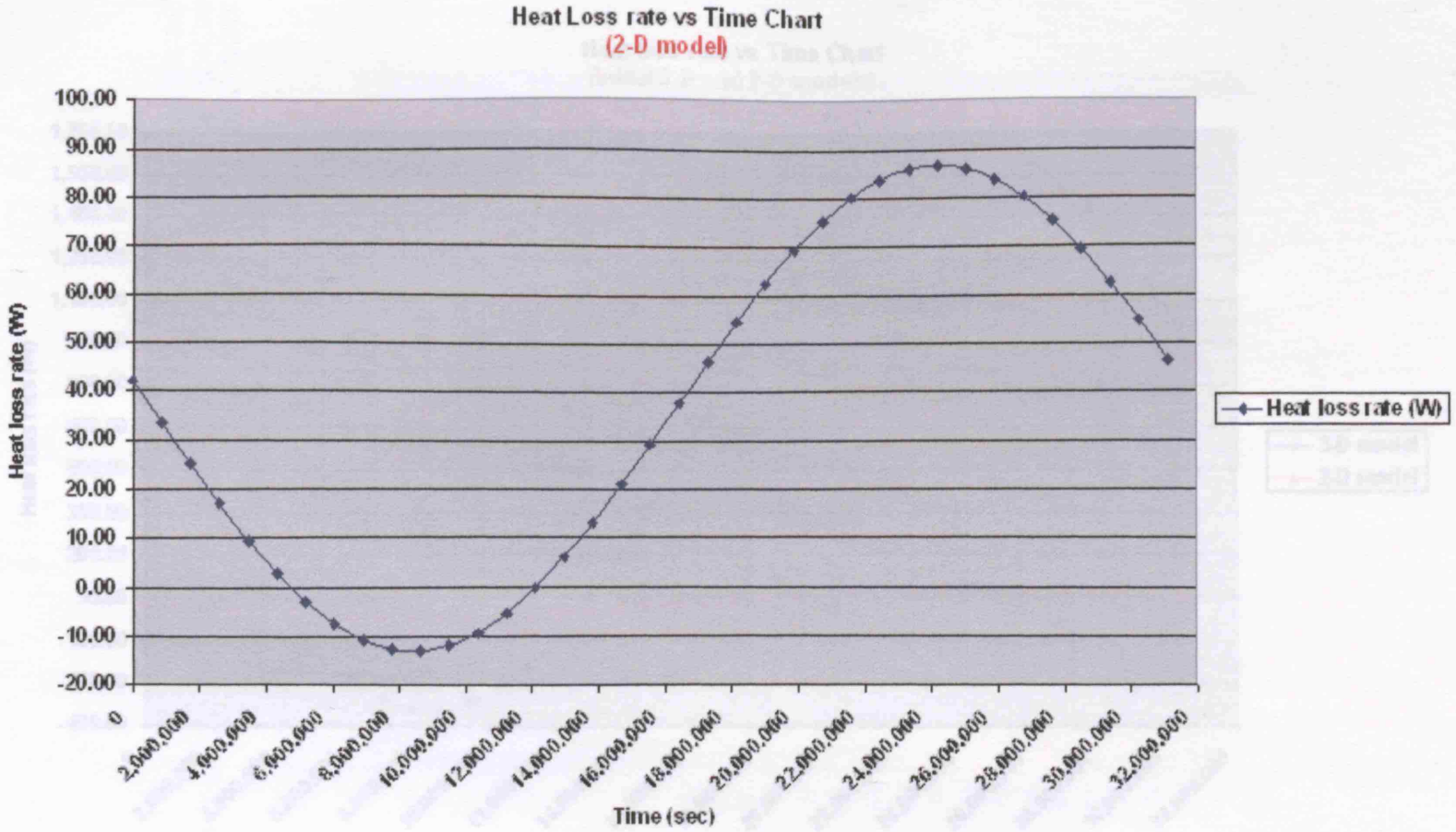

Figure 5.6: Heat loss rate vs Time Chart (2-D model)

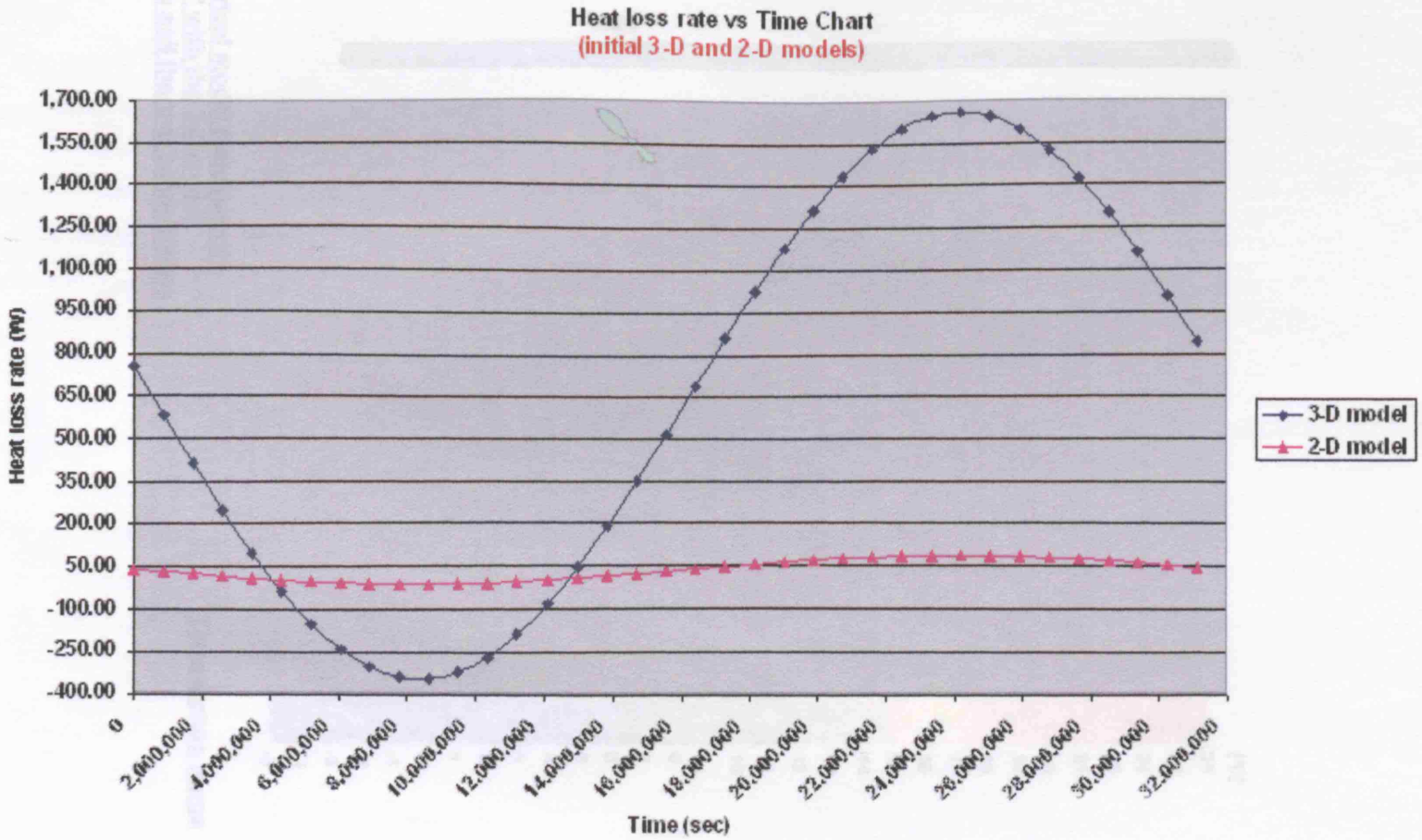

Figure 5.7: Heat loss rate vs Time Chart (3-D vs 2-Dmodel)

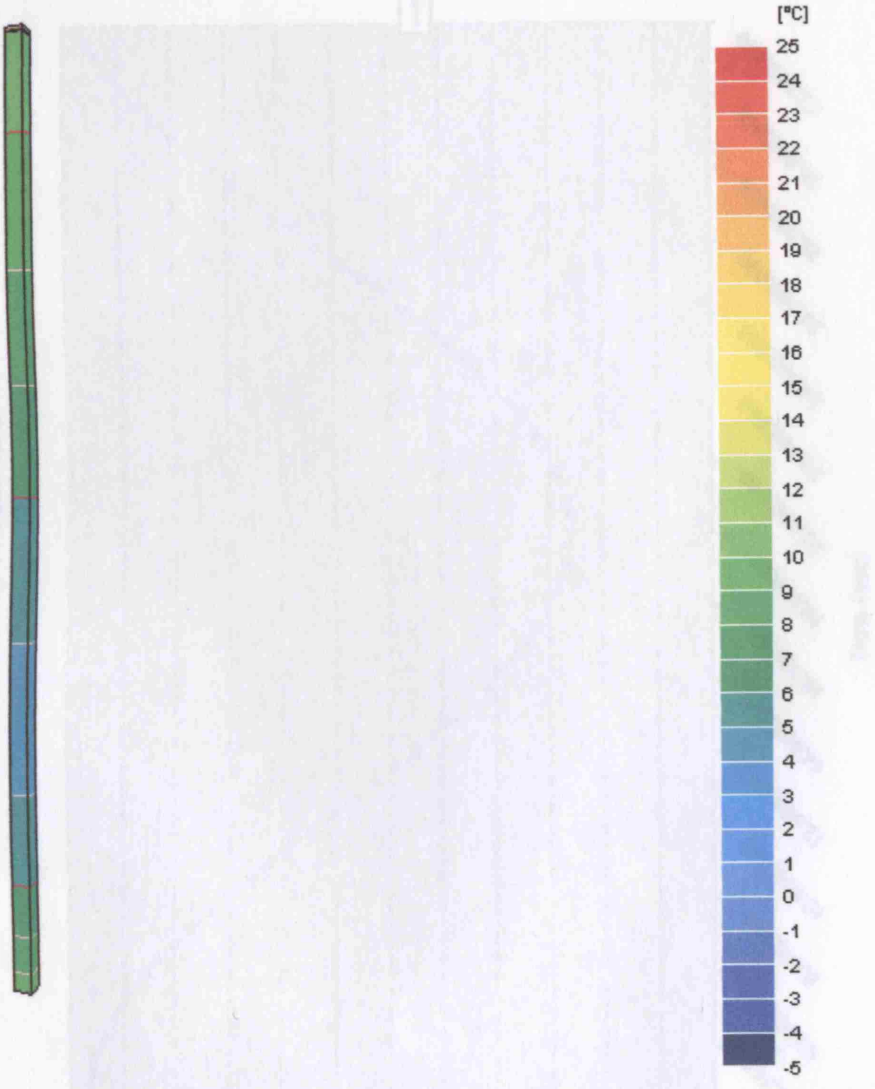

1-D Numerical model (calculated)
'Match' with the 2-D model
(change of the soil thermal conductivity)

Temperature range

Figure 5.8: Temperature results of the 1-D numerical model's calculation ('match' with the 2-D model)

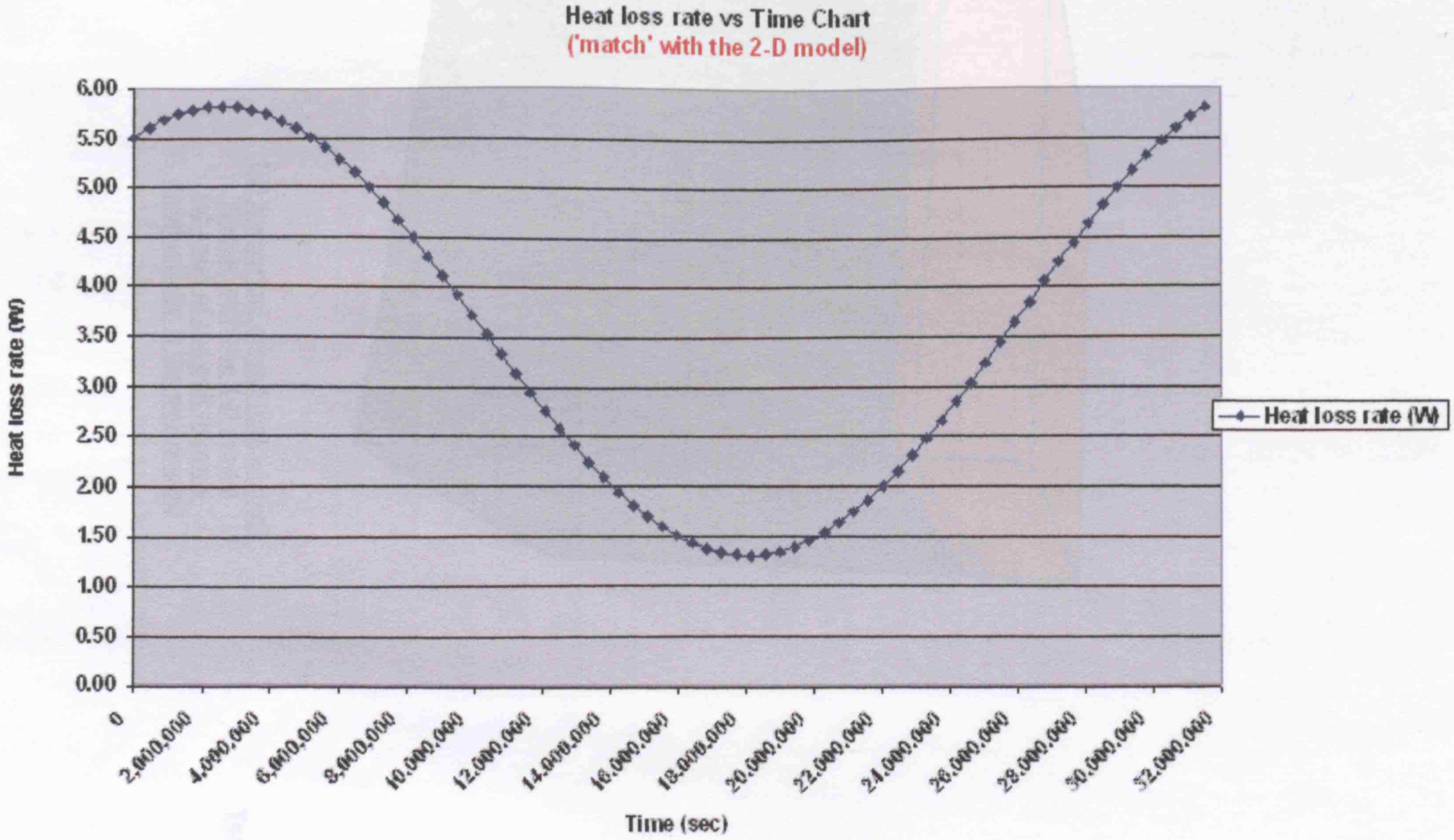

Figure 5.9: Heat loss rate vs Time Chart (1-D model/ 'match with the 2-D model)

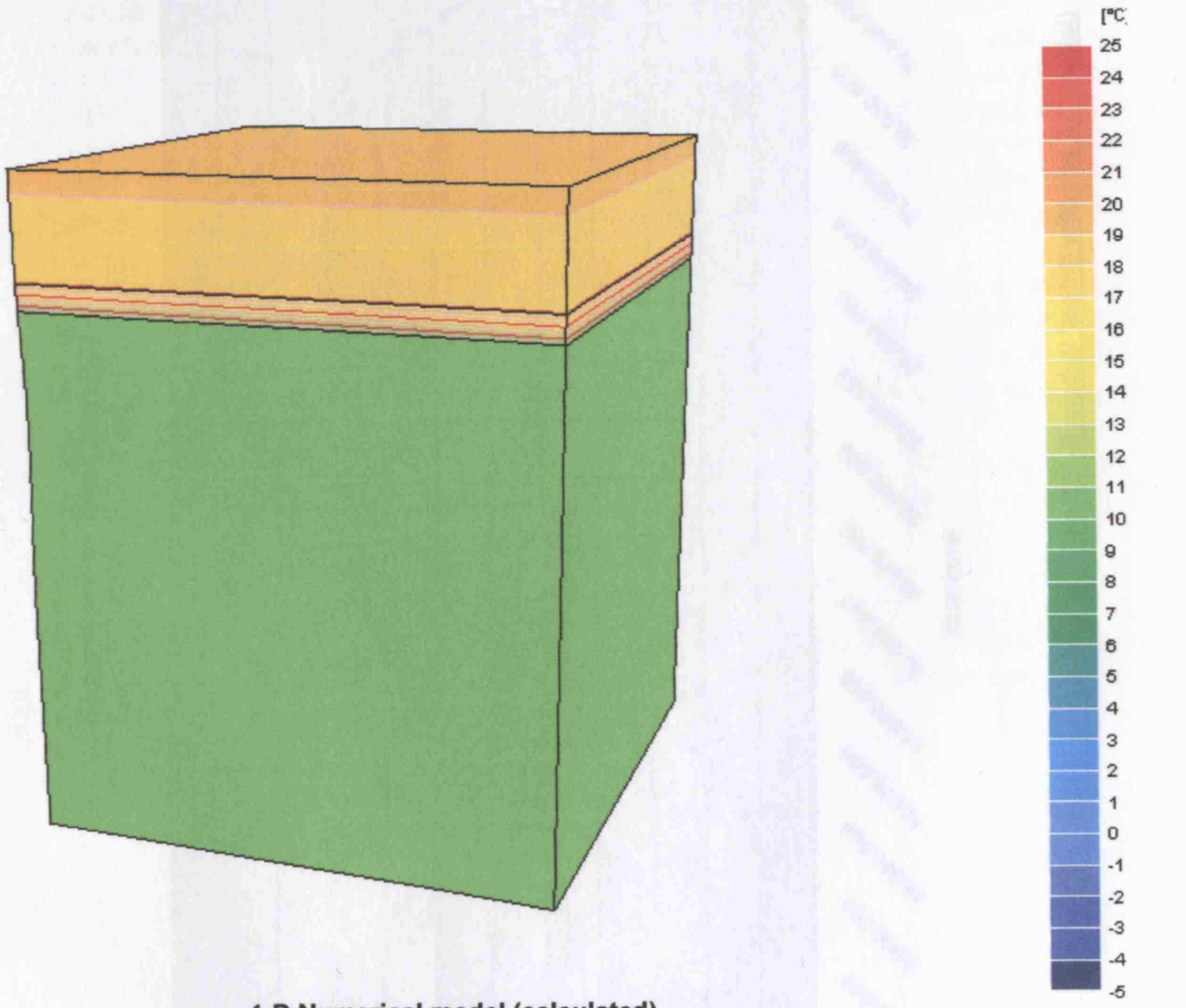

Figure 5.10: Temperature results of the 1-D numerical model's calculation ('match' with the 3-D model)

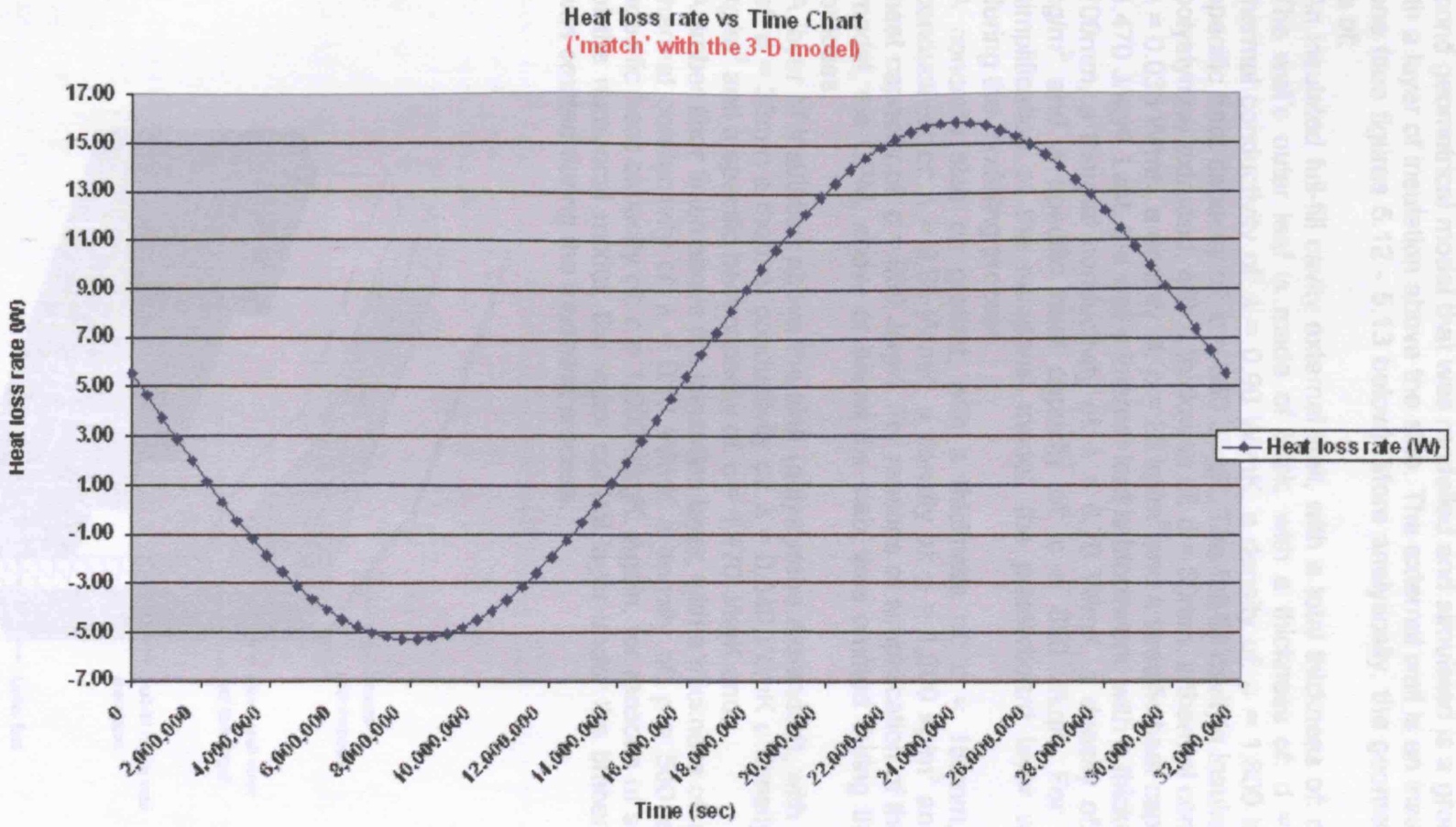

Figure 5.11: Heat loss rate vs Time Chart (1-D model/ 'match with the 3-D model)

5.3.2 Ground bearing floor with insulated cavity wall geometrical model

The second geometrical model that was modelled and simulated is a ground bearing floor with a layer of insulation above the slab. The external wall is an insulated full-fill cavity one (see figures 5.12 - 5.13 below). More analytically, the geometrical model consists of:

- An insulated full-fill cavity external wall, with a total thickness of: d = 300mm. The wall's outer leaf is made of brick, with a thickness of: d = 150mm, a thermal conductivity of: λ = 0.90 W/mK, a density of: ρ = 1,800 kg/m^3 and a specific heat capacity of: c = 850 J/kgK. The full-fill cavity's insulation layer is polystyrene extruded, with a thickness of: d = 50mm, a thermal conductivity of: λ = 0.035 W/mK, a density of: ρ = 25 kg/m^3 and a specific heat capacity of: c = 1,470 J/kgK. Last, the wall's internal leaf is blockwork, with a thickness of: d = 100mm, a thermal conductivity of: λ = 0.70 W/mK, a density of: ρ = 1,600 kg/m^3 and a specific heat capacity of: c = 850 J/kgK. For reasons of simplification of the numerical model, the plasterboard layer was omitted during the modeling process,
- A concrete slab on ground, with a thickness of: d = 150mm, a thermal conductivity of: λ = 0.85 W/mK, a density of: ρ = 1,600 kg/m^3 and a specific heat capacity of: c = 930 J/kgK. For reasons of simplification of the numerical model, the DPM, above or below the slab, was omitted during the modeling process,
- A layer of insulation above the slab (polystyrene expanded), with a thickness of: d = 30mm a thermal conductivity of: λ = 0.040 W/mK a density of: ρ = 20 kg/m^3 and a specific heat capacity of: c = 1,470 J/kgK and,
- A timber floor finish above the insulation layer, with a thickness of: d = 20mm a thermal conductivity of: λ = 0.13 W/mK a density of: ρ = 500 kg/m^3 and a specific heat capacity of: c = 1,600 J/kgK. Again, for reasons of simplification of the numerical model, the vapor control layer under the timber floor finish was omitted during the modeling process.

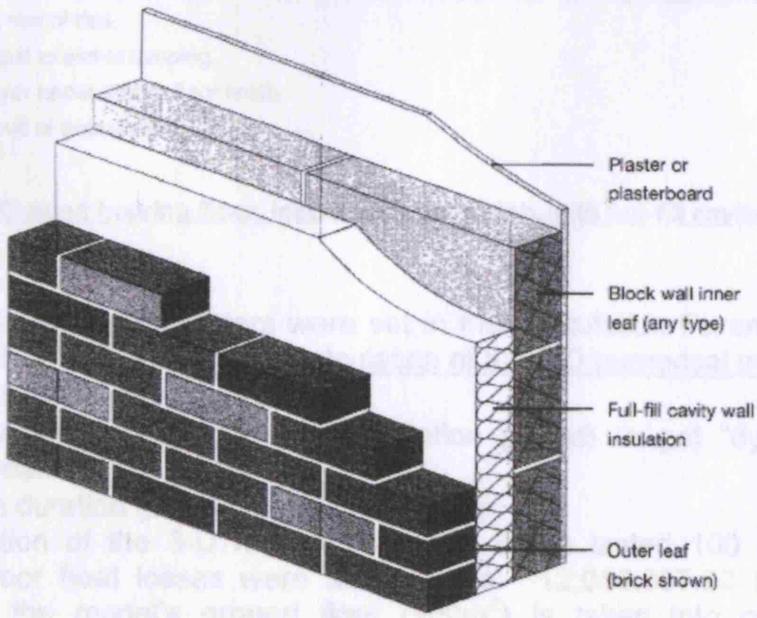

Figure 5.12 - Constructional detail of the full-fill cavity wall [83]

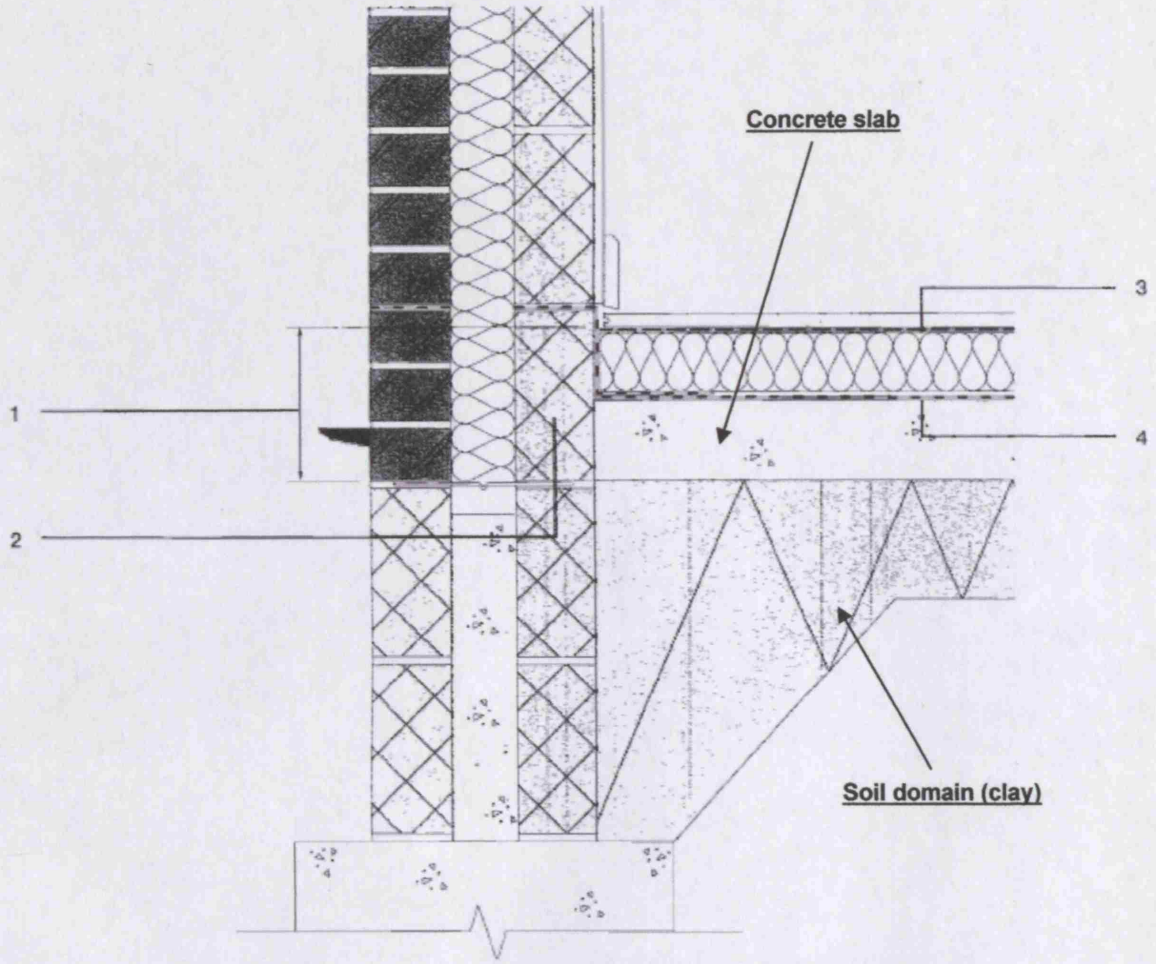

Notes

1. Continue wall insulation at least 150mm below top of floor insulation (or perimeter insulation where screed is used) and support on a row of ties.
2. Course may be split to assist tamping.
3. Vapour control layer under timber floor finish.
4. DPM may be above or below slab.

Figure 5.13 - Ground bearing floor, insulation above slab, with full-fill cavity wall [83]

The following calculation parameters were set in the Calculation Parameters dialog box of the "VOLTRA" software (for the calculation of the 3-D numerical model):

- Time step interval: 5 days.
- Start-up calculation duration (pre-simulation period) to get "dynamic" start values: 1 year.
- Calculation duration (simulation period): 1 year.

After the calculation of the 3-D numerical model, which lasted 100 minutes, the annual ground floor heat losses were found to be: ~12,055,957.92 kJ or, if the surface area of the model's ground floor (100m^2) is taken into consideration: ~120,559.58 kJ/ m^2. Then, the 2-D & 1-D numerical models were 'derived' from the 3-D model, following the procedure described in Chapter 1 - §1.2.

The respective results for the specific models are presented in the Table 5.2 below:

Table 5.2

Numerical model	Annual ground floor heat losses (kJ)	Ground floor surface area (m^2)	Annual ground floor heat losses per unit surface area (kJ/m^2)
Two-dimensional (2-D)	~712,601.28	10	~71,260.13
One-dimensional (1-D)	~9,145.44	1	~9,145.44

Last, the 'equalization' of the 1-D with the 2-D & 3-D models, as far as the annual ground floor heat losses per unit surface area are concerned, was performed. For the 1-D & 2-D models, it was found that, setting the value (in the 1-D model) of the soil thermal conductivity (λ) equal to: ~ 19.16 W/mk (from: 1.5 W/mk), a 'match' of the two models was achieved. As for the 'equalization' process of the 1-D & 3-D models, which is the primary aim of this work, the following results were derived:

- After several simulations with different soil thermal conductivity values for each one, it was found that, setting the value of 'λ' equal to: ~ 51.09 W/mk (from: 1.5 W/mk), a 'match' of the two models was achieved,
- The change of the soil density (ρ) or the soil specific heat capacity (c) values (in the 1-D model) had almost no effect on the 'equalization' process of the two specific numerical models,
- The soil depth of the 1-D model again turned out to be the most significant simulation parameter, as far as its influence on the annual ground floor heat losses per unit surface area and, consequently, on the 'equalization' process is concerned. A **90%** decrease of the initial soil depth (from: 50m to 5m) increased the annual ground floor heat losses by: **~1,800%** (from: **~9,145.44 kJ/m^2** to: **~164,661.12 kJ/m^2**), while a **98%** decrease of the soil depth (from: 50m to 1m) increased the annual ground floor heat losses by: **~2,091%** (from: **~9,145.44 kJ/m^2** to: **~191,289.60 kJ/m^2**)! In this specific case (soil depth: 1m), the annual ground floor heat losses per unit surface area derived from the 1D model - as in "TAS" simulations - were: **~158.67%** of the 3-D model's respective ones **(~120,559.58 kJ/m^2)**, which best represents the real conditions, due to the 3-D nature of the heat transfer. Last, setting the value of the soil depth equal to: 15.507m (from: 1m), a 'match' of the two models was achieved and,
- 'Removing' the insulation layer above the floor slab did not, surprisingly, bring about any changes in the annual ground floor heat losses (per unit surface area). The specific 1-D model is presented in the following page (figure 5.14):

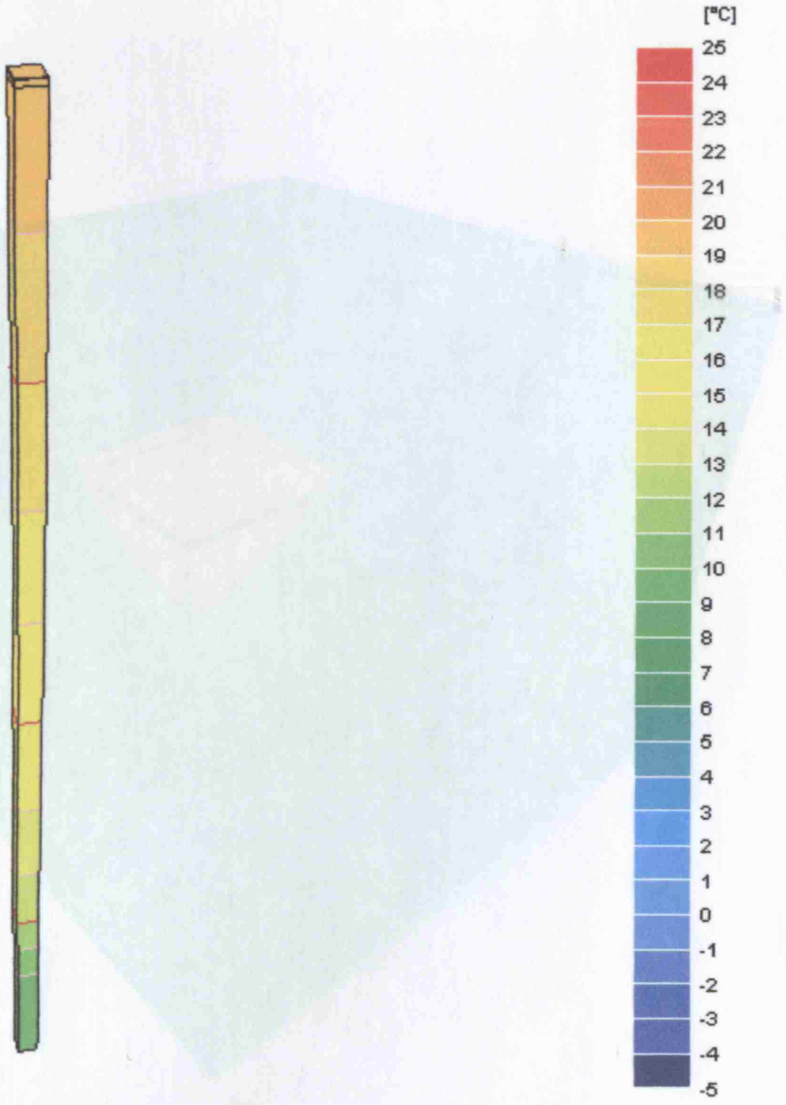

1-D Numerical model (calculated)
No insulation layer above the slab

Temperature range

Figure 5.14: Temperature results of the 1-D numerical model's calculation (no insulation above slab)

The initial 3-D & 2-D models, as well as, the 1-D numerical models that, 'matched' them, as far as the annual ground floor heat losses per unit surface area are concerned, along with a graphical representation of these models heat loss rate (W) change in relation with time (sec), are presented in the figures 5.15-5.25 below. A detailed presentation of the whole 'equalization' process is made in the attached Appendix D.

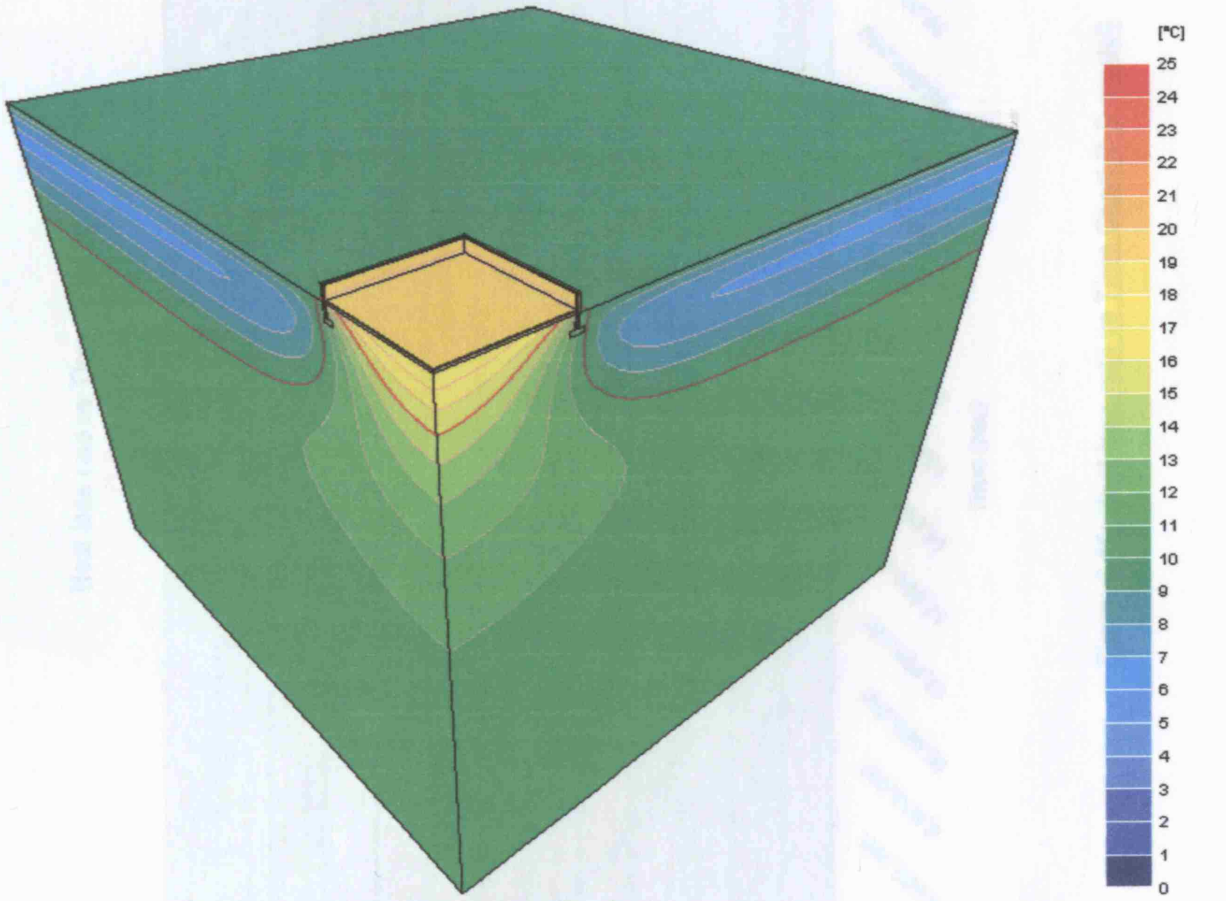

Initial 3-D Numerical model (calculated) **Temperature range**

Figure 5.15: Temperature results of the 3-D numerical model's calculation

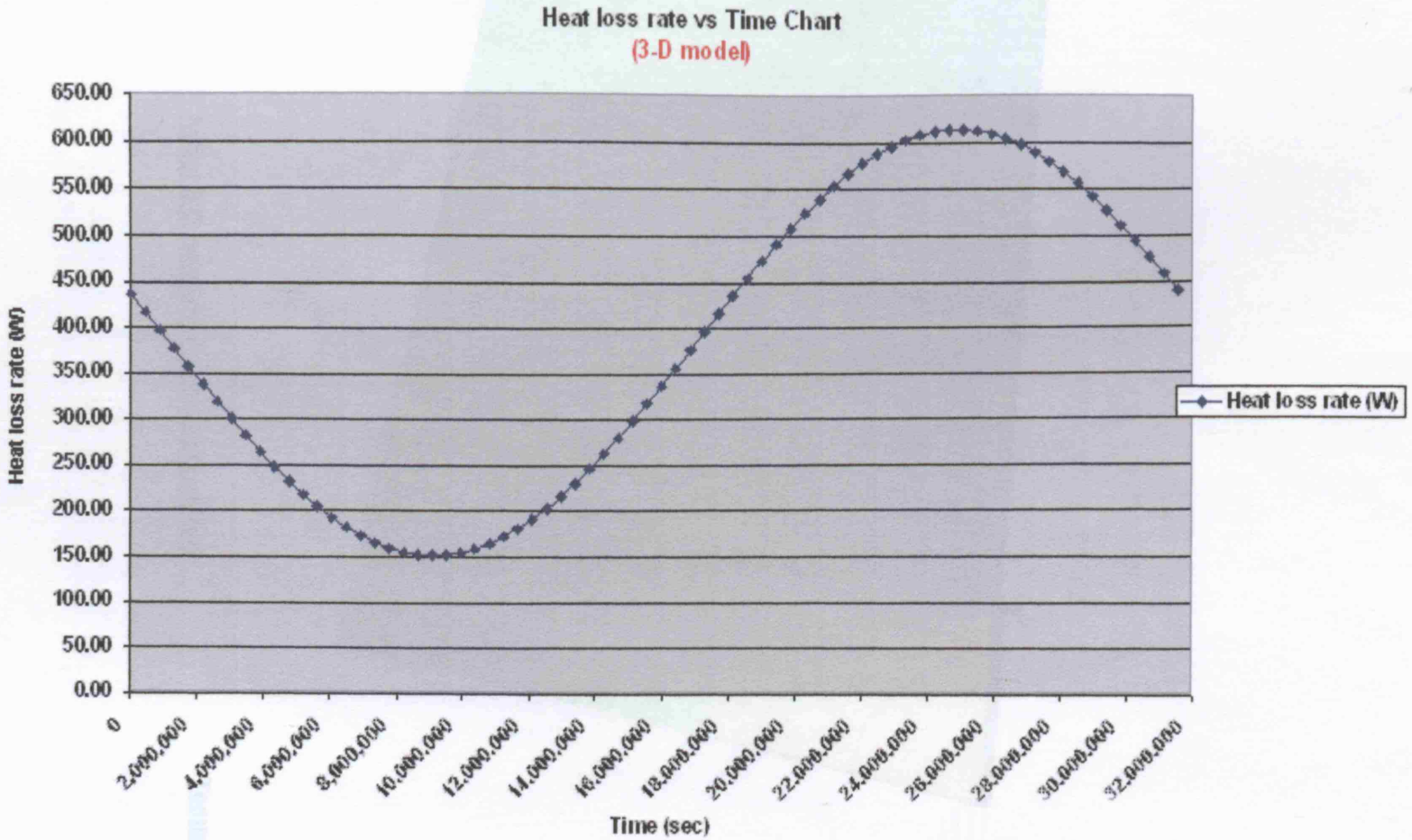

Figure 5.16: Heat loss rate vs Time Chart (3-D model)

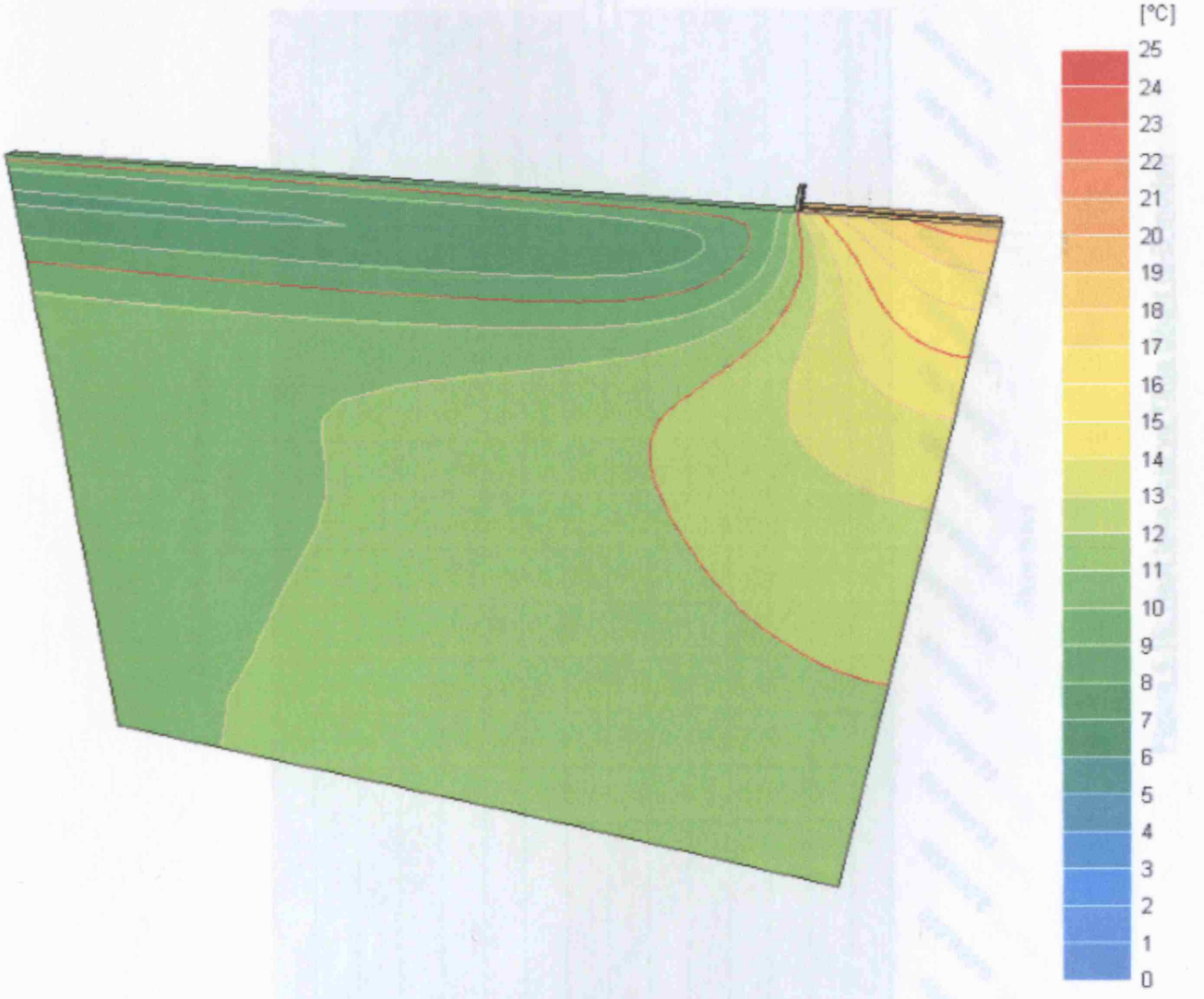

Figure 5.17: Temperature results of the 2-D numerical model's calculation

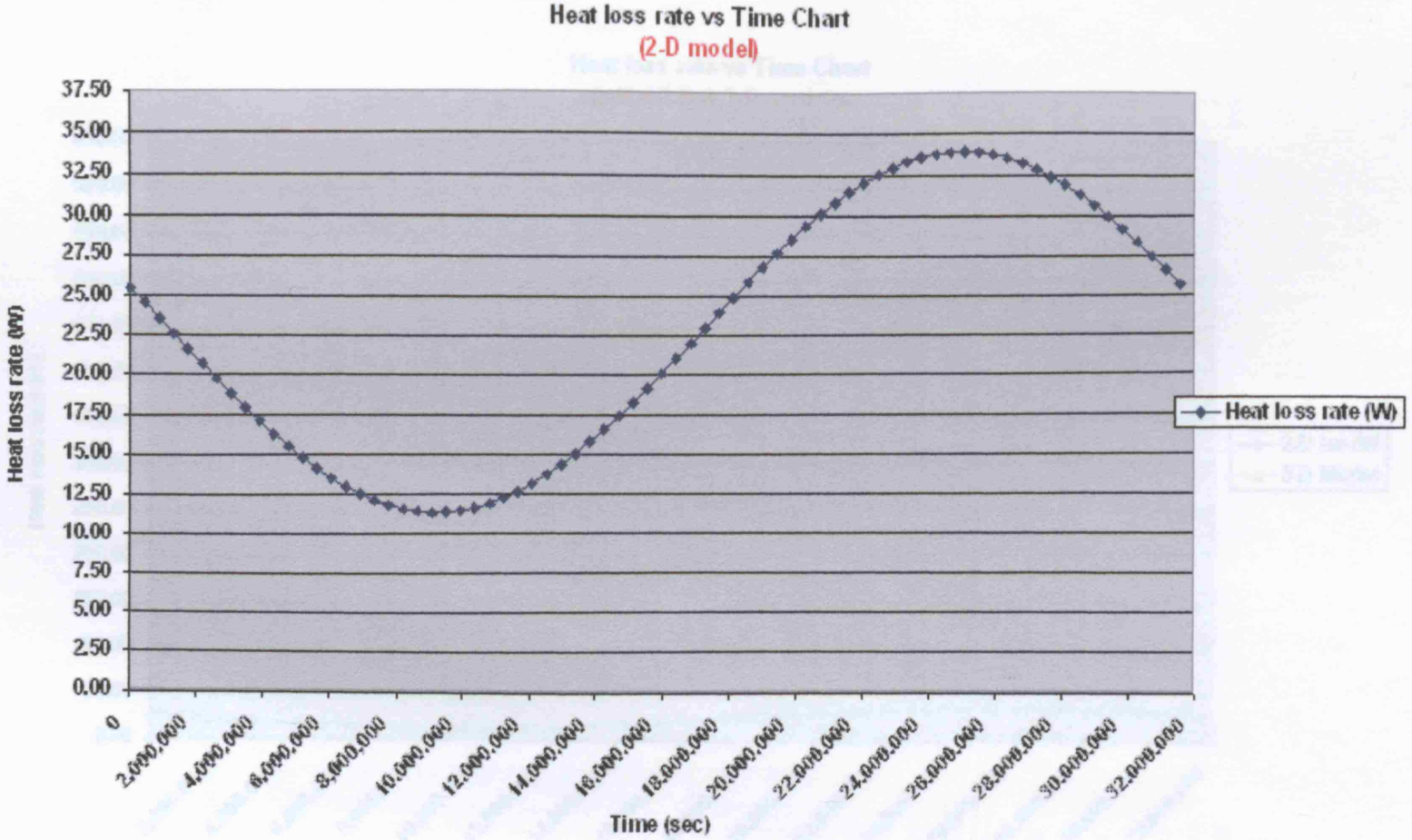

Figure 5.18: Heat loss rate vs Time Chart (2-D model)

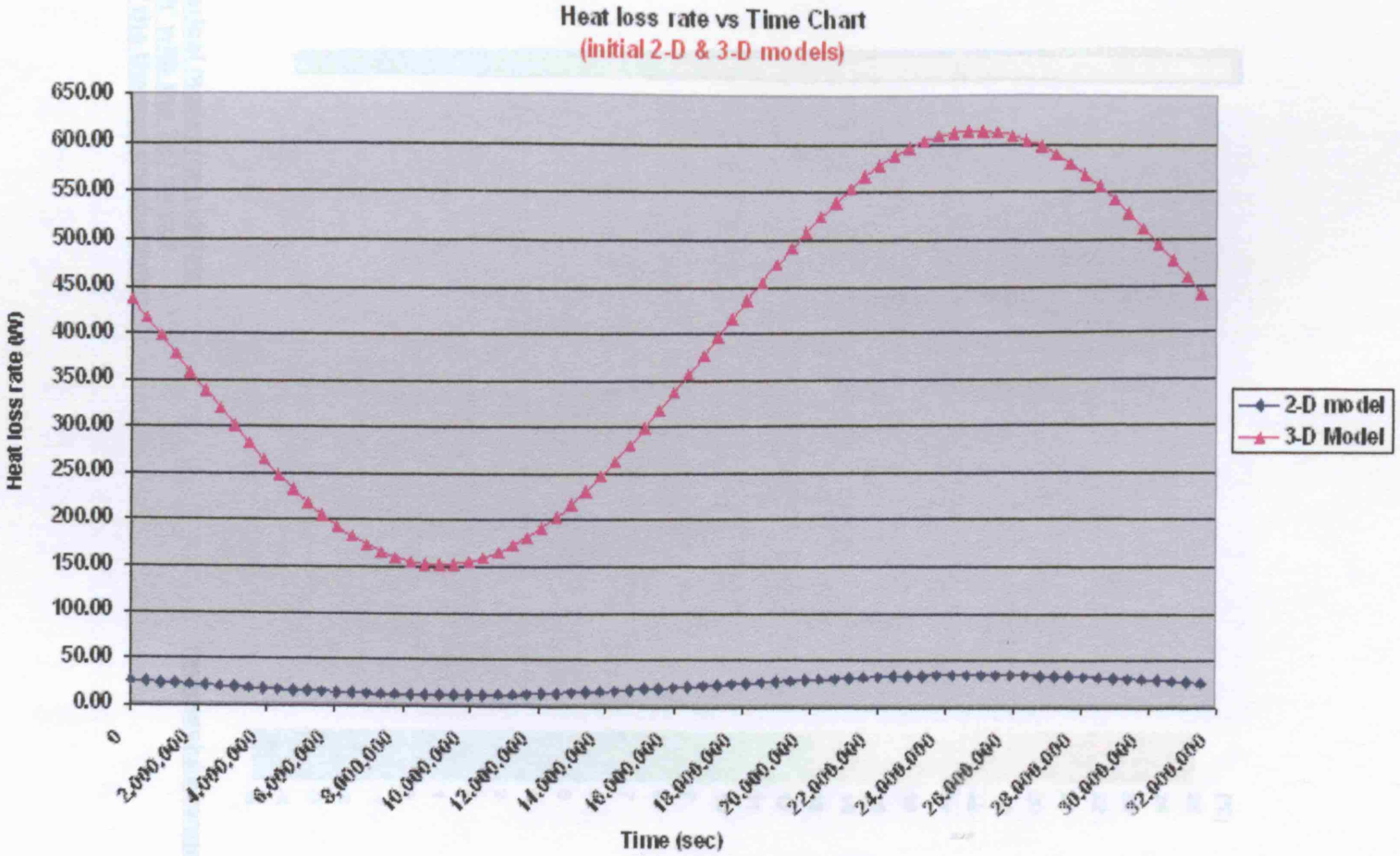

Figure 5.19: Heat loss rate vs Time Chart (3-D vs 2-Dmodel)

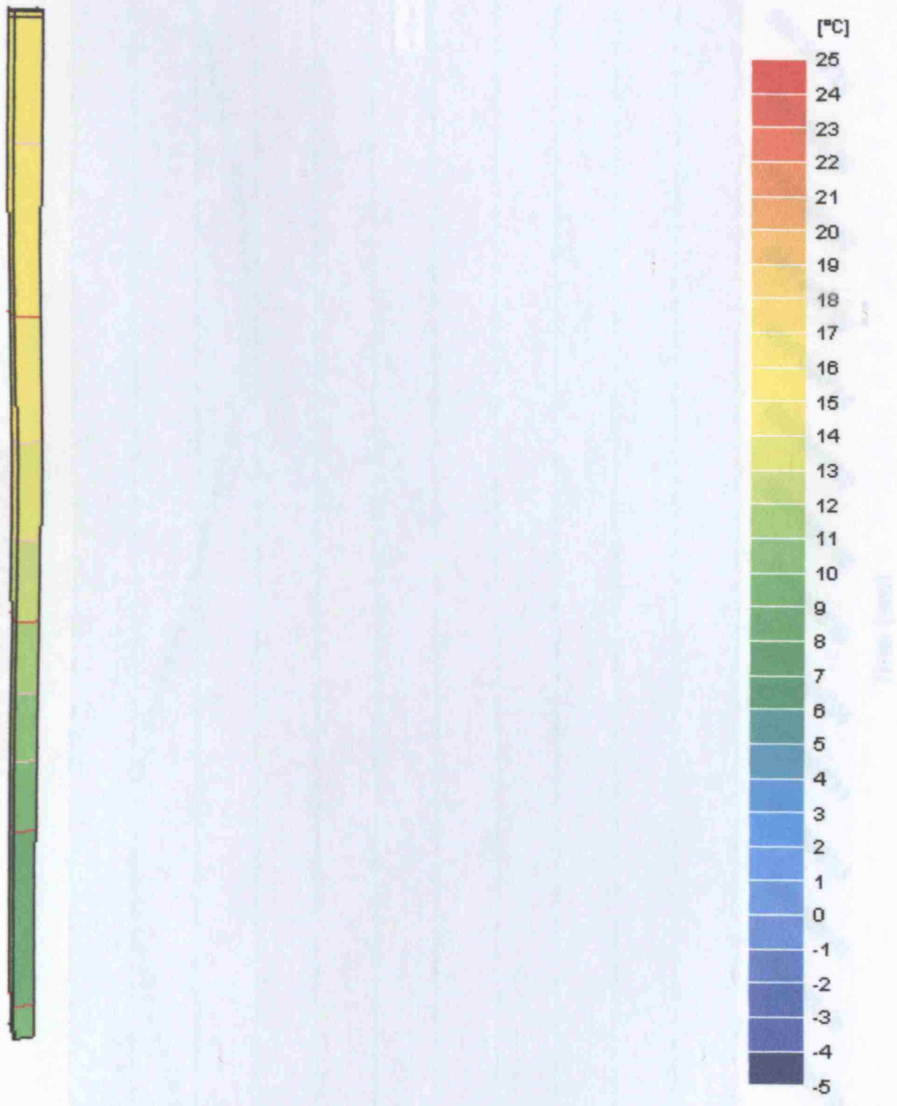

Figure 5.20: Temperature results of the 1-D numerical model's calculation ('match' with the 2-D model)

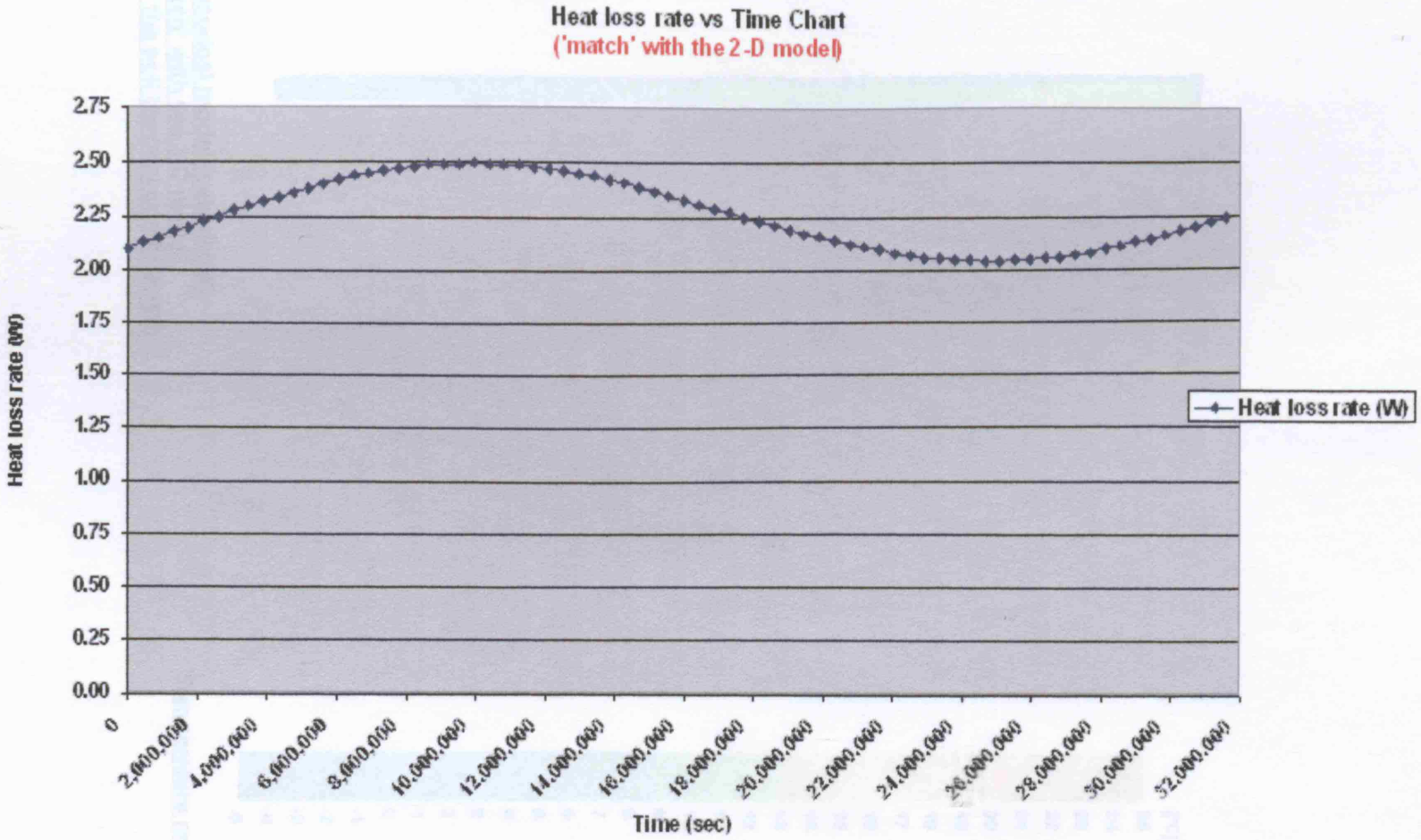

Figure 5.21: Heat loss rate vs Time Chart ('match' with the 2-D model)

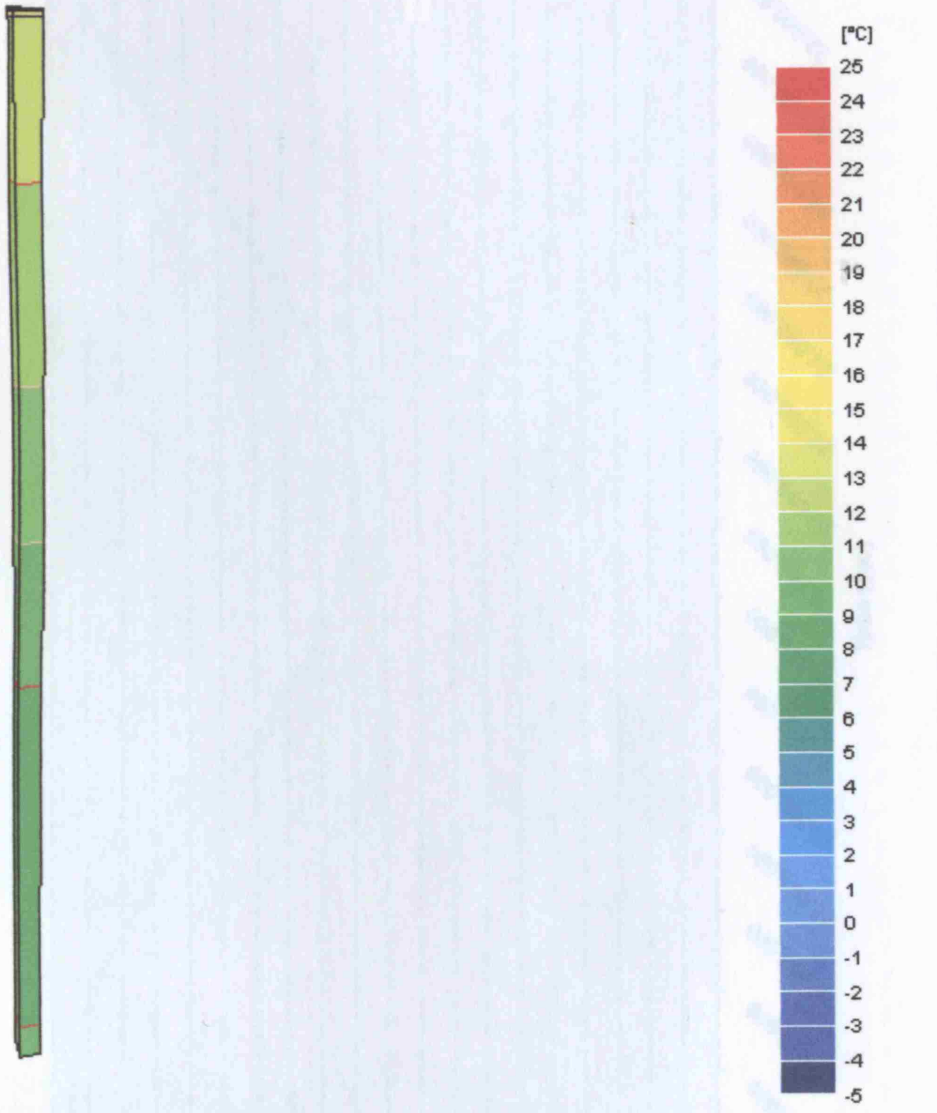

Figure 5.22: Temperature results of the 1-D numerical model's calculation ('match' with the 2-D model, due to change of the soil thermal conductivity)

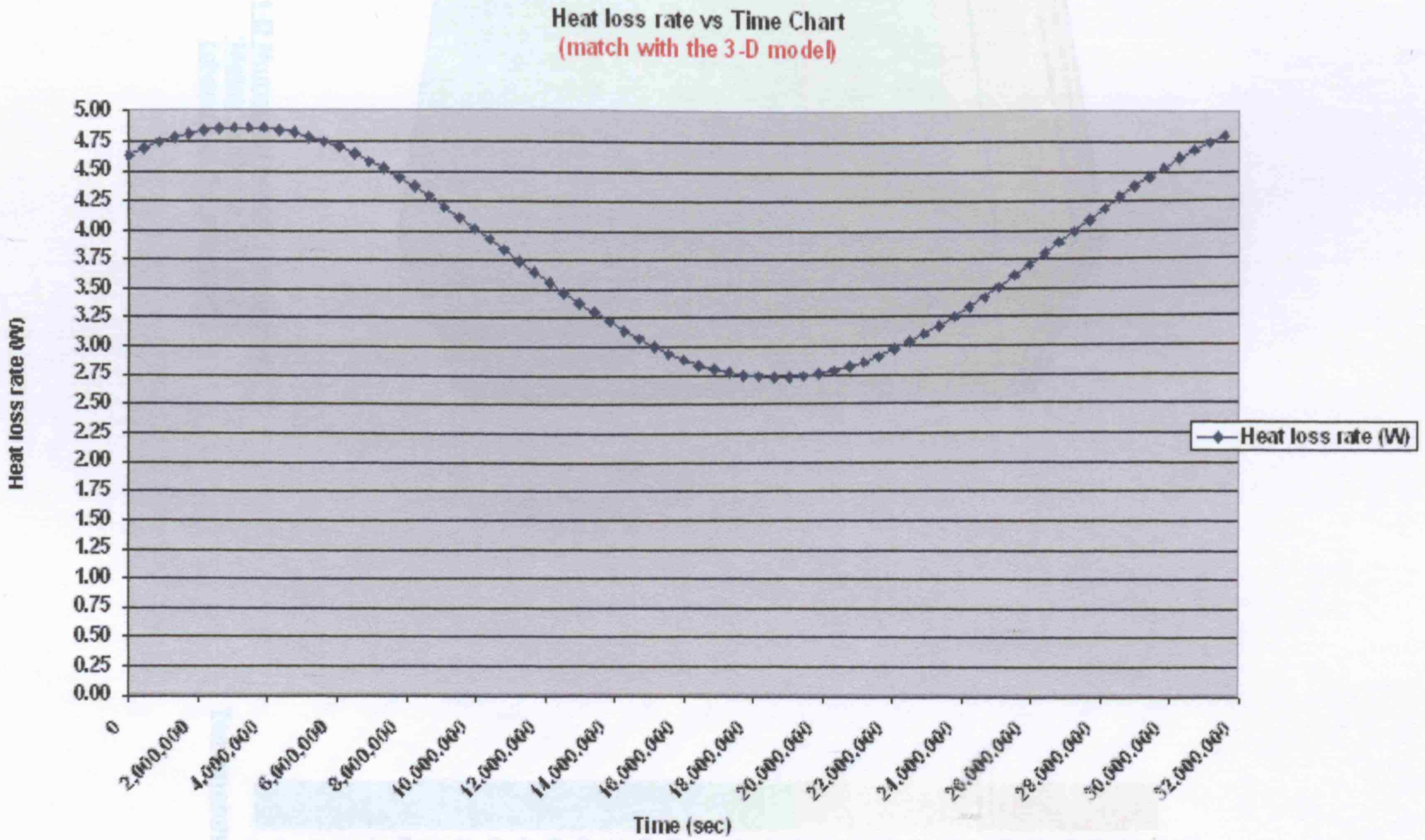

Figure 5.23: Heat loss rate vs Time Chart
(1-D model/ 'match' with the 3-D model due to change of the soil thermal conductivity)

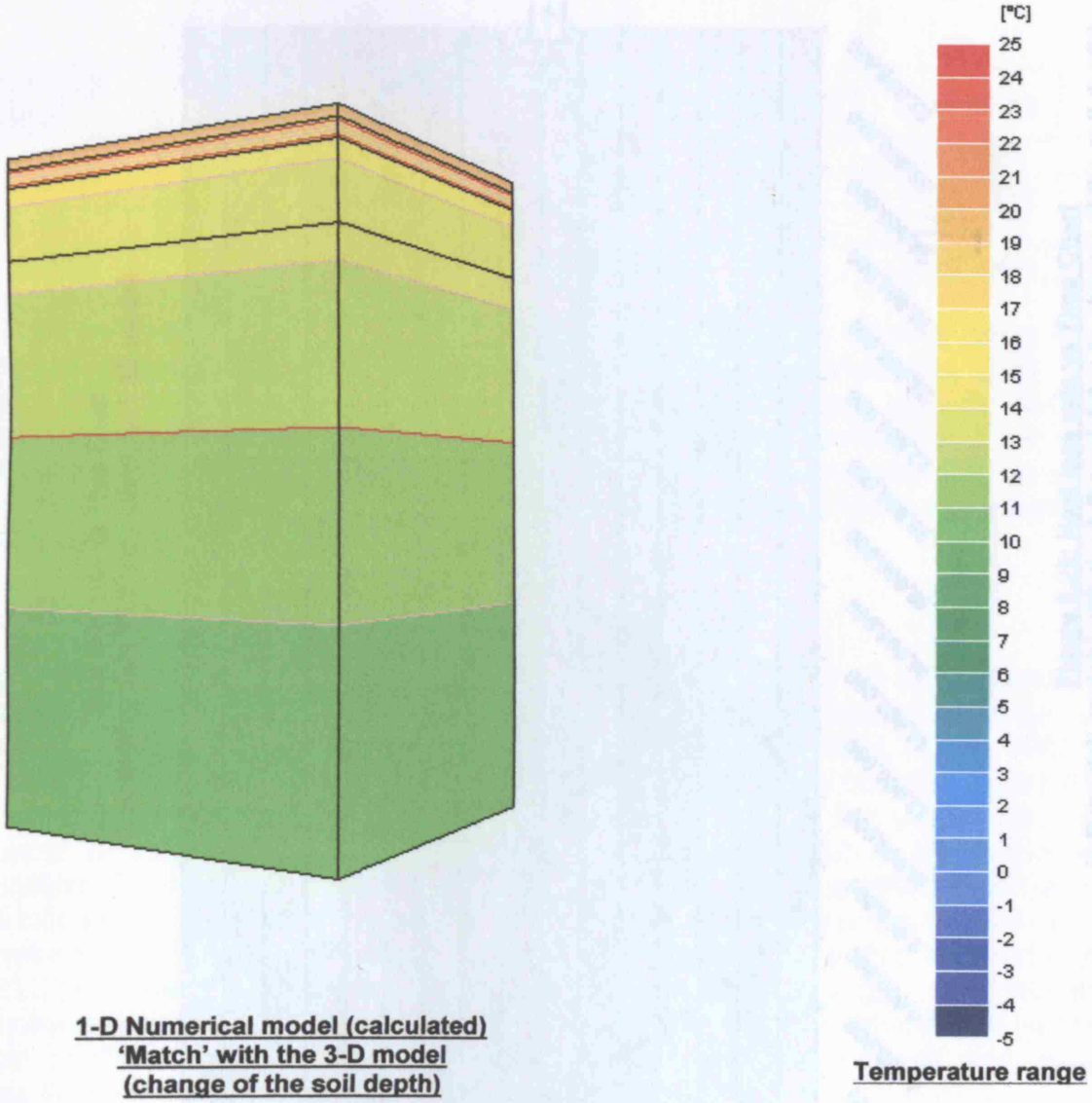

Figure 5.24: Temperature results of the 1-D numerical model's calculation ('match' with the 2-D model, due to change of the soil depth)

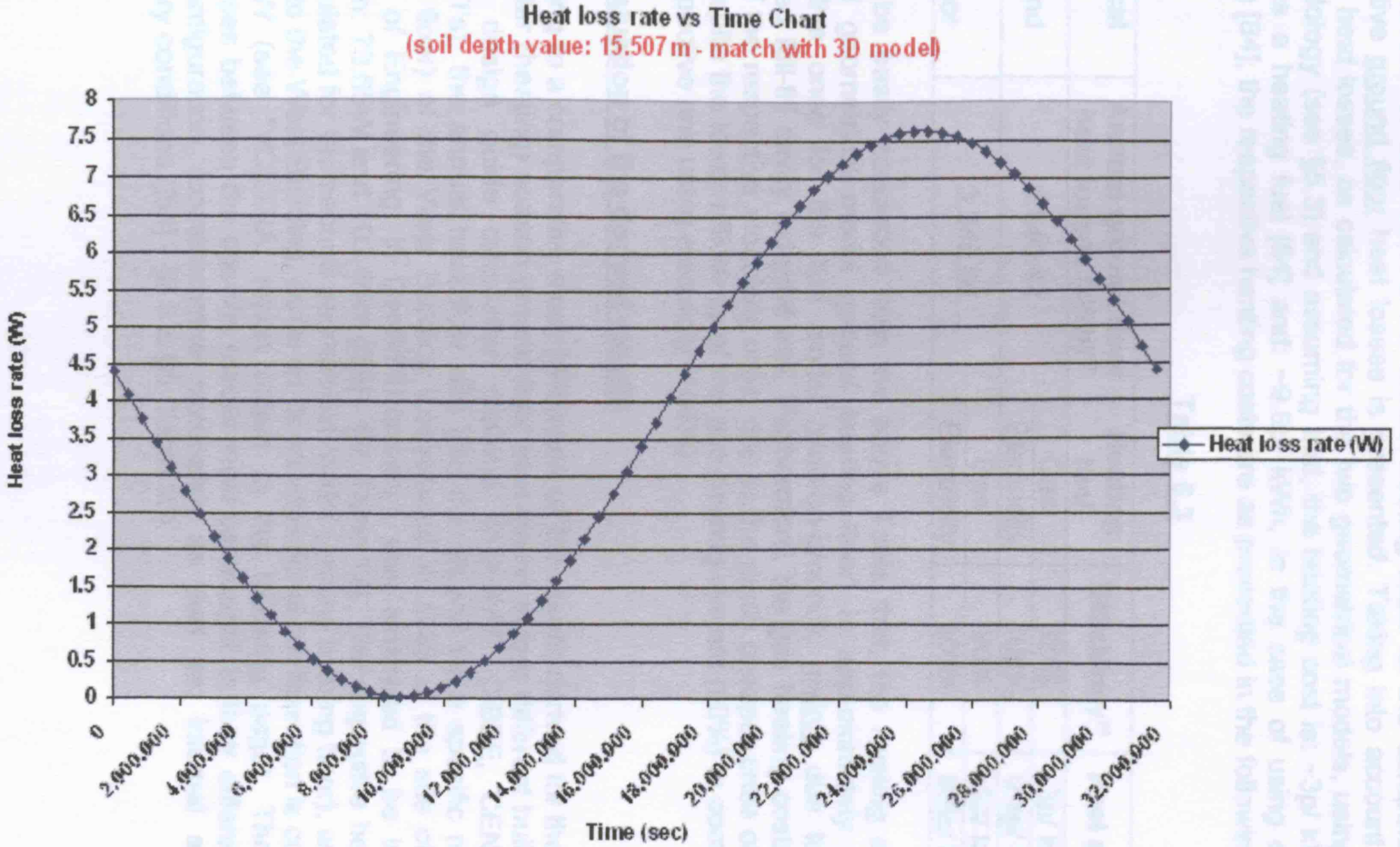

Figure 5.25: Heat loss rate vs Time Chart
(1-D model/ 'match' with the 3-D model due to change of the soil depth)

5.4 Heating costs

In this section an estimation of the annual heating costs for the 'compensation' of the respective ground floor heat losses is presented. Taking into account the specific annual heat losses, as calculated for the two geometrical models, using this work's methodology (see §5.3) and assuming that, the heating cost is: ~3p/ kWh, if gas is used as a heating fuel [84] and: ~9.8p/ kWh, in the case of using electricity for heating [84], the respective heating costs are as presented in the following Table 5.3:

Table 5.3

Geometrical model	Annual ground floor heat losses (kWh)[18]	Heating fuel	Efficiency[19]	Fuel price	Heating cost (£)
Slab-on-ground	5,640.42	Gas	90%	3p/ kWh	**188.01**
		Electricity	100%	9.8p/ kWh	**552.76**
Ground bearing floor	3,348.88	Gas	90%	3p/ kWh	**111.63**
		Electricity	100%	9.8p/ kWh	**328.19**

It can be easily concluded from the above Table that, the heating costs for the second geometrical model (ground bearing floor) is approximately 60% of the respective ones for the first model (slab-on-ground), mainly due to the better insulated full-fill cavity external wall. Furthermore, the gas heating costs are almost 34% of the respective electricity ones, due to the much cheaper price of natural gas and despite the lower efficiency of the gas heating system (90%) in comparison with the respective one using electricity (100%).

5.5 Evaluation of the derived results

According to a comparative study [54] made on the results derived for the annual and the winter (heating) season ground floor heat losses in four different buildings, using various design guide calculation methods (ASHRAE, CIBSE, CEN, AICVF & KRARTI's), the annual heat flow rate into the ground for a specific region (lower ground floor) of the West Building (constructed in 1989 at the site of the Cardiff School of Engineering, in Cardiff University), was estimated to be in the range between: 73.65W and 103.45W {[54] - §6, Table 12}. The respective heat flow rate, as calculated for the second geometrical model (ground bearing floor), which is more similar to the West Building, as far as its constructional configuration is concerned, is: 383.06W (see "VOLTRA" report output in the following page). The 'observed' differences between the specific results must be 'sought' in their different geometry and configuration (constructional materials), as well as, internal and external boundary conditions {[54] - §2.3 & §6, Table 10}.

[18]: 1kJ = 10^{-3}MJ = 10^{-3}x (1/3.6) kWh ~ 2.78x10^{-4}kWh [85]

[19]: A gas condensing boiler with 90% efficiency is assumed for the gas heating system.

VOLTRA Report Output

VOLTRA data file: Slab on ground_Cavity wall_2years_5days_sin_prec.vtr

Column 1: Time [sec]
Column 2: Colour 12, sum of heat flows into object (ground floor) [W]
Column 3: Colour 12, sum of heat flows out of object (ground floor) [W]

Column 1	Column 2	Column 3
0	436.27	0.00
432000	416.89	0.00
864000	397.24	0.00
1296000	377.47	0.00
1728000	357.72	0.00
2160000	338.14	0.00
2592000	318.87	0.00
3024000	300.07	0.00
3456000	281.86	0.00
3888000	264.39	0.00
4320000	247.78	0.00
4752000	232.15	0.00
5184000	217.63	0.00
5616000	204.32	0.00
6048000	192.33	0.00
6480000	181.73	0.00
6912000	172.61	0.00
7344000	165.03	0.00
7776000	159.06	0.00
8208000	154.74	0.00
8640000	152.10	0.00
9072000	151.15	0.00
9504000	151.92	0.00
9936000	154.38	0.00
10368000	158.53	0.00
10800000	164.33	0.00
11232000	171.74	0.00
11664000	180.71	0.00
12096000	191.17	0.00
12528000	203.05	0.00
12960000	216.24	0.00
13392000	230.67	0.00
13824000	246.22	0.00
14256000	262.77	0.00
14688000	280.21	0.00
15120000	298.41	0.00
15552000	317.22	0.00
15984000	336.52	0.00
16416000	356.16	0.00
16848000	375.99	0.00
17280000	395.87	0.00
17712000	415.66	0.00
18144000	435.19	0.00
18576000	454.34	0.00
19008000	472.95	0.00
19440000	490.90	0.00
19872000	508.05	0.00
20304000	524.26	0.00
20736000	539.43	0.00
21168000	553.44	0.00

Column 1	Column 2	Column 3
21600000	566.19	0.00
22032000	577.57	0.00
22464000	587.52	0.00
22896000	595.95	0.00
23328000	602.80	0.00
23760000	608.03	0.00
24192000	611.59	0.00
24624000	613.45	0.00
25056000	613.61	0.00
25488000	612.06	0.00
25920000	608.82	0.00
26352000	603.90	0.00
26784000	597.35	0.00
27216000	589.22	0.00
27648000	579.55	0.00
28080000	568.44	0.00
28512000	555.95	0.00
28944000	542.18	0.00
29376000	527.24	0.00
29808000	511.23	0.00
30240000	494.27	0.00
30672000	476.49	0.00
31104000	458.02	0.00
31536000	439.00	0.00

Average heat flow rate into the ground floor: 383.06W

Chapter 6

Conclusions

In the work presented hereby, an estimation of the annual ground floor heat losses using a 1-D numerical model was attempted. Two different geometrical models (constructional details of buildings ground floors) were modelled and simulated, using the thermal analysis computer programs: "TRISCO" & "VOLTRA" and the respective annual heat losses (per unit surface area) were estimated.
Prior to the modelling and simulation of the specific geometrical models, the buildings heat losses via the ground 'phenomenon' was briefly, but concisely, described. The presentation in question started with an analysis of the ground heat transfer mechanisms and the most important soil thermal properties which influence the specific 'phenomenon': the soil thermal conductivity and the soil (volumetric) heat capacity. A mention made of the available calculation methods of the buildings heat losses via the ground continued the presentation of the specific 'phenomenon'. While the influence of the soil stratification and the ground water flow on the phenomenon was very briefly presented, special attention was given to the respective one of the soil moisture transfer. The fact that, the couplings between soil heat and soil moisture transfer cannot be assumed having a negligible influence was highlighted, analyzed and commented.
After the presentation of the buildings heat losses via the ground 'phenomenon', as summarily described previously and before the modelling and simulation of the two 'main' geometrical models examined within the context of this work, a validation of the methodology used for the estimation of the annual ground floor heat losses ("TRISCO" & "VOLTRA" thermal analysis computer programs) was attempted. For this purpose, three 'trial' numerical models (one of 1-D, one of 2-D and one of 3-D heat transfer) were tested. The respective results derived, verified the high precision of the used methodology.
As far as the numerical simulation of the two 'main' geometrical models is concerned, the results derived for the annual ground floor heat losses from the 3-D ones - namely, the numerical models which best represent the buildings heat losses via the ground 'phenomenon', due to the 3-D nature of the heat transfer - were in relatively good agreement with respective measurements taken for the heat losses of the West Building's ground floor in Cardiff University [54], which represents a building suitable for such a comparison, as far as its location (UK) and constructional configuration are concerned. The calculated heating costs, necessary the 'compensation' of the 3-D models' annual ground floor heat losses, are also considered to be realistic.

Regarding the primary aim of the work presented hereby, which is the 'equalization' of the 1-D with the respective 3-D numerical model as far as the annual ground floor heat losses per unit surface area are concerned or, in other words, the estimation of the specific heat losses using a 1-D numerical model, the results derived, showed that, the most significant - the one with the greatest influence - simulation parameter for this aim to be achieved, is the soil depth. This is completely expected, since, in the 1-D numerical models, the soil depth represents the heat 'getaway' path. The shorter the length of this path (soil depth), the bigger the rate of heat being transferred from indoors to outdoors via the buildings ground floors and the ground (soil) itself and so, the greater the amount of the (annual) heat losses through the specific building element.

The soil thermal conductivity (λ) is the second most influential simulation parameter on the 'equalization' process of the 1-D & 3-D numerical models, as derived by the various numerical calculations performed. This is expected, too, since the thermal conductivity of a material represents the rate at which heat is transferred by conduction to the temperature gradient.

While the results derived, demonstrated the significant influence of the soil thermal conductivity on the 'equalization' process of the 1-D & 3-D numerical models, the same does not apply for two other soil thermal properties: the density (ρ) and the specific heat capacity (c). The respective results derived from the relevant numerical calculations performed, showed that, the influence of the specific soil thermal properties on the annual ground floor heat losses is insignificant.

As far as the errors possibly introduced in the process of estimating the annual buildings ground floors heat losses using a 1-D numerical model (simulation of the heat transfer process in one-dimension) are concerned, a first step towards this 'direction' was made in this work. In the various such simulations tools (like "TAS" thermal analysis software) used for the estimation of the heat losses (gains) - those through the buildings ground floors included - it is a common practice that, the soil is modelled with a depth of: 1m. However, the results derived from the numerical simulation of the two 'main' geometrical models examined herein, showed that, there is a great discrepancy (approximately: -38% for the first and: +59% for the second model) between the 3-D numerical models - which best represent the real conditions, due to the three-dimensional nature of the heat transfer through the ground - and the respective 1-D ones, which 'incorporate' a soil depth of: 1m - as, namely, generally happens when using the specific simulation tools. In order for the specific discrepancies to be 'eliminated', a soil depth of: 1m (instead of: 50m - correct value), but with a soil thermal conductivity of: 17.31W/mK (instead of: 1.5W/mK - correct value), was defined for the first and of: 50m, along with a soil thermal conductivity of: 51.09W/mK (instead of: 1.5W/mK - correct value), for the second numerical model, as 'revealed' by the 'equalization' process in each case. It is concluded, therefore, from the aforementioned that, the common practice of modelling the soil with a depth of: 1m, when estimating (annual) ground floor heat losses using a 1-D numerical model, is not completely correct, but bigger or smaller discrepancies occur. Furthermore, the definition of the 'proper' soil depth value depends on the specific numerical model (its geometry, configuration and simulation parameters), as well as, the soil type and its thermal properties, the thermal conductivity being the most significant one. Consequently, it is strongly recommended that, when estimating (annual) ground floor heat losses (gains) using a 1-D numerical model, a 'correction factor' should be taken into account in the relevant calculations. This factor depends on the specific case and can only be calculated precisely using a 3-D numerical model, as in this work.

On the other hand, taking into consideration that, the 3-D numerical models best represent the estimation of the annual ground floor heat losses, the calculation of the 'derived' initial 2-D & 1-D numerical models (following the procedure described in Chapter 1 - §1.2), for the both geometrical models examined in this work, showed that, the annual ground floor heat losses per unit surface area estimated by the specific 2-D models are approximately: 58% of the 3-D models' respective ones, while the heat losses estimated by the 1-D models, are about: 5.5% of the 3-Ds' respective ones.
It must be noted, however, at this point that, the aforementioned conclusions, drawn from the results given by the numerical modelling and simulation of the two 'main' geometrical models (constructional details) examined in this work, refer only to the specific numerical models and simulation parameters, namely: geometry and constructional configuration of the models, boundary conditions (internal & external), pre-simulation and main simulation period, simulation time step and grid refinement, as well as, size of the physical domain and thermal properties of the soil beneath each model's ground floor. This means that, different, for example, external boundary conditions - possibly taking into account the effect, of snow coverage, precipitation amount or vegetation, which, however, cannot be simulated with the specific version of the thermal analysis computer program used in this work [20] - or time dependent soil thermal properties - possibly also accounting for the effect of the couplings between soil heat and soil moisture transfer, which, again, is not possible with "VOLTRA's" specific version [20] - would lead to different results and, probably, to different conclusions from the ones mentioned previously, as far as the significance of the (1-D numerical model's) soil depth or the soil thermal conductivity in the 'equalization' process of the 1-D & 3-D numerical models or, even more, the definition of the 'proper' soil depth value when estimating ground floor heat losses (gains) using a 1-D numerical model, are concerned. Therefore, a generalization of the specific conclusions should be avoided.
Last, a brief mention of the limitations imposed during the elaboration of this work is considered both necessary and useful to be made. The PCs used for the numerical modelling and simulation of the two 'main' geometrical models, as well as, the specific version of "VOLTRA" itself [20], did not allow, due to practical ('incompatibility' of the computer program's hardware key with USB ports, PCs' and computer program's limited capacities) and temporal (submission deadline of this work) constraints, further 'development' of this work, as far as the modelling and simulation of some more geometrical models are concerned. It is the author's strong belief, nevertheless, that, the numerical models examined herein, achieved sufficiently the aim of this work.

Acknowledgements

The work presented hereby was completed thanks to the undivided attention, help and guidance from both: Dr Mike Davies and Dr Dejan Mumovic. Therefore, their contribution to the completion of this work is gratefully acknowledged.

References

[1] Mulholland J., Dr Howard St., Roberts C. Best practice series, Vol. 4: Energy management in buildings. Lincoln: Institute of Environmental Management & Assessment, 2003.

[2] Clarke JA, Maver TW. Advanced design tools for energy conscious building design: development and dissemination. Building and Environment 1991;26:25-34.

[3] Rees S.W., Adjali M.H., Zhou Z., Davies M., Thomas H.R. Ground heat transfer effects on the thermal performance of earth-contact structures. Renewable and Sustainable Energy Reviews 2000;4:213-265.

[4] The Building Regulations 2000, Approved Document L1: Conservation of fuel and power in dwellings, 2002 ed. Office of the Deputy Prime Minister, 2002.

[5] The Building Regulations 2000, Approved Document L1A: Conservation of fuel and power in new dwellings, 2006 ed. Office of the Deputy Prime Minister, 2006.

[6] Claridge DE. Design methods for earth-contact heat transfer. In: Boer K, editor. Advances in solar energy. Boulder, CO: American Solar Energy Society, 1987; p. 305-50.

[7] Shipp PH. Basement, crawlspace, and slab-on-grade thermal performance. In: Proc. Of ASHRAE/DOE Conference on Thermal Performance of the Exterior Envelopes of Buildings, Las Vegas, Nevada, 6-9 December, 1983; p. 160-79.

[8] Claesson J., Hagentoft C.-E. Heat loss to the ground from a building - I. General theory. Building and Environment 1991;26(2):195-208.

[9] Bahnfleth WP. Three-dimensional modelling of heat transfer from slab floors. Technical Manuscript, USA Construction Engineering Research Laboratory, 1989; p.194.

[10] Adjali M.H., Davies M., Littler J. Earth-contact heat flows: review and application of guidance predictions, Building Services Eng. Res. Technol. 1998;19 (3): 111-121.

[11] Adjali M.H., Davies M., Ni Riain C., Littler MA J.G. In situ measurements and numerical simulation of heat transfer beneath a heated ground floor slab. Energy and Buildings 2000;33: 75-83.

[12] Janssen H. The influence of soil moisture transfer on building heat loss via the ground. Ph.D. thesis, Catholic University of Leuven, Belgium, 2002.

[13] Janssen H., Carmeliet J., Hens H. The influence of soil moisture transfer on building heat loss via the ground. Building and Environment 2004;39: 825 - 836.

[14] Deru M. A model for ground-coupled heat and moisture transfer from buildings, Ph.D. thesis, Colorado State University, United States, 2001.

[15] Bahnfleth WP. A three-dimensional numerical study of slab-on-grade heat transfer, Ph.D. thesis, University of Illinois, United States, 1989.
[16] Hagentoft C.-E. Heat loss to the ground from a building. Ph.D. thesis, Lund University of Technology, Sweden, 1988.
[17] Anderson BR. Calculation of the steady-state heat transfer through a slab-on-ground floor, Building and Environment 1991;26: 405-15.
[18] TRISCO: computer program to calculate 3D & 2D steady-state heat transfer in objects described in a rectangular grid using the energy balance technique Version 10.0w - 2002 PHYSIBEL.
[19] Principles of heat transfer [online]. Available from: <http://canteach.candu.org/library/20043804.pdf> [Accessed June 23 2006].
[20] VOLTRA: computer program to calculate 3D & 2D transient heat transfer in objects described in a rectangular grid using the energy balance technique - Version 4.0w - 2003 PHYSIBEL.
[21] Transient heat transfer [online]. Available from: <http://www.algor.com/products/analysis_types/thermal/trans_therm.asp> [Accessed July 19 2006].
[22] Adjali M.H., Davies M., Littler J. Three-dimensional earth-contact heat flows: a comparison of simulated and measured data for a buried structure. Renewable Energy 1998;15: 356-359.
[23] BSI: BS EN ISO 7345. Thermal insulation - Physical quantities and definitions. British Standards Institution, London, UK, 1996.
[24] Wakao N., Kato K. Effective thermal conductivity of packed beds. Journal of Chemical Engineering of Japan 1969;2(1): 24-33.
[25] De Vries D.A. The thermal conductivity of soil, Mededelingen van de Landbouwhogeschool te Wageningen, 52(1);1952:1-73, [Translated by Building Research Station (Library Communication No. 759), UK].
[26] Rees S.W., Zhou Z., Thomas H.R. The influence of soil moisture content variations on heat losses from earth-contact structures: an initial assessment. Building and Environment 2001;36: 157-165.
[27] Soil Mechanics A [online]. Available from: <http://www.civil.usyd.edu.au/courses/civl2410/sma2.ppt#296,41,Slide41> [Accessed July 20 2006].
[28] Rees S.W., Zhou Z., Thomas H.R. Ground heat transfer: A numerical simulation of a full-scale experiment. Building and Environment, 2005.
[29] De Vries D.A. In: Van Wisk WR, editor. Physics of plant environment. Amsterdam: North-Holland Publishing Company. 1966; p. 211-35.
[30] Farouki OT. Thermal properties of soils. Trans Tech Publications, 1986.
[31] Clark SP. Handbook of physical constants. Geological Society of America. 1966; 97: 78-96.
[32] Analytical models [online]. Available from: <http://serc.carleton.edu/introgeo/mathstatmodels/Analytical.html> [Accessed July 20 2006].
[33] Wright AJ. Heat flows from solid ground floors in buildings: simple calculation model. Building Serv Eng Res Technol1988;9(4): 177-82.
[34] Latta JK, Boileau GG. Heat losses from house basements. Canadian Builders 1969;19(10): 39-42.
[35] ASHRAE handbook of fundamentals. Atlanta, USA: American Society of Heating, Refrigerating and Air-conditioning Engineers Inc, 1993.

[36] Kusuda T, Bean JW. Simplified methods for determining seasonal heat loss from uninsulated slab-on-grade floors. ASHRAE Transactions 1984;90(1B): 611-32.
[37] Macey HH. Heat loss through a solid floor. Journal of the Institute of Fuel, 1949;22: 369-371.
[38] Muncey R.W.R., Spencer J.W. Heat loss into the ground under a house. In: C.J. Hoogendoorn and N.H. Afgan (eds), "Energy conservation in heating, cooling and ventilating buildings", 1978; 649-660.
[39] Anderson B.R. The effect of edge insulation on the steady-state heat transfer through a slab-on-ground floor. Building and Environment 1993;28: 361-367.
[40] Numerical models [online]. Available from: <http://serc.carleton.edu/introgeo/mathstatmodels/Numerical.html> [Accessed July 20 2006].
[41] Finite-difference time-domain method [online]. Available from: <http://en.wikipedia.org/wiki/FDTD> [Accessed July 21 2006].
[42] Finite element analysis [online]. Available from: <http://en.wikipedia.org/wiki/Finite_element_analysis> [Accessed July 21 2006].
[43] Shipp P.H., Pfender E., Blight TP. Thermal-characteristics of a large earth-sheltered building. Underground Space 1981;6(1):53-64.
[44] Parker DS. Simplified method for determining below grade heat loss. In: Proceedings of the 9th Biannual Congress of the International Solar Energy Society, Montreal, Canada, 23-29 June 1986, vol. 1. p. 254-61.
[45] Parker DS. F-factor correlations for determining earth contact heat loads. ASHRAE Transactions 1987;93(1):784-90.
[46] Akridge JM, Poulos JFJ. The Decremented Average Ground Temperature Method for predicting the thermal performance of underground walls. ASHRAE Transactions 1983;89(2A):49-60.
[47] Mitalas GP. Calculation of basement heat loss. ASHRAE Transactions 1983;89(1):420-38.
[48] Mitalas GP. Calculation of below-grade residential heat loss: low rise residential building. ASHRAE Transactions 1987;93(1):743-83.
[49] Yard DC., Morton-Gibson M., Mitchell JW. Simplified dimensionless relations for heat loss from basements. ASHRAE Transactions 1984;90(1B):633-43.
[50] Krarti M, Choi S. Simplified method for foundation heat loss calculation. ASHRAE Transactions 1996;102(1):140-52.
[51] Wang FS. Mathematical modelling and computer simulation of insulation systems in below grade applications. In: Proceedings of ASHRAE/DOE Conference on Thermal performance of the exterior envelopes of buildings, Orlando, Florida, 3-5 December 1979, 1981. p. 456-71.
[52] Thermal properties of building structures. In: CIBSE GUIDE, A3. The Chartered Institution of Building Services Engineers, London, UK, 1986.
[53] BSI: BS EN ISO 13370. Thermal performance of buildings - heat transfer via the ground - calculation methods. British Standards Institution, London, UK, 1998.
[54] Adjali M.H., Davies M., Rees S.W. A comparative study of design guide calculations and measured heat loss through the ground. Building and Environment 2004; 39:1301-1311.

[55] CEN, European Committee for Standardisation. Thermal performance of buildings - heat exchange with the ground - calculation method. CEN/TC 89, Office for Official Publications of the European Communities, Luxembourg, 1992.
[56] Krarti M., Gabbard S. Heat transfer in layered soils beneath partially insulated slab-on-grade floors, Proceedings of the ASHRAE-DOE conference "Thermal performance of the exterior envelope of Buildings VI", Clearwater Beach, Florida, 1992; pp. 87-94.
[57] Delsante A.E. The effect of water table depth on steady-state heat transfer through a slab-on-ground floor. Building and Environment 1993; 28: 369-372.
[58] Hagentoft C.-E. Heat losses and temperature in the ground under a building with and without ground water flow-II. Finite ground water flow rate. Building and Environment 1996; 31: 13-19.
[59] Ewen J., Thomas H.R. The thermal probe - a new method and its use on an unsaturated sand. Geotechnique 1987;37(1):91-105.
[60] Yong RN, Warkentin BP. Soil properties and behaviour. Oxford, UK: Elsevier Scientific Publishing, 1975.
[61] Karim C. Abbaspour. Modelling Soil Processes: All about Soil Physics! (for Modelling Flow and Transport) [online]. Available from: <http://www.polyql.ethz.ch/concepts/soilphysics/AllAboutSoilPhysics.pdf> [Accessed June 10 2006].
[62] Scott CR. An introduction to soil mechanics and foundations. London, UK: Applied Science Ltd, 1980.
[63] Hydraulic conductivity [online]. Available from: <http://en.wikipedia.org/wiki/Hydraulic_conductivity> [Accessed July 22 2006].
[64] Nakano M, Amemiya Y, Fujii K. Saturated and unsaturated hydraulic conductivity of swelling clays. Soil Sci J 1986;141(1):1-6.
[65] Hall DGM, Reeve MJ, Thomasson AJ, Wright VF. Water retention, porosity and density of field soils. Soil Survey of England and Wales, Technical monograph No. 19, 1977.
[66] Croney D, Coleman JD. Soil structure in relation to soil suction (pF). Soil Sci J 1954;5(1):75-84.
[67] Russo D, Bresler E. Field determinations of soil hydraulic properties for statistical analyses. Soil Sci Soc Am J 1980;44:697-702.
[68] Alonso EE, Gens A, Hight DW. Special problem soils - general report (Session 5). In: Proc. 9th European Conf. Soil Mech. and Found. Engng, Dublin, Ireland, 1987. p. 1087-146.
[69] Thomas H.R., He Y., Ramesh A., Zhou Z., Villar MV., Cuevas J. Heating unsaturated soil - An experimental and numerical investigation. In: Proceedings of the Third European Conference on Numerical Methods in Geotechnical Engineering - ECONMIG 94, Manchester, UK, 1994. p. 181-6.
[70] Advection [online]. Available from: <http://ww2010.atmos.uiuc.edu/(Gh)/guides/mtr/af/adv/adv.rxml> [Accessed July 15 2006].
[71] Geiger R. The climate near the ground, Harvard University Press, Cambridge, 1971.
[72] Van Bavel C.H.M., Hillel D.I. Calculating potential and actual evaporation from a bare soil surface by simulation of concurrent flow of water and heat, Agricultural Meteorology, 1976; 17: 453-476.
[73] Albedo [online]. Available from: <http://en.wikipedia.org/wiki/Albedo> [Accessed July 15 2006].

[74] Gilpin R.R. and Wong B.K. "Heat-valve" effects in the ground thermal regime, Journal of Heat Transfer, 1976; 98: 537-542.
[75] Gerson H. dos Santos, Nathan Mendes. Simultaneous heat and moisture transfer in soils combined with building simulation. Energy and Buildings 2006; 38:303-314.
[76] Environmental Engineering Science 1 - Thermal Comfort [online]. Available from: <http://www.esru.strath.ac.uk/Courseware/Class-16293/6-Comfort.pdf> [Accessed July 18 2006].
[77] BSI: BS EN ISO 10211-1 (incorporating corrigendum No. 1): Thermal bridges in building construction - Calculation of heat flows and surface temperatures - Part 1: General methods. British Standards Institution, London, UK, 1996.
[78] CIBSE GUIDE A: Environmental Design. The Chartered Institution of Building Services Engineers, London, UK, 1999.
[79] Delsante A.E., Stokes A.N., Walsh P.J. Application of Fourier transforms to periodic heat flow into the ground under a building, Int. J. Heat Mass Transfer, 1983; 26: 121-132.
[80] Geving S. Averaging of climatic data and its effect on moisture transfer calculations, IEA ANNEX 24, Report T2-N-94/04, 1994.
[81] TAS Next Generation Thermal Analysis Software - Version 9.0.7 - 2004 EDSL.
[82] Discretization [online]. Available from: <http://en.wikipedia.org/wiki/Discretization> [Accessed July 19 2006].
[83] Limiting thermal bridging and air leakage: Robust construction details for dwellings and similar buildings (incorporating amendment 1). Norwich: TSO, 2002.
[84] Domestic retail market report - March 2006 [online]. Available from: <http://www.ofgem.gov.uk/temp/ofgem/cache/cmsattach/15610_DRMR_March 2006_pdf> [Accessed August 4 2006].
[85] Randall McMullan. Environmental science in building, 5th ed. New York: Palgrave Macmillan, 2002.

Appendix A

Information about the "VOLTRA" thermal analysis computer program

A.1 Minimum system requirements

- "VOLTRA" is a 32-bit Windows program.
- A PC running under Windows 95 SP2, Windows 98, Windows NT 4 SP4, Windows 2000 or higher.
- 512 Mb RAM allows to solve a system of about 1,000,000 nodes.
- 1Gb RAM allows to solve about 3,000,000 nodes.
- Super VGA monitor (with screen resolution set to at least 800 x 600).
- CD-ROM drive for installing the software.

A software license of "VOLTRA" is protected by a hardware key, provided by PHYSIBEL to the end user.

A.2 Program functions

For the time dependent boundary conditions "VOLTRA" refers to time functions: either an external function or an internal function. An external time function is defined in a separate data file, with extension .fte (temperature function), .fir (imposed flux function), .ffh (power function) or .fvr (ventilation function). The program FUNCEDIT allows to edit these files (the program's version used in this work does not include the specific program). An internal time function is a built-in program function, defined by one or more parameters. "VOLTRA" contains five built-in functions, which are described further in this section. For the temperature dependent material properties (thermal conductivity and specific heat) "VOLTRA" refers to temperature functions.

A.3 Materials thermal properties

Compared to the "TRISCO" Colors window the following differences occur in "VOLTRA":

- Two material properties concerning the thermal capacity are added: the material density ρ (in kg/m^3), and the specific heat capacity c (in J/kgK). These properties are also loaded when a material is selected from the material database.
- The properties: λ *(thermal conductivity)*, c *(specific heat capacity)*, θ *(boundary condition temperature)*, q *(boundary condition heat flux)*, θ_a *(boundary condition air temperature)*, Pc *(convective power into air cavity)* and θ_r *(boundary condition radiation temperature)* can refer to functions (defined in the Functions window) via function reference names.

A.4 Calculation parameters

The Calculation Parameters dialog box:
Compared to "TRISCO" some new parameters concerning the time dimension occur:

- Time step: this is the time distance between two successive dynamic system calculations (about the time format: days, hours, minutes and seconds are separated by colons).
- Start-up calculation duration: this is the time duration before the actual start of the calculation (where reporting starts) with the purpose to get good dynamic start values.
- Calculation duration: duration of the dynamic calculation during which time step results and report items can be saved (e.g. to produce a graphic animation). The calculation start is always at time 0000:00:00:00 (i.e. 0 days, 0 hours, 0 minutes, 0 seconds).
- Day number at start of calculation: number between 1 and 365 to indicate the day in the year where the calculation starts. This is important when the used (external) function is related to a calendar date: e.g. a test reference year, with hourly climatic data of a typical year in a given location. The start date of the external function may be different from the start date of the calculation.

References for Appendix A

[A.1] VOLTRA: computer program to calculate 3D & 2D transient heat transfer in objects described in a rectangular grid using the energy balance technique - Version 4.0w - 2003 PHYSIBEL.

Appendix B

Predictive models for the soil thermal conductivity

Mathematically the problem of expressing the soil thermal conductivity as a function of the conductivities and volume ratios of its constituents is analogous to expressing the electrical conductivity or the dielectric constant of a granular material in terms of volume ratios and the electrical conductivities (or dielectric constants) of its constituents [B.1].
Early attempts at solving the problem made use of the electric conductivity or dielectric constant of two-phase materials. If the soil constituents are assumed to have a distribution parallel to the direction of heat flow, the thermal conductivity of the soil can be expressed as [B.1]:

$$\lambda = \chi_1\lambda_1 + \chi_2\lambda_2 \quad , \tag{B.1}$$

where: χ_1 and χ_2 are volume fractions and λ_1 and λ_2 represent thermal conductivities of constituents, e.g. water and solid mineral. Eq. (B.1) is known as the "*weighted arithmetic mean*", which, as shown below, is considered to over-estimate the soil thermal conductivity {[B.2], as found in [B.1]}.
An alternate approach is to assume that the soil constituents have a series distribution that is perpendicular to the direction of heat flow. In this case, the soil thermal conductivity may be expressed as [B.1]:

$$\lambda = \frac{\lambda_1\lambda_2}{\chi_1\lambda_2 + \chi_2\lambda_1} \tag{B.2}$$

This is the so-called "*weighted harmonic mean*" equation, which is known to under-estimate the thermal conductivity of the soil {[B.2], as found in [B.1]}.
Woodside and Messmer {[B.2], as found in [B.1]} have used a "*weighted geometric mean*" equation to represent the thermal conductivity, in the following form:

$$\lambda = \lambda_1^{\chi_1}\lambda_2^{\chi_2} \tag{B.3}$$

This approach was found to give an intermediate value between the "*weighted arithmetic mean*" and the "*weighted harmonic mean*" equation.
Figure B.1 below presents a comparison of soil thermal conductivity values calculated from the "*weighted arithmetic mean*", "*weighted harmonic mean*" and "*weighted geometric mean*" equations. The results are plotted against porosity (volume of voids divided by the total volume of soil) [B.1]:

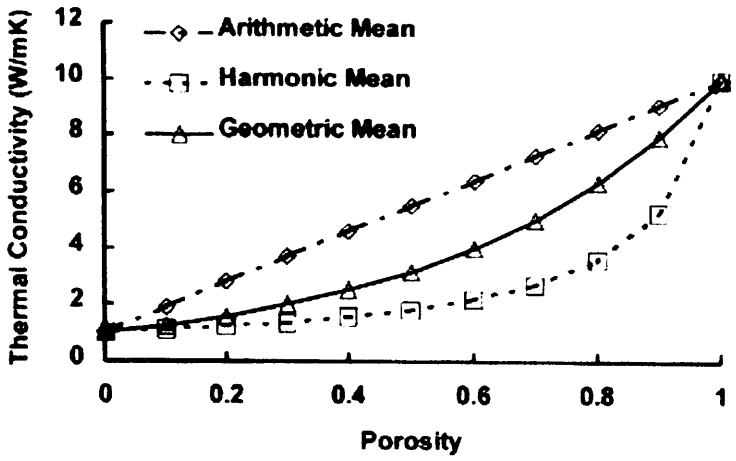

Figure B.1: The relationship between thermal conductivity and porosity [B.1]

The porosity indicates the maximum water content a soil can achieve. The Table B.1, below, includes a summary of porosity values that may be expected for a variety of different soil types:

Soil type	Porosity range (%)
(1) Uniform materials	
(a) Equal spheres (theoretical values)	$26.0 < \eta < 47.6$
(b) Standard Ottawa sand	$33.0 < \eta < 44.0$
(c) Clean, uniform sand (fine or medium)	$29.0 < \eta < 50.0$
(d) Uniform, inorganic silt	$29.0 < \eta < 52.0$
(2) Well-graded materials	
(a) Silty sand	$23.0 < \eta < 47.0$
(b) Clean, fine to coarse sand	$17.0 < \eta < 49.0$
(c) Micaceous sand	$29.0 < \eta < 55.0$
(d) Silty sand and gravel	$12.0 < \eta < 46.0$
(3) Mixed soils	
(a) Sandy or silty clay	$20.0 < \eta < 64.0$
(b) Skip-graded silty clay with stones or rock fragments	$17.0 < \eta < 50.0$
(c) Well-graded gravel, sand, silt and clay mixture	$11.0 < \eta < 41.0$
(4) Clay soils	
(a) Clay (30–50% clay sizes)	$33.0 < \eta < 71.0$
(b) Colloidal clay (<0.002 mm ≥ 50%)	$37.0 < \eta < 92.0$
(5) Organic soils	
(a) Organic silt	$35.0 < \eta < 75.0$
(b) Organic clay (30–50% clay sizes)	$41.0 < \eta < 81.0$

Table B.1: Typical porosity values for different soil types - [B.3], as found in [B.1]

The above Eq. (B.1), (B.2) & (B.3) can be easily extended for a soil containing more than two constituents. For parallel distribution [B.1]:

$$\lambda = \gamma_1\lambda_1 + \gamma_2\lambda_2 + \gamma_3\lambda_3 \quad \text{(B.4)},$$

and for series distribution [B.1]:

$$\lambda = \frac{\lambda_1\lambda_2\lambda_3}{\gamma_1\lambda_2\lambda_3 + \gamma_2\lambda_3\lambda_1 + \gamma_3\lambda_1\lambda_2} \quad \text{(B.5)}$$

The "*weighted geometric mean*" is then given as [B.1]:

$$\lambda = \prod_{i=1}^{n}\lambda_i^{\gamma_i}, \quad \text{(B.6)}$$

where: n is the number of constituents. The Greek capital letter 'Π' is used to imply product terms.
Johansen {[B.4], as found in [B.5]} proposed an approach which relates thermal conductivity (λ) to the dry (λ_{dry}) and saturated states (λ_{sat}) of a soil of the same density:

$$\lambda = (\lambda_{sat} - \lambda_{dry})Ke + \lambda_{dry} \quad \text{(B.7)}$$

Eq. (B.7) includes a normalised thermal conductivity value called "*Kersten number*" (*Ke*), which is dimensionless. The relationship between *Ke* and the degree of saturation (S_r) of a soil is effectively linear (both parameters range between zero and one). For unsaturated unfrozen soils, *Ke* can be obtained from Eq. (B.8), for coarse soils or Eq. (B.9), for fine soils [B.5]:

$$Ke \simeq 0.7 \log S_r + 1.0. \quad \text{(B.8)}$$

$$Ke \simeq \log S_r + 1.0. \quad \text{(B.9)}$$

As mentioned previously, the porosity of the soil structure is recognised to be an important parameter when considering soil thermal conductivity. Since the soils microstructure is an important parameter, two expressions were suggested for the thermal conductivity of the soils dry state: the first is for the natural soils {Eq. (B.10)} and the second for the crushed materials {Eq. (B.11)} [B.5]:

$$\lambda_{dry} = 0.039n^{-2.2} \pm 25\%. \quad \text{(B.10)}$$

$$\lambda_{dry} = \frac{0.135\gamma_d + 64.7}{2700 - 0.947\gamma_d} \pm 20\%. \quad \text{(B.11)}$$

where: n is the porosity and γ_d is the dry density (kg/m^3).

For saturated soils, it has been shown that, variations in their microstructure have relatively little influence on the thermal conductivity. The "*weighted geometric mean*" equation can, therefore, be used to calculate values of the soils thermal conductivity and their respective volume fractions, as illustrated below [B.5]:

$$\lambda_{soil} = \lambda_s^{(1-m)} \lambda_w^{m} \quad \text{(B.12)}$$

where: the thermal conductivity of the solid phase (λ_s) can be expressed as:

$$\lambda_s = \lambda_q^{q} \lambda_o^{(1-q)} \quad \text{(B.13)}$$

Eq. (B.13) is based upon the quartz content (q) expressed as a fraction of the total solids content. Johansen [B.5] recommended that, the thermal conductivity value of quartz (λ_q) can be taken as: 7.7 W/mK, while the respective value for other minerals (λ_o) can be assumed to be approximately: 2.0 W/mK. However, this method, though acknowledges the importance of the degree of saturation on soil thermal conductivity, tends to derive relatively poor predictions of its values for low degrees of saturation and for small alterations of moisture content at low degrees of saturation.

The most widely, however, accepted physical model for soil thermal conductivities was derived by De Vries {[B.6], as found in [B.7]}. Although this model appears difficult to use, it offers considerable flexibility over some of the other models described herein. For moist soils, he assumed the liquid phase as a continuous medium in which solid grains and small air pockets are uniformly distributed. The overall thermal conductivity can, then, be expressed as:

$$\lambda = \frac{\sum_{\Pi=1}^{4} k_\Pi \theta_\Pi \lambda_\Pi}{\sum_{\Pi=1}^{4} k_\Pi \theta_\Pi} \quad \text{(B.14)}$$

where: θ_Π is the volume fraction (m^3/m^3) of component Π {(1) water, (2) air, (3) quartz, (4) non-quartz; organic matter is not considered}, k_Π the ratio of the thermal gradients (-) in component Π and in the bulk material, and λ_Π is the thermal conductivity (W/mK) of component Π. The thermal conductivities of the different soil constituents are listed in the following Table B.2. For moist air, however, the effect of latent heat transfer by thermal vapor diffusion is to be added to the dry air thermal conductivity, given in Table B.2.

Constituent Π	Number	Vol. spec. heat C_Π (MJ/m³K)	Thermal conductivity λ_Π (W/mK)
water	1	4.180 *	-0.908 + 8.34 10^{-3} T – 1.10 10^{-5} T^2 *
dry air	2	1.2122 10^{-3} *	6.19 10^{-3} + 6.41 10^{-5} T #
quartz	3	1.9228 *	22.3 - 7.21 10^{-2} T + 7.41 10^{-5} T^2 *
other minerals	4	1.9228 *	2.0 &

* Farouki [1981] # Kimball et al. [1976] & Johansen [1975]

Table B.2: Volumetric specific heat and thermal conductivity of the soil constituents- [B.8], [B.9] & [B.10] as found in [B.7]

In addition to the theoretical methods presented above, the soil thermal conductivity has frequently been expressed in terms of empirical equations. However, these equations tend to be suitable only for the particular soils, tested under designated conditions and therefore, they lack generality [B.1].
For example, an empirical expression for thermal conductivity was presented by Makowski and Mochlinski {[B.11], as found in [B.1]}. This expression can be written in SI units as:

$$\lambda = (a \log_{10} m + b)10^{z} \quad \text{(B.15)}$$

where:

$$a = 0.1424 - 0.000465p \quad b = 0.0419 - 0.000313p \quad \text{(B.16)}$$

and:

$$z = 6.24\rho_d \times 10^{-4} \quad \text{(B.17)}$$

In Eq. (B.15), m is the moisture content of the soil as a percentage of dry soil weight, ρ_d is the dry density and p is the percentage of clay in the soil.
On the other hand, *Thomas et al.* {[B.12], as found in [B.1]} provided the following relationship between the soil thermal conductivity and its degree of saturation:

$$\lambda = 0.62 + 3.976S_l + 2.687S_l \log(S_l) - 3.313S_l^2 \quad \text{(B.18)}$$

where: S_l is the degree of saturation of water.

References for Appendix B

[B.1] Rees S.W., Adjali M.H., Zhou Z., Davies M., Thomas H.R. Ground heat transfer effects on the thermal performance of earth-contact structures. Renewable and Sustainable Energy Reviews 2000;4:213-265.

[B.2] Woodside W, Messmer JH. Thermal conductivities of porous media I: unconsolidated soils. J Appl Phys 1961;32(9):1699-706.

[B.3] Hough BK. In: Basic soils engineering. New York: Ronald Press, 1969; p. 634.

[B.4] Johansen O. Thermal conductivity of soils. PhD thesis, Trondheim, Norway, 1975 (CRREL Draft Translation 637, 1977), ADA 044002.

[B.5] Rees S.W., Zhou Z., Thomas H.R. Ground heat transfer: A numerical simulation of a full-scale experiment. Building and Environment, 2005.

[B.6] De Vries D.A. Thermal properties of soils, "Physics of the plant environment," Van Wijk W.R. (eds), North-Holland, Amsterdam, 1966.

[B.7] Janssen H. The influence of soil moisture transfer on building heat loss via the ground. Ph.D. thesis, Catholic University of Leuven, Belgium, 2002.

[B.8] Farouki O.T. "Thermal properties of soil", CRREL Monograph 81-8, 1981.

[B.9] Johansen O. "Thermal conductivity of soils", Ph.D. thesis, Trondheim University, Norway, , 1975.

[B.10] Kimball B.A., Jackson R.D., Reginato R.J., Nakayama F.S., Idso S.B. Comparison of field-measured and calculated soil heat fluxes. "Soil Science Society of America Journal". 1976 ; 40: 18-25.

[B.11] Makowski MW, Mochlinski K. An evaluation of two rapid methods of assessing the thermal resistivity of soil. Proc Instn Elect Engng 1956;103:453-64 [Part A].

[B.12] Thomas H.R., He Y., Ramesh A., Zhou Z., Villar MV., Cuevas J. Heating unsaturated clay - an experimental and numerical investigation. In: Smith IM, editor. Proc. 3rd Euro. Con. on Numer. Methods in Geotech. Engng - ECONMIG 94, Manchester, UK, 1994. p. 181-6.

Appendix C
Validation of the used methodology

First model: One-dimensional heat transfer (half a square column)
Nodes: 798 [C.1] & [C.2]

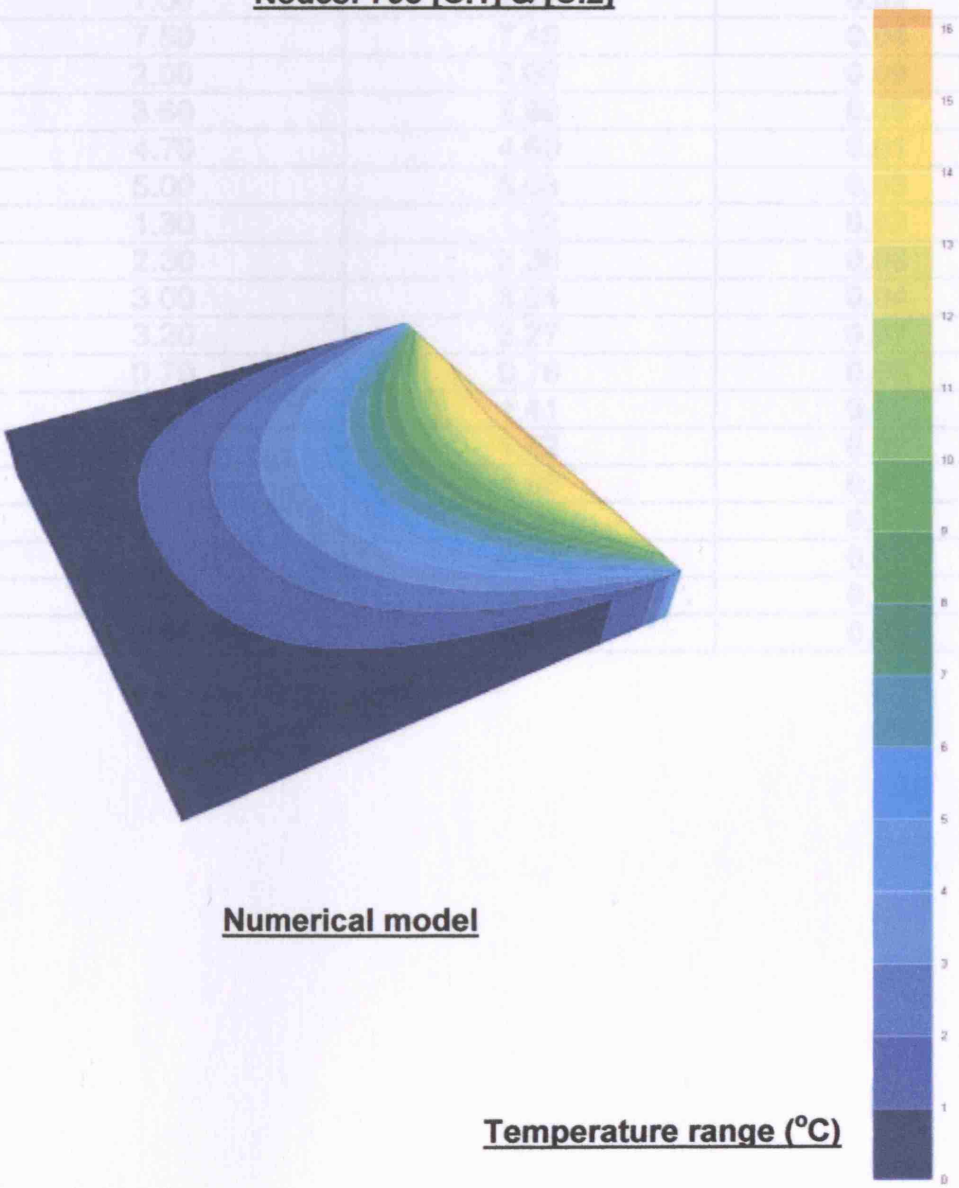

Numerical model

Temperature range (°C)

Comparison of the derived results (Design calculation method vs work's methodology)

➢ **Temperatures comparison**

Grid Node	Temperatures results (°C)		Results difference (°C/ °K)
	Design calculation method	Work's methodology*	
1	9.70	9.62	**0.08**
2	13.40	13.31	**0.09**
3	14.70	14.67	**0.03**
4	15.10	15.03	**0.07**
5	5.30	5.30	**0.00**
6	8.60	8.61	**0.01**
7	10.30	10.28	**0.02**
8	10.80	10.78	**0.02**
9	3.20	3.27	**0.07**
10	5.60	5.64	**0.04**
11	7.00	7.02	**0.02**
12	7.50	7.46	**0.04**
13	2.00	2.09	**0.09**
14	3.60	3.69	**0.09**
15	4.70	4.69	**0.01**
16	5.00	5.03	**0.03**
17	1.30	1.32	**0.02**
18	2.30	2.36	**0.06**
19	3.00	3.04	**0.04**
20	3.20	3.27	**0.07**
21	0.70	0.78	**0.08**
22	1.40	1.41	**0.01**
23	1.80	1.82	**0.02**
24	1.90	1.96	**0.06**
25	0.30	0.37	**0.07**
26	0.60	0.67	**0.07**
27	0.80	0.86	**0.06**
28	0.90	0.93	**0.03**

*: **TRISCO - Temperatures in Node BCs**

TRISCO data file: Andreasmodel-1.trc

	X	Y	Z	t [°C]
1:	7	4		9.62
2:	7	9		13.31
3:	7	14		14.67
4:	7	19		15.03
5:	9	4		5.30
6:	9	9		8.61
7:	9	14		10.28
8:	9	19		10.78
9:	10	4		3.27
10:	10	9		5.64
11:	10	14		7.02
12:	10	19		7.46
13:	11	4		2.09
14:	11	9		3.69
15:	11	14		4.69
16:	11	19		5.03
17:	12	4		1.32
18:	12	9		2.36
19:	12	14		3.04
20:	12	19		3.27
21:	13	4		0.78
22:	13	9		1.41
23:	13	14		1.82
24:	13	19		1.96
25:	15	4		0.37
26:	15	9		0.67
27:	15	14		0.86
28:	15	19		0.93

X, Y & Z: Grid coordinates

Second model: Two-dimensional heat transfer
Nodes: 30,060

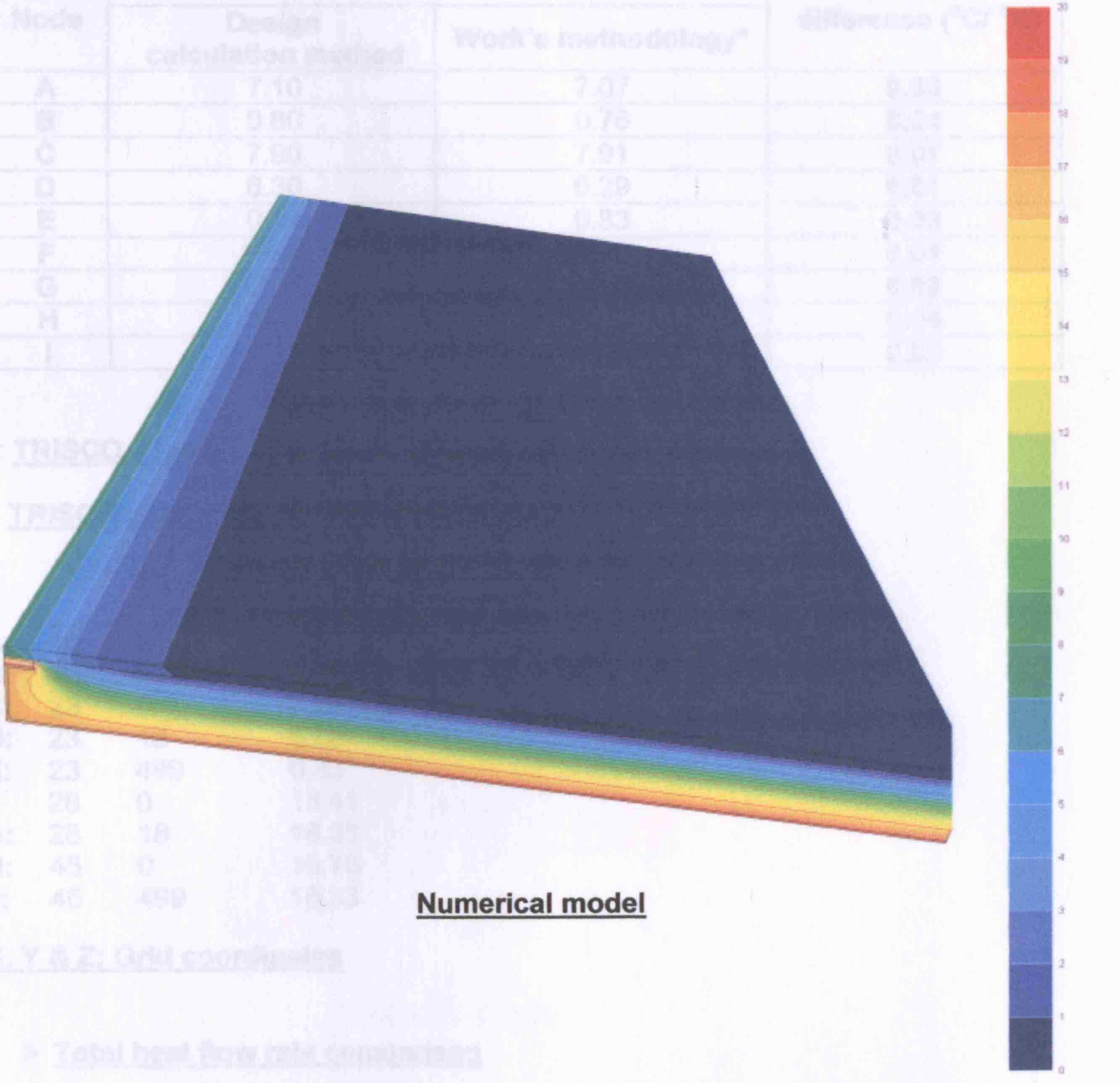

Numerical model

Temperature range (°C)

Comparison of the derived results (Design calculation method vs work's methodology)

➢ **Temperatures comparison**

Grid Node	Temperatures results (°C)		Results difference (°C/ °K)
	Design calculation method	Work's methodology*	
A	7.10	7.07	**0.03**
B	0.80	0.76	**0.04**
C	7.90	7.91	**0.01**
D	6.30	6.29	**0.01**
E	0.80	0.83	**0.03**
F	16.40	16.41	**0.01**
G	16.30	16.33	**0.03**
H	16.80	16.76	**0.04**
I	18.30	18.33	**0.03**

*: **TRISCO - Temperatures in Node BCs**

TRISCO data file: Andreasmodel-2.trc

	X	Y	Z	t [°C]
A:	16	0		7.07
B:	16	499		0.76
C:	23	0		7.91
D:	23	18		6.29
E:	23	499		0.83
F	28	0		16.41
G:	28	18		16.33
H:	45	0		16.76
I:	45	499		18.33

X, Y & Z: Grid coordinates

➢ **Total heat flow rate comparison**

Total heat flow rate results (W/m)		Results difference (W/m)
Design calculation method	Work's methodology	
9.50	9.51	**0.01**

Third model: Three-dimensional heat transfer
Nodes: 997,680

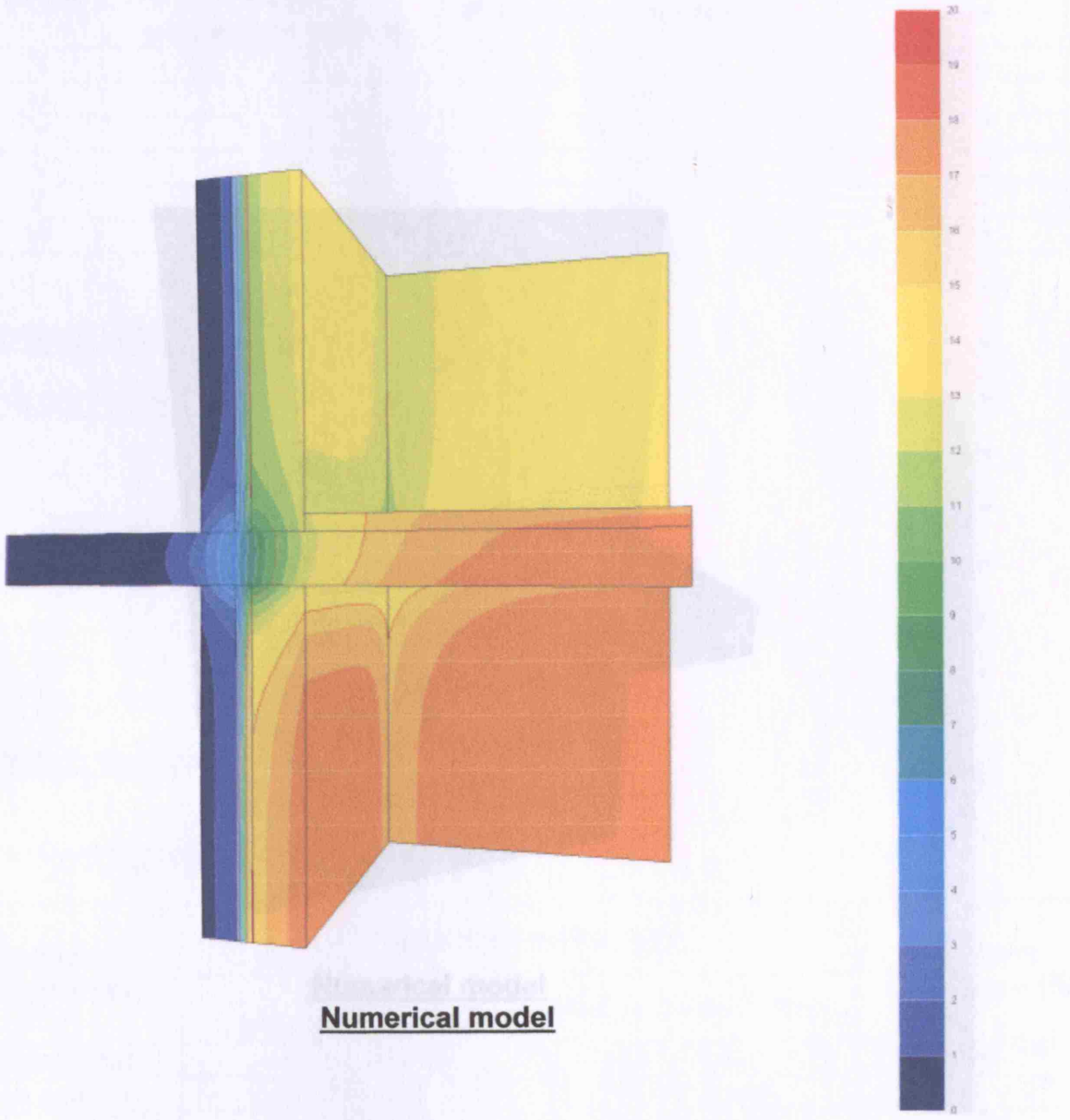

Numerical model

Temperature range (°C)

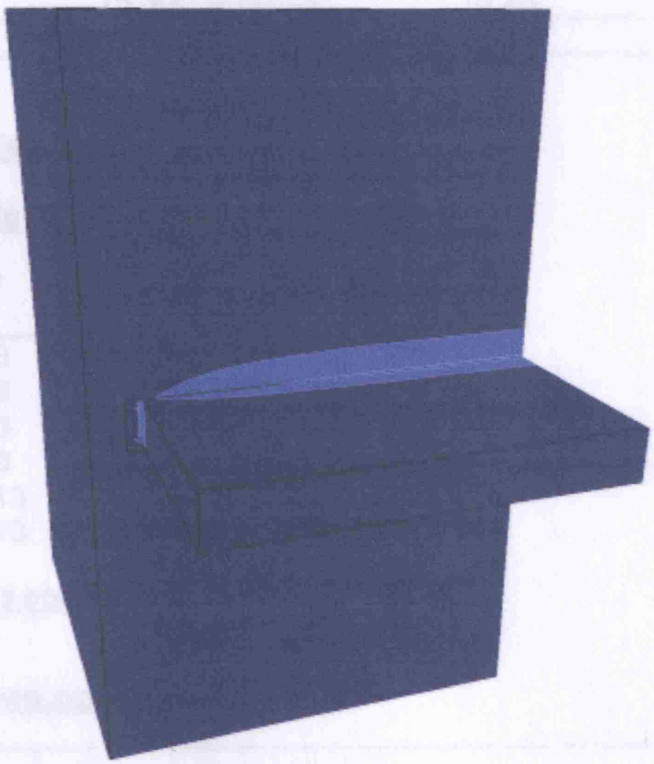

Numerical model

Temperature range (°C)

Comparison of the derived results (Design calculation method vs work's methodology)

➢ Temperatures comparison

Grid Node	Temperatures results (°C)		Results difference (°C/ °K)
	Design calculation method	Work's methodology*	
X	12.60	12.55	**0.05**
U	12.90	12.90	**0.00**
Y	11.10	11.10	**0.10**
V	11.30	11.18	0.12 > 0.10[1]
Z	15.30	15.28	**0.02**
W	16.40	16.40	**0.00**

*: **TRISCO - Temperatures in node BCs**

TRISCO data file: Andreasmodel-3.trc

	X	Y	Z	t [°C]
X:	109	83	50	12.55
U:	109	83	24	12.90
Y:	75	83	50	11.00
V:	75	83	24	11.18
Z:	75	213	50	15.28
W:	75	213	24	16.40

X, Y & Z: Grid coordinates

➢ Heat flows comparison

Boundary Condition	Heat flows results (W)		Results difference (%)
	Design calculation method	Work's methodology	
α (outside)	-46.30 (loss)	-46.26 (loss)	8.64 > 2[20]
β (upstairs)	-14.00 (loss)	-14.03 (loss)	21.43 > 2[20]
γ (downstairs)	+60.30 (gain)	+60.29 (gain)	**1.66**

[20]: Further grid refinement, which would result in more precise results, could not be calculated, due to the limited PC's capacity

References for Appendix C

[C.1] TRISCO: computer program to calculate 3D & 2D steady-state heat transfer in objects described in a rectangular grid using the energy balance technique Version 10.0w - 2002 PHYSIBEL.

[C.2] VOLTRA: computer program to calculate 3D & 2D transient heat transfer in objects described in a rectangular grid using the energy balance technique - Version 4.0w - 2003 PHYSIBEL.

Appendix D

"VOLTRA" calculations data

D.1 SLAB ON GROUND NUMERICAL MODEL [D.1]

The calculations done for all the numerical models (3-D, 2-D & 1-D) of the specific constructional detail (slab-on-ground with insulation below the slab and an un-insulated compact external wall), the respective derived results and the conclusions drawn from them, are presented below. Furthermore, the Tables: D.1, D.2 & D.3, which follow, summarize all the relevant numerical data of the calculations done.

➢ CALCULATIONS 'DIARY' AND DERIVED CONCLUSIONS

• THREE-DIMENSIONAL (3-D) MODELS: 979,120 nodes

1. The calculation of the model with: no pre-simulation ("*pre-conditioning*") time, a main simulation time of: 2 years and a time-step interval of: 5 days, lasted: 190 mins but, no results were derived as far as the heat loss/gain rate (W) for every time-step interval is concerned. So, the annual heat loss (J) cannot be calculated for the specific model.

2. The calculation of the model with: a pre-simulation time of: 1 year, a main simulation time of: 1 year and a time-step interval of: 5 days, lasted: 180 mins but, no results were derived as far as the heat loss/gain rate (W) for every time-step interval is concerned. So, the annual heat loss (J) cannot be calculated for the specific model.

3. The calculation of the model with: a pre-simulation time of: 1 year, a main simulation time of: 1 year and a time-step interval of: 10 days, lasted: 110 mins. The results derived - as far as the heat flow rate (W) at the end of the simulation time is concerned - diverged: ~11% from the results of the calculation described in §2.

4. The calculation of the model with: a pre-simulation time of: 1 year, a main simulation time of: 1 year and a time-step interval of: 15 days, lasted: 85 mins. The results derived, diverged only: ~1.2% from the results of the calculation described in §3.

5. The calculation of the model with: a pre-simulation time of: 1 year, a main simulation time of: 1 year and a time-step interval of: 20 days, lasted: 60 mins. The results derived, diverged only: ~1.18% from the results of the calculation described in §4.

Conclusion: Since the model described in §3 is the most precise one - the one with the shortest time step interval - that can derive results and since, it does not differ a lot - as far as the results derived for the heat flow rate (W) at the end of the simulation time are concerned - from the models described in §4 & 5, then it is concluded that, is the most 'reliable' one to be compared with the respective 2-D & 1-D models, as far as the estimation of the annual (ground floor) heat losses is concerned. The heat losses in question, as estimated by the specific model, are: 20,305,494.72 kJ or, if the surface area of the model's ground floor (100m^2) is taken into consideration: ~203,054.95 kJ/ m^2.

1. The calculation of the model with: no pre-simulation time, a main simulation time of: 2 years and a time-step interval of: 20 days, lasted: 70 mins. The results derived, diverged: ~6.4% from the results of the calculation described in §5 (the respective calculation with a pre-simulation time of: 1 year).

2. The calculation of the model with: no pre-simulation time, a main simulation time of: 2 years and a time-step interval of: 15 days, lasted: 90 mins. The results derived, diverged: ~7.22% from the results of the calculation described in §4 (the respective calculation with a pre-simulation time of: 1 year).

3. The calculation of the model with: no pre-simulation time, a main simulation time of: 2 years and a time-step interval of: 10 days, lasted: 110 mins. The results derived, diverged: ~12.75% from the results of the calculation described in §3 (the respective calculation with a pre-simulation time of: 1 year).

Conclusion: There is a divergence of: ~ 8.79% in average - as far as the results derived for the heat flow rate at the end of the simulation time are concerned - between the calculations with a pre-simulation time of: 1 year (and a main simulation time of: 1 year) and the ones with no pre-simulation time (but, with a main simulation time of: 2 years).

- **TWO-DIMENSIONAL (2-D) MODELS: 11,258 nodes**

1. The calculation of the model with: no pre-simulation time, a main simulation time of: 2 years and a time-step interval of: 5 days, lasted less than 1 min.

2. The calculation of the model with: no pre-simulation time, a main simulation time of: 2 years and a time-step interval of: 10 days, lasted less than 1 min. The results derived - as far as the heat flow rate (W) at the end of the simulation time is concerned - diverged: ~14% from the results of the simulation described in §1.

3. The calculation of the model with: no pre-simulation time, a main simulation time of: 2 years and a time-step interval of: 15 days, lasted less than 1 min. The results derived, diverged unnoticeably from the results of the calculation described in §2.

4. The calculation of the model with: no pre-simulation time, a main simulation time of: 2 years and a time-step interval of: 20 days, lasted less than 1 min. The results derived, again diverged unnoticeably from the results of the calculation described in §2.

5. The calculation of the model with: no pre-simulation time, a main simulation time of: 2 years and a time-step interval of: 1 day, lasted approximately 2mins. The results derived, had no difference from the respective results of the calculation described in §2.

6. The calculation of the model with: no pre-simulation time, a main simulation time of: 2 years and a time-step interval of: 1 hour, lasted 60 mins. The results derived, diverged: ~17.32% from the results of the calculation described in §2.

7. The calculation of the model with: a pre-simulation time of: 1 year, a main simulation time of: 1 year and a time-step interval of: 5 days, lasted less than 1min. The results derived, had no difference from the results of the calculation described in §1 (the respective calculation with no pre-simulation time).

8. The calculation of the model with: a pre-simulation time of: 1 year, a main simulation time of: 1 year and a time-step interval of: 1 hour, lasted 60mins. The results derived, had no difference from the results of the calculation described in §6 (the respective calculation with no pre-simulation time) and the respective ones of the calculation described in §7.

9. The calculation of the model with: a pre-simulation time of: 1 year, a main simulation time of: 1 year and a time-step interval of: 1 day, lasted less than 1min. The results derived, had no difference both from the results of the calculation described in §5 (the respective calculation with no pre-simulation time) and the respective ones of the calculation described in §7.

10. The calculation of the model with: a pre-simulation time of: 1 year, a main simulation time of: 1 year and a time-step interval of: 10 days, lasted less than 1min. The results derived, diverged: ~11% both from the results of the calculation described in §2 (the respective calculation with no pre-simulation time) and the respective ones of the calculation described in §7.

11. The calculation of the model with: a pre-simulation time of: 1 year, a main simulation time of: 1 year and a time-step interval of: 15 days, lasted less than 1min. The results derived, diverged: ~5.04% from the results of the calculation described in §3 (the respective calculation with no pre-simulation time) and ~12.66% from the respective ones of the calculation described in §7.

12. The calculation of the model with: a pre-simulation time of: 1 year, a main simulation time of: 1 year and a time-step interval of: 20 days, lasted less than 1min. The results derived, diverged: ~3.05% from the results of the calculation described in §4 (the respective calculation with no pre-simulation time) and ~14.26% from the respective ones of the calculation described in §7.

Conclusions:

– **There is a divergence of: ~ 6.36% in average - as far as the results derived for the heat flow rate at the end of the simulation time are concerned - between the calculations with a pre-simulation time of: 1 year (and a main simulation time of: 1 year) and the ones with no pre-simulation time (but, with a main simulation time of: 2 years) and,**

– **The model described in §10 is a 'reliable' one to be compared with the respective 3-D & 1-D models, as far as the estimation of the annual (ground floor) heat losses is concerned. This is because, the results in question derived from this calculation, diverge only: 0.92% from the respective ones of the calculation described in §7 (see figures D.1 & D.2 in the next two pages), although the results divergence between the two calculations - as far as the heat flow rate at the end of the simulation time is concerned - is: ~11%. The annual ground floor heat losses, as estimated by the specific model, are:** 1,139,814.72 kJ, **or, if the surface area of the model's ground floor (10m^2) is taken into consideration:** ~113,981.47 kJ/ m^2.

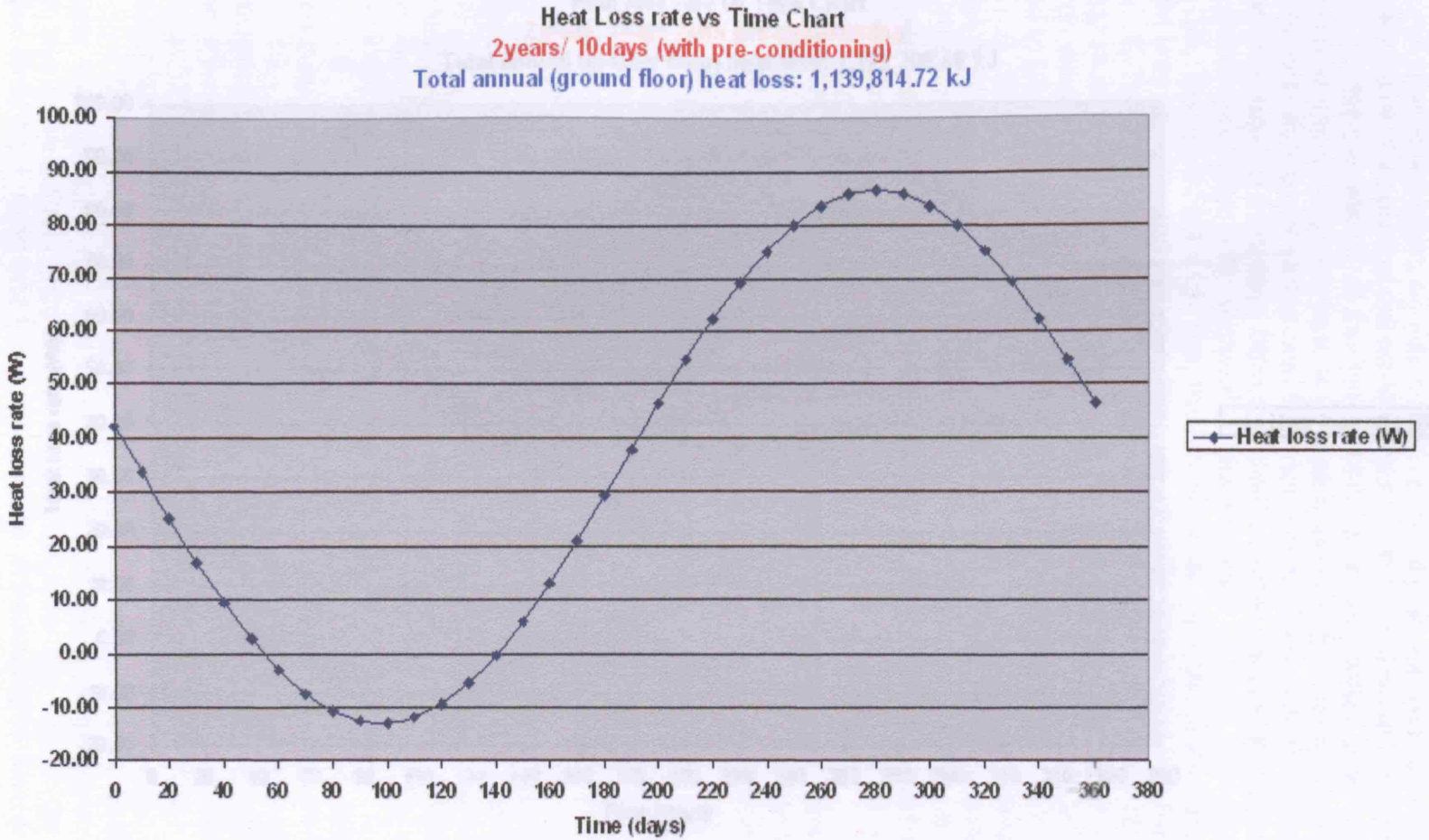

Figure D.1 - Heat loss rate vs Time Chart (2-D model/ 2years per 10 days with pre-conditioning)

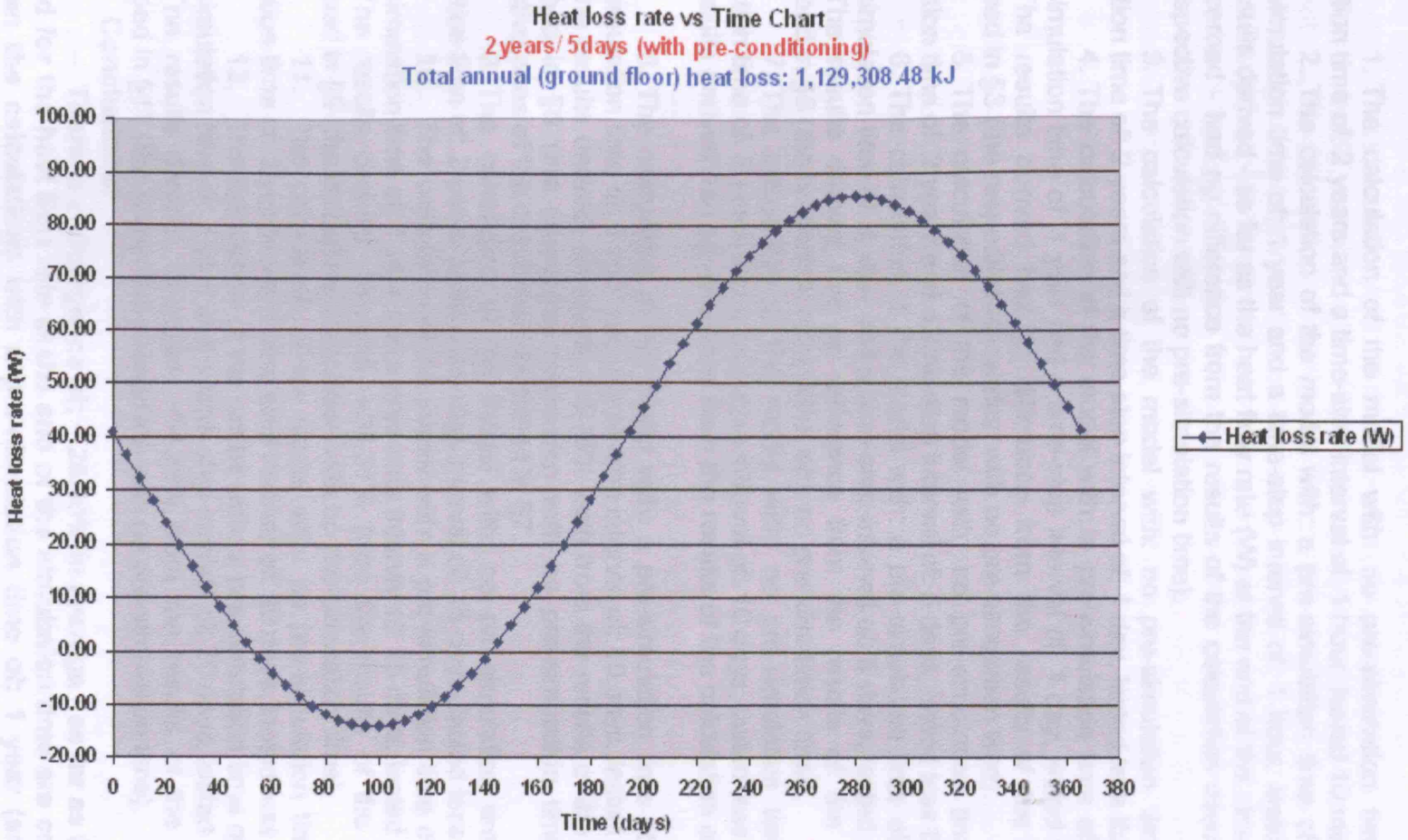

Figure D.2 - Heat loss rate vs Time Chart (2-D model/ 2years per 5 days with pre-conditioning)

- **ONE-DIMENSIONAL (1-D) MODELS: 224 nodes**

1. The calculation of the model with: no pre-simulation time, a main simulation time of: 2 years and a time-step interval of: 1 hour, lasted 10 mins.

2. The calculation of the model with: a pre-simulation time of: 1 year, a main simulation time of: 1 year and a time-step interval of: 1 hour, lasted 10 mins. The results derived - as far as the heat flow rate (W) at the end of the simulation time is concerned - had no difference from the results of the calculation described in §1 (the respective calculation with no pre-simulation time).

3. The calculation of the model with: no pre-simulation time, a main simulation time of: 2 years and a time-step interval of: 1 day, lasted less than 1 min.

4. The calculation of the model with: a pre-simulation time of: 1 year, a main simulation time of: 1 year and a time-step interval of: 1 day, lasted less than 1 min. The results derived had no difference from the results of the calculation described in §3 (the respective calculation with no pre-simulation time).

5. The calculation of the model with: no pre-simulation time, a main simulation time of: 2 years and a time-step interval of: 5 days, lasted less than 1 min.

6. The calculation of the model with: a pre-simulation time of: 1 year, a main simulation time of: 1 year and a time-step interval of: 5 days, lasted less than 1 min. The results derived had no difference from the results of the calculation described in §5 (the respective calculation with no pre-simulation time).

7. The calculation of the model with: no pre-simulation time, a main simulation time of: 2 years and a time-step interval of: 10 days, lasted less than 1 min. The results derived had no difference from the results of the calculation described in §5.

8. The calculation of the model with: a pre-simulation time of: 1 year, a main simulation time of: 1 year and a time-step interval of: 10 days, lasted less than 1 min. The results derived, diverged: ~15.15% both from the results of the calculation described in §6 (the respective calculation with no pre-simulation time) and the respective ones of the calculation described in §7.

9. The calculation of the model with: no pre-simulation time, a main simulation time of: 2 years and a time-step interval of: 15 days, lasted less than 1 min.

10. The calculation of the model with: a pre-simulation time of: 1 year, a main simulation time of: 1 year and a time-step interval of: 15 days, lasted less than 1 min. The results derived, diverged: ~26.31% from the results of the calculation described in §9 (the respective calculation with no pre-simulation time).

11. The calculation of the model with: no pre-simulation time, a main simulation time of: 2 years and a time-step interval of: 20 days, lasted less than 1 min.

12. The calculation of the model with: a pre-simulation time of: 1 year, a main simulation time of: 1 year and a time-step interval of: 20 days, lasted less than 1 min. The results derived, diverged: ~34.89% from the results of the calculation described in §11 (the respective calculation with no pre-simulation time).

Conclusions:

– **There is a divergence of: ~ 25.45% in average - as far as the results derived for the heat flow rate at the end of the simulation time are concerned - between the calculations with a pre-simulation time of: 1 year (and a main simulation time of: 1 year) and the ones with no pre-simulation time (but, with a main simulation time of: 2 years). The longest the time-step interval of the calculation, the biggest the specific divergence.**

– **The model described in §6 is a 'reliable' one to be compared with the respective 3-D & 2-D models, as far as the estimation of the annual (ground floor) heat losses is concerned. This is because the results in question derived from this simulation, diverge: 13.97% from the respective ones of the calculation described in §8 (see figures D.3 & D.4 in the next two pages) - as opposed to the respective 2-D models, whose divergence is only: 0.92%. So, the calculation of §6 is chosen as more precise, due to its shorter time-step interval (5 days, as opposed to 10 days). The annual ground floor heat losses, as estimated by the specific model, are:** 8,830.08 kJ, **or, since the surface area of the model's ground floor is:** $1m^2$, **then:** 8,830.08 kJ/ m^2.

- **'EQUALIZATION' OF THE THREE MODELS**

After the 'determination' of the three models (3-D, 2-D & 1-D) to be 'compared', the next step is to 'equalize' the specific models. This means that, the annual ground floor heat losses per unit surface area of the 1-D model (8,830.08kJ/m^2) should be the same with the respective ones of the 2-D (~113,981.47 kJ/m^2) and the 3-D (~203,054.95 kJ/m^2) models. This will be achieved by changing the values of the simulation parameters of the 1-D model, as described below:

– **'EQUALIZATION' OF THE 2-D & 1-D MODELS**

♦ **SOIL THERMAL CONDUCTIVITY (λ)**

As mentioned in Chapter 2, the soil thermal conductivity (λ) was found to comparatively be the most important parameter, as far as the earth-contact heat transfer part of the overall simulation process is concerned, according to a sensitivity study [D.2] made on the results derived from the simulation of a 3-D numerical model of a test room. Therefore, the first simulation parameter to be changed, in order for the 'equalization' of the two specific models to be achieved, was the soil thermal conductivity. After several calculations with different values for the soil thermal conductivity for each of them, it was found that, setting the value of 'λ' equal to: ~ 59.89 W/mk (from: 1.5 W/mk), a 'match' of the two models was achieved.

– **'EQUALIZATION' OF THE 3-D & 1-D MODELS**

♦ **SOIL THERMAL CONDUCTIVITY (λ)**

As with the 2-D & 1-D models, the first simulation parameter to be changed, in order for the equalization of the two specific models to be achieved, was the soil thermal conductivity. After several calculations with different soil thermal conductivity values for each, it was found that, setting the value of 'λ' from: 1.5 W/mK (initial value) to: ~ $2.5x10^6$ W/mk, a 'match' of the two models was achieved by: ~84.7% {the annual ground floor heat losses derived from the 1-D model were: 84.7% (171,983.52 kJ/m^2) of the respective ones (~203,054.95 kJ/m2) derived from the 3-D model}. Further increase of the 'λ' value, did not result in 'match' of the two models.

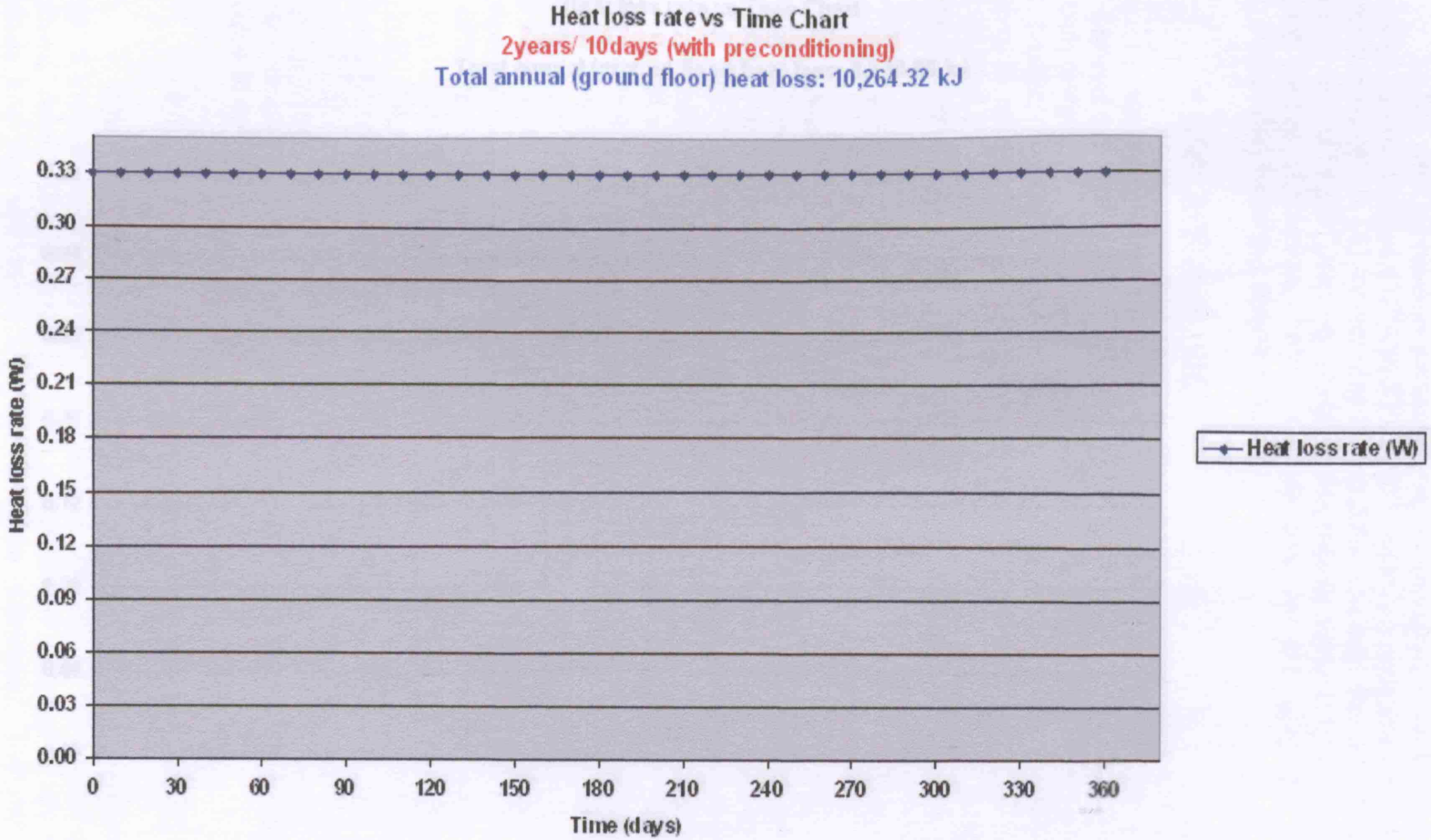

Figure D.3 - Heat loss rate vs Time Chart (1-D model/ 2years per 10 days with pre-conditioning)

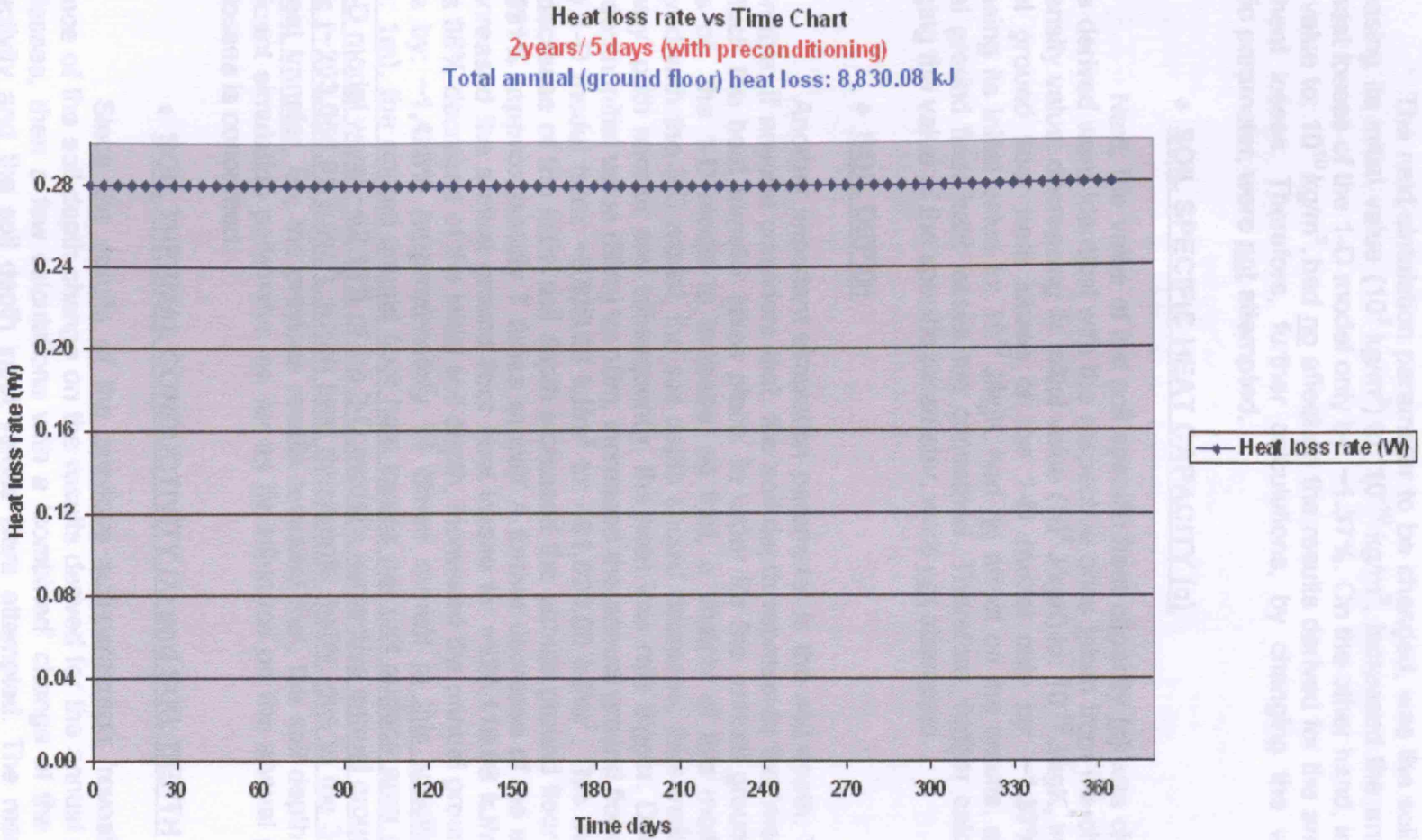

Figure D.4 - Heat loss rate vs Time Chart (1-D model/ 2years per 5 days with pre-conditioning)

♦ SOIL DENSITY (ρ)

The next simulation parameter to be changed, was the soil density (ρ). Decreasing its initial value (10^3 kg/m^3) to: 10^{-10} kg/m^3, increased the annual ground floor heat losses of the 1-D model only by: **~1.37%**. On the other hand, increasing its initial value to: 10^{10} kg/m^3, had no affect on the results derived for the annual ground floor heat losses. Therefore, further calculations, by changing the value of the specific parameter, were not attempted.

♦ SOIL SPECIFIC HEAT CAPACITY (c)

Next, the value of the soil specific heat capacity (c) was changed. The results derived were identical with the respective ones taken from the change of the soil density value: decreasing its initial value (10^3 J/kgK) to: 10^{-10} J/kgK, increased the annual ground floor heat losses of the 1-D model only by: **~1.37%**, whereas, increasing its initial value to: 10^{10} J/kgK, had no affect on the results, as far as the annual ground floor heat losses are concerned. Therefore, further calculations, by changing the value of the specific parameter, were not attempted.

♦ SOIL DEPTH

Another important simulation parameter is the soil depth. This is quite reasonable, if anyone considers that, the soil depth represents the 'medium' (path) via which the heat transfer takes place. In order for the annual ground floor heat losses of the 1-D model to increase, so that, a 'match' of this model could be achieved with the 3-D model, the soil depth should decrease, thus making the heat 'getaway' path shorter and subsequently, the heat loss rate bigger. Decreasing the soil's depth initial value (50m) to: 10m, increased the annual ground floor heat losses of the 1-D model from: **~8,830.08 kJ/m^2** to: **~61,020.00 kJ/m^2**. This means that, a **90%** decrease of the initial soil depth increased the annual ground floor heat losses by: **~691% (approximately 7 times more)!** A further decrease of the soil depth to: 1m increased the annual ground floor heat losses to: **~126,118.08 kJ/m^2**, meaning that, a **98%** decrease of the initial soil depth, increased the annual ground floor heat losses by: **~1,428% (approximately 14 times more)!** In this specific case (soil depth: 1m), the annual ground floor heat losses per unit surface area derived from the 1-D model were: **~62.11%** of the 3-D model's respective annual ground floor heat losses (**~203,054.95 kJ/m^2**), which best represents reality, due to the 3-D nature of the heat transfer. So, the previous results revealed that, the soil depth is the most significant simulation parameter, as far as its influence on the annual ground floor heat losses is concerned.

♦ SOIL THERMAL CONDUCTIVITY (λ) and SOIL DEPTH

Since the results of the previous sub-paragraph 'revealed' a great influence of the soil depth change on the results derived for the annual ground floor heat losses, then a few calculations with a 'combined' change of the soil thermal conductivity and the soil depth input values were attempted. The results derived, showed that, with a soil thermal conductivity value of: 17.31 W/mK (from: 1.5 W/mK) and a soil depth value of: 1m (from: 50m), a 'match' of the two models was achieved.

➢ SYNOPSIS OF THE NUMERICAL MODELS

- **THREE-DIMENSIONAL (3-D)**
  Nodes: 979,120
  Internal Boundary Condition Surface (Floor) Area: 100m^2

Table D.1

VOLTRA File Title (*.vtr)	Pre-simulation Period (years)	(Main) Simulation Period (years)	Time-step (days)	Calculation Time (min)	Internal Boundary Condition Heat Loss Rate (W)	Comments
Slab on ground_sin_2years_5days		2	5	190[21]	186.61	
Slab on ground_sin_2years_5days_prec	1	1	5	180[22]	744.97	
Slab on ground_sin_2years_10days		2	10	110	744.87	
Slab on ground_sin_2years_10days_prec	1	1	10	110	839.60	
Slab on ground_sin_2years_15days		2	15	90	914.23	
Slab on ground_sin_2years_15days_prec	1	1	15	85	848.92	
Slab on ground_sin_2years_20days		2	20	70	913.58	
Slab on ground_sin_2years_20days_prec	1	1	20	60	858.57	

[21]: No intermediate results for every time-step (5 days) were derived after the end of the calculation time; this happened twice. So, the annual heat loss cannot be calculated for the specific model.
[22]: No intermediate results for every time-step (5 days) were derived after the end of the calculation time; this happened three (3) times. So, the annual heat loss cannot be calculated for the specific model.

- **TWO-DIMENSIONAL**
  Nodes: 11,258
  Internal Boundary Condition Surface (Floor) Area: 10m^2

Table D.2

VOLTRA File Title (*.vtr)	Pre-simulation Period (years)	(Main) Simulation Period (years)	Time-step (days)	Calculation Time (min)	Internal Boundary Condition Heat Loss Rate (W)	Comments
Slab on ground_sin_2D_2years_1day		2	1	2	41.35	
Slab on ground_sin_2D_2years_1day_prec	1	1	1	2	41.35	
Slab on ground_sin_2D_2years_1hour		2	1/24 (1hr)	60	41.35	
Slab on ground_sin_2D_2years_1hour_prec	1	1	1/24 (1hr)	60	41.35	
Slab on ground_sin_2D_2years_5days		2	5	Very quick[23]	41.35	
Slab on ground_sin_2D_2years_5days_prec	1	1	5	-//-	41.35	
Slab on ground_sin_2D_2years_10days		2	10	-//-	41.34	
Slab on ground_sin_2D_2years_10days_prec	1	1	10	-//-	46.46	
Slab on ground_sin_2D_2years_15days		2	15	-//-	49.73	
Slab on ground_sin_2D_2years_15days_prec	1	1	15	-//-	47.34	
Slab on ground_sin_2D_2years_20days		2	20	-//-	49.70	
Slab on ground_sin_2D_2years_20days_prec	1	1	20	-//-	48.23	

[23]: Less than one (1) minute.

- **ONE-DIMENSIONAL**
  Nodes: 224
  Internal Boundary Condition Surface (Floor) Area: 1m^2

Table D.3

VOLTRA File Title (*.vtr)	Pre-simulation Period (years)	(Main) Simulation Period (years)	Time-step (days)	Calculation Time (min)	Internal Boundary Condition Heat Loss Rate (W)	Comments
Slab on ground_sin_1D_2years_1day		2	1	Very quick[3]	0.28	
Slab on ground_sin_1D_2years_1day_prec	1	1	1	-//-	0.28	
Slab on ground_sin_1D_2years_1hour		2	1/24 (1hr)	10	0.28	
Slab on ground_sin_1D_2years_1hour_prec	1	1	1/24 (1hr)	10	0.28	
Slab on ground_sin_1D_2years_10days		2	10	Very quick[3]	0.28	
Slab on ground_sin_1D_2years_10days_prec	1	1	10	-//-	0.28	
Slab on ground_sin_1D_2years_15days		2	15	-//-	0.28	
Slab on ground_sin_1D_2years_15days_prec	1	1	15	-//-	0.38	
Slab on ground_sin_1D_2years_20days		2	20	-//-	0.28	
Slab on ground_sin_1D_2years_20days_prec	1	1	20	-//-	0.43	
Slab on ground_sin_1D_2years_5days		2	5	-//-	0.28	
Slab on ground_sin_1D_2years_5days_prec	1	1	5	-//-	0.28	
Slab on ground_sin_1D_2years_5days_prec_cond2D.vtr	1	1	5	-//-	5.81[24]	λ = 59.8861 W/mK
Slab on ground_sin_1D_2years_5days_prec_cond3D	1	1	5	-//-	9.26[25]	$\lambda = 2.5 \times 10^6$ W/mK
Slab on ground_sin_1D_2years_5days_prec_dens3D	1	1	5	-//-	0.28	$\rho = 10^{10}$ kg/m^3
Slab on ground_sin_1D_2years_5days_prec_dens3D'	1	1	5	-//-	0.30	$\rho = 10^{-10}$ kg/m^3

[24]: Match with the 2-D Model.
[25]: 84.7% match with the 3-D Model.

VOLTRA File Title (*.vtr)	Pre-simulation Period (years)	(Main) Simulation Period (years)	Time-step (days)	Calculation Time (min)	Internal Boundary Condition Heat Loss Rate (W)	Comments
Slab on ground_sin_1D_2years_5days_prec_ sphc3D	1	1	5	-//-	0.28	$c = 10^{10}$ J/kgK
Slab on ground_sin_1D_2years_5days_prec_ sphc3D'	1	1	5	-//-	0.30	$c = 10^{-10}$ J/kgK
Slab on ground_sin_1D_2years_5days_prec_ depth1	1	1	5	-//-	4.59	Soil depth = 1m
Slab on ground_sin_1D_2years_5days_prec_ depth5	1	1	5	-//-	4.42	Soil depth = 5m
Slab on ground_sin_1D_2years_5days_prec_ depth1_cond3D	1	1	5	-//-	5.55[26]	Soil depth = 1m & $\lambda = 17.31$ W/mK

[26]: Match with the 3-D Model.

D.2 GROUND BEARING FLOOR NUMERICAL MODEL [D.1]

The calculations done for all the models (3-D, 2-D & 1-D) of the specific constructional detail (ground bearing floor with insulation above slab and a full-fill cavity external wall), the respective derived results and the conclusions drawn from them, are presented below. Furthermore, the Tables: D.4, D.5 & D.6, which follow, summarize all the relevant numerical data of the calculations done.

➢ CALCULATIONS 'DIARY' AND DERIVED CONCLUSIONS

• THREE-DIMENSIONAL (3-D) MODELS: 791,504 nodes

1. The calculation of the model with: no pre-simulation time, a main simulation time of: 2 years and a time-step interval of: 1 day, lasted: 70 mins. After the specific time interval the PC 'crashed' and so, no results were derived. Then, the same calculation was repeated again from the start, but after three hours the PC 'crashed' again. So, once more, no results were derived.

2. The calculation of the model with: no pre-simulation time, a main simulation time of: 2 years and a time-step interval of: 10 days, lasted: 60 mins.

3. The calculation of the model with: no pre-simulation time, a main simulation time of: 2 years and a time-step interval of: 20 days, lasted: 40 mins. The results derived - as far as the heat flow rate (W) at the end of the simulation time is concerned - diverged: ~30% from the results of the calculation described in §2.

4. The calculation of the model with: no pre-simulation time, a main simulation time of: 2 years and a time-step interval of: 30 days, lasted: 35 mins. The results derived - as far as the heat flow rate (W) at the end of the simulation time is concerned - diverged: ~1.5% from the results of the calculation described in §3.

5. The calculation of the model with: no pre-simulation time, a main simulation time of: 2 years and a time-step interval of: 40 days, lasted: 20 mins. The results derived, diverged: ~3% from the results of the calculation described in §3.

6. The calculation of the model with: no pre-simulation time, a main simulation time of: 2 years and a time-step interval of: 5 days, lasted: 105 mins. The results derived, were similar with the respective ones of the calculation described in §2.

7. The calculation of the model with: no pre-simulation time, a main simulation time of: 2 years and a time-step interval of: 15 days, lasted: 85 mins. The results derived, were similar with the respective ones of the calculation described in §3, but not similar with the respective ones of the calculations described in §2 & §6.

8. The calculation of the model with: a pre-simulation time of: 1 year, a main simulation time of: 1 year and a time-step interval of: 5 days, lasted: 100 mins. The results derived - as far as the heat flow rate (W) at the end of the simulation time is concerned - had no difference from the respective ones of the calculation described in §6 (the respective calculation with no pre-simulation time).

9. The calculation of the model with: a pre-simulation time of: 4 years, a main simulation time of: 1 year and a time-step interval of: 5 days, lasted: 255 mins. The results derived - as far as the heat flow rate (W) at the end of the simulation time is concerned - diverged less than: 1% from the results of the calculation described in §8.

Conclusions:

– There is a divergence of: ~ 32% in average - as far as the results derived for the heat flow rate at the end of the simulation time are concerned - between the calculations with a time-step interval of: 5 or 10 days and the respective ones with a time-step interval of: 15, 20, 30 or 40 days (no pre-simulation time and main simulation time: 2 years).

– The increase of the pre-simulation time from: 1 to 4 years had little influence on the results derived from the calculation described in §8.

– Since the model described in §8 is the most precise one - the one with the shortest time step interval - that can derive results and since, it does not differ a lot - as far as the results derived for the heat flow rate (W) at the end of the simulation time are concerned - from the models described in §2 & §9, then it is concluded that, is the most 'reliable' one to be compared with the respective 2-D & 1-D models, as far as the estimation of the annual (ground floor) heat losses is concerned. The heat losses in question, as estimated from the specific model, are: ~12,055,957.92 kJ or, if the surface area of the model's ground floor (100m^2) is taken into consideration: ~120,559.58 kJ/ m^2.

- **TWO-DIMENSIONAL (2-D) MODELS: 15,244 nodes**

1. The calculation of the model with: no pre-simulation time, a main simulation time of: 2 years and a time-step interval of: 20 days, lasted less than 1 min.

2. The calculation of the model with: no pre-simulation time, a main simulation time of: 2 years and a time-step interval of: 1 day, lasted approximately 3 mins. The results derived - as far as the heat flow rate (W) at the end of the simulation time is concerned - diverged: ~8.97% from the results of the calculation described in §1.

3. The calculation of the model with: no pre-simulation time, a main simulation time of: 2 years and a time-step interval of: 1 hour, lasted 60 mins. The results derived, diverged: ~8.97% from the results of the calculation described in §1, but had no difference from the respective ones of the calculation described in §2.

4. The calculation of the model with: no pre-simulation time, a main simulation time of: 2 years and a time-step interval of: 5 days, lasted less than 1 min. The results derived, had no difference from the respective ones of the calculation described in §3.

5. The calculation of the model with: no pre-simulation time, a main simulation time of: 2 years and a time-step interval of: 30 mins, lasted 120 mins, but then, the PC 'crashed'. So, no results were derived.

6. The calculation of the model with: a pre-simulation time of: 1 year, a main simulation time of: 1 year and a time-step interval of: 5 days, lasted less than 1min. The results derived, had no difference from the results of the calculation described in §4 (the respective calculation with no pre-simulation time).

7. The calculation of the model with: a pre-simulation time of: 4 years, a main simulation time of: 1 year and a time-step interval of: 5 days, lasted approximately 2.5 mins. The results derived, had little difference (~0.43%) from the results of the calculation described in §6 (the respective calculation with a pre-simulation time of: 1 year).

Conclusions:

– Since the model described in §6 has no difference - as far as the results derived for the heat flow rate at the end of the simulation time are concerned - with the models described in §2, 3 & 4, which are the most precise ones than can be calculated, then is concluded that, it is a 'reliable' model to be compared with the respective 3-D & 1-D models, as far as the estimation of the annual (ground floor) heat losses is concerned. The heat losses in question, as estimated from the specific model, are: ~712,601.28 kJ **or, if the surface area of the model's ground floor (**10m^2**) is taken into consideration:** ~71,260.13 kJ/ m^2.

– The increase of the pre-simulation time from: 1 to 4 years, had little influence on the results of the calculation described in §6, as far as the heat flow rate at the end of the simulation time is concerned.

- **ONE-DIMENSIONAL (1-D) MODELS: 208 nodes**

1. The calculation of the model with: no pre-simulation time, a main simulation time of: 2 years and a time-step interval of: 5 days, lasted less than 1 min.

2. The calculation of the model with: a pre-simulation time of: 1 year, a main simulation time of: 1 year and a time-step interval of: 5 days, lasted less than 1 min. The results derived - as far as the heat flow rate (W) at the end of the simulation time is concerned - had little difference (~3.33%) from the results of the calculation described in §1 (the respective calculation with no pre-simulation time).

3. The calculation of the model with: a pre-simulation time of: 4 years, a main simulation time of: 1 year and a time-step interval of: 5 days, lasted less than 1 min. The results derived, had little difference (~7.14%) from the results of the calculation described in §2 (the respective calculation with a pre-simulation time of: 1 year).

Conclusion: Since the model described in §2 has little difference - as far as the results derived for the heat flow rate at the end of the simulation time are concerned - with the ones described in §1 & 3, then is concluded that, it is a 'reliable' model to be compared with the respective 2-D & 1-D models, as far as the estimation of the annual (ground floor) heat losses is concerned. The heat losses in question, as estimated from the specific model, are: ~9,145.44 kJ **or, since the surface area of the model's ground floor is:** 1m^2**, then:** ~9,145.44 kJ/ m^2.

- **'EQUALIZATION' OF THE THREE MODELS**

After the 'determination' of the three models (3-D, 2-D & 1-D) to be 'compared' has been completed then, the next step is to 'equalize' the specific models. This means that, the annual ground floor heat losses per unit surface area of the 1-D model (9,145.44 kJ/m^2) should be 'made' the same with the respective ones of the 2-D (~71,260.13 kJ/m^2) and the 3-D (~120,559.58 kJ/m^2) models. This will be achieved by changing the values of the simulation parameters of the 1-D model, as described in the next paragraphs:

– 'EQUALIZATION' OF THE 2-D & 1-D MODELS

♦ SOIL THERMAL CONDUCTIVITY (λ)

As with the first geometrical model, the first simulation parameter that was changed during the 'equalization' process was the soil thermal conductivity (λ). After several calculations with different values for the soil thermal conductivity for each of them, it was found that, setting the value of 'λ' from: 1.5 W/mK (initial value) to: ~ 19.16 W/mk, a 'match' of the two models was achieved.

– 'EQUALIZATION' OF THE 3-D & 1-D MODELS

♦ SOIL THERMAL CONDUCTIVITY (λ)

Similarly with the 2-D & 1-D models, the first simulation parameter to be changed, in order for the 'equalization' of the two specific models to be achieved, was the soil thermal conductivity (λ). After several calculations with different soil thermal conductivity values for each one, it was found that, setting the value of 'λ' from: 1.5 W/mK (initial value) to: ~ 51.09 W/mk, a 'match' of the two models was achieved.

♦ SOIL DENSITY (ρ)

The next simulation parameter to be changed, was the soil density (ρ). Increasing its initial value (10^3 kg/m^3) to: 10^{10} kg/m^3, had no affect on the results derived for the annual ground floor heat losses. On the other hand, decreasing its initial value to: 10^{-10} kg/m^3 reduced the annual ground floor heat losses of the 1-D model only by: **~1.32%**. Therefore, further calculations, by changing the value of the specific parameter, were not attempted.

♦ SOIL SPECIFIC HEAT CAPACITY (c)

Next, the value of the soil specific heat capacity (c) was changed. The results derived were identical with the respective ones taken from the change of the soil density value: decreasing its initial value (10^3 J/kgK) to: 10^{-10} J/kgK reduced the annual ground floor heat losses of the 1-D model only by: **~1.32%**, whereas, increasing its initial value to: 10^{10} J/kgK, had no affect on the results, as far as the annual ground floor heat losses are concerned. Therefore, further calculations, by changing the value of the specific parameter, were not attempted.

♦ SOIL DEPTH

Another important simulation parameter is the soil depth, since it represents, as mentioned during the 'equalization' process of the first geometrical model, the path via which the heat transfer takes place. So, decreasing the soil's depth initial value (50m) to: 10m, increased the annual ground floor heat losses of the 1-D model from: **~9,145.44 kJ/m^2** to: **~164,661.12 kJ/m^2**. This means that, a **90%** decrease of the initial soil depth increased the annual ground floor heat losses by: **~1,800% (approximately 18 times more)!**

A further decrease of the soil depth to: 1m increased the annual ground floor heat losses to: **~191,289.60 kJ/m^2**, meaning that, a **98%** decrease of the initial soil depth increased the annual ground floor heat losses by: **~2,091% (approximately 21 times more)!** In this specific case (soil depth: 1m), the annual ground floor heat losses per unit surface area derived from the 1D model were: **~158.67%** of the 3-D model's respective annual ground floor heat losses (**~120,559.58 kJ/m^2**), which best represents reality, due to the 3-D nature of the heat transfer. So, the previous results reveal that, the soil depth is the most significant simulation parameter, as far as its influence on the annual ground floor heat losses is concerned. A 'match' of the two models was finally achieved with a soil depth value of: **15.507m**.

- **NO INSULATION LAYER ABOVE THE FLOOR SLAB**

As strange as it may seem, 'removing' the insulation layer above the floor slab did not bring about any changes in the annual ground floor heat losses, as concluded by the calculation of the specific 1-D model.

➢ SYNOPSIS OF THE NUMERICAL MODELS

- **THREE-DIMENSIONAL (3-D)**
  Nodes: 791,504
  Internal Boundary Condition Surface (Floor) Area: 100m^2

Table D.4

VOLTRA File Title (*.vtr)	Pre-simulation Period (years)	(Main) Simulation Period (years)	Time-step (days)	Calculation Time (min)	Internal Boundary Condition Heat Loss Rate (W)	Comments
Slab on ground_Cavity wall[27]				10	770.75	
Slab on ground_Cavity wall_1year_1day[7]		1	1	85	770.75	
Slab on ground_Cavity wall_1year_20days[7]		1	20	8	770.75	
Slab on ground_Cavity wall_2years_1day[7]		2	1	165	770.75	
Slab on ground_Cavity wall_2years_20days[7]		2	20	12	770.75	
Slab on ground_Cavity wall_2years_1day_sin		2	1	----[28]		
Slab on ground_Cavity wall_1year_10days_sin		1	10	30	455.26	
Slab on ground_Cavity wall_2years_5days_sin		2	5	105	439.00	
Slab on ground_Cavity wall_2years_5days_sin_4prec	4	1	5	255	440.45	
Slab on ground_Cavity wall_2years_5days_sin_prec	1	1	5	100	439.00	
Slab on ground_Cavity wall_2years_10days_sin		2	10	60	438.99	
Slab on ground_Cavity wall_2years_15days_sin		2	15	85	476.50	
Slab on ground_Cavity wall_2years_20days_sin		2	20	40	476.47	
Slab on ground_Cavity wall_2years_30days_sin		2	30	20	476.12	
Slab on ground_Cavity wall_2years_40days_sin		2	40	20	475.66	

[27]: Constant function for the external boundary condition air temperature.
[28]: No results derived, because the PC 'crashed'; this happened twice.

- **TWO-DIMENSIONAL**
  Nodes: 15,244
  Internal Boundary Condition Surface (Floor) Area: $10m^2$

Table D.5

VOLTRA File Title (*.vtr)	Pre-simulation Period (years)	(Main) Simulation Period (years)	Time-step (days)	Calculation Time (min)	Internal Boundary Condition Heat Loss Rate (W)	Comments
Slab on ground_Cavity wall_2years_1day_sin_2D		2	1	3	25.65	
Slab on ground_Cavity wall_2years_1hour_sin_2D		2	1/24 (1hr)	60	25.65	
Slab on ground_Cavity wall_2years_5days_sin_2D		2	5	Very quick[3]	25.65	
Slab on ground_Cavity wall_2years_5days_sin_2D_4prec	4	1	5	2.5	25.76	
Slab on ground_Cavity wall_2years_5days_sin_2D_prec	1	1	5	Very quick[3]	25.65	
Slab on ground_Cavity wall_2years_20days_sin_2D		2	20	Very quick[3]	27.95	
Slab on ground_Cavity wall_2years_30minutes_sin_2D		2	1/48 (0.5 hr)	120[29]		

[29]: The PC 'crashed' after 120min of calculation time and so, no results were derived.

- **ONE-DIMENSIONAL**
  Nodes: 208
  Internal Boundary Condition Surface (Floor) Area: $1m^2$

Table D.6

VOLTRA File Title (*.vtr)	Pre-simulation Period (years)	(Main) Simulation Period (years)	Time-step (days)	Calculation Time (min)	Internal Boundary Condition Heat Loss Rate (W)	Comments
Slab on ground_Cavity wall_2years_5days_sin_1D		2	5	Very quick[3]	0.29	
Slab on ground_Cavity wall_2years_5days_sin_1D_prec	1	1	5	-//-	0.30	
Slab on ground_Cavity wall_2years_5days_sin_1D_4prec	4	1	5	-//-	0.28	
Slab on ground_Cavity wall_2years_5days_sin_1D_prec_cond2D	1	1	5	-//-	2.24[30]	λ = 19.158 W/mK
Slab on ground_Cavity wall_2years_5days_sin_1D_prec_cond3D	1	1	5	-//-	4.80[31]	λ = 51.089 W/mK
Slab on ground_Cavity wall_2years_5days_sin_1D_prec_dens3D	1	1	5	-//-	0.30	$\rho = 10^{10}$ kg/m^3
Slab on ground_Cavity wall_2years_5days_sin_1D_prec_dens3D'	1	1	5	-//-	0.29	$\rho = 10^{-10}$ kg/m^3
Slab on ground_Cavity wall_2years_5days_sin_1D_prec_sphc3D	1	1	5	-//-	0.30	$c = 10^{10}$ J/kgK
Slab on ground_Cavity wall_2years_5days_sin_1D_prec_sphc3D'	1	1	5	-//-	0.29	$c = 10^{-10}$ J/kgK
Slab on ground_Cavity wall_2years_5days_sin_1D_prec_depth1	1	1	5	-//-	6.14	Soil depth = 1n
Slab on ground_Cavity wall_2years_5days_sin_1D_prec_depth5	1	1	5	-//-	5.41	Soil depth = 5n
Slab on ground_Cavity wall_2years_5days_sin_1D_prec_depth3D	1	1	5	-//-	4.41[11]	Soil depth = 15.507m
Slab on ground_Cavity wall_2years_5days_sin_1D_prec_no insul	1	1	5	-//-	0.29	No insulation

[30]: Match with the 2-D Model.
[31]: Match with the 3-D Model.

References for Appendix D

[D.1] VOLTRA: computer program to calculate 3D & 2D transient heat transfer in objects described in a rectangular grid using the energy balance technique - Version 4.0w - 2003 PHYSIBEL

[D.2] M.H. Adjali, M. Davies and J. Littler. Three-dimensional earth-contact heat flows: a comparison of simulated and measured data for a buried structure. Renewable Energy 1998;15: 356-359.